NASA-JSC CONTRACT NAS9-14641

FINAL PROGRESS REPORT

May 1, 1975 - March 31, 1984

PRINCIPAL INVESTIGATOR

Manning J. Correia, Ph.D.
Professor
Departments of Otolaryngology and Physiology & Biophysics
The University of Texas Medical Branch
Galveston, Texas 77550-2778

TABLE OF CONTENTS

I. COMMUNICATIONS RESULTING FROM THIS CONTRACT - 1977/1984

1. Brassard, J.R.; Correia, M.J. A computer program for fitting multimodal density functions. Comput. Prog. Biomed. 7: 1-20; 1977.

2. Anderson, D.J.; Correia, M.J. The detection and analysis of point processes in biological signals. Special Issue "Biological Signal Processing Analysis." Proc. IEEE 65: 773-780; 1977.

3. Correia, M.J.; Landolt, J.P. A point process analysis of the spontaneous activity of anterior semicircular canal units in the anesthetized pigeon. Biol. Cybern. 27: 199-213; 1977.

4. Correia, M.J.; Guedry, Jr., F.E. The vestibular system: basic biophysical and physiological mechanisms. IN: Handbook of Behavioral Neurobiology, Vol. 1, Sensory Integration., R.B. Masterton, ed. New York, Plenum Press; 1978: 353-407.

5. Ni, M.-D.; Correia, M.J.; Rae, J.L.; Koblasz, A.J. A real-time minicomputer program for calculation of transfer function and coherence function by digital Fourier methods. MIMI 77' Proc. of the Montreal Int. Show and Symp. on Mini and Microcmputers, Nov. 11-18, 1977, Montreal, Canada. Long Beach, CA: IEEE Catalog #77CH1347-4C; 1978: 205-212.

6. Correia, M.J.; Eden, A.R.; Westlund, K.N.; Coulter, J.D. Autoradiographic demonstration of auditory and vestibular pathways in the pigeon by means of anterograde transneural transport. Soc. Neurosci. Abst. 5: 18; 1979.

7. Eden, A.R.; Correia, M.J. Horseradish peroxidase identification of four separate groups of vestibular efferent neurons in the adult pigeon. Soc. Neurosci. Abst. 5: 691; 1979.

8. Eden, A.R.; Correia, M.J. A study of the relationship between HRP-labeled vestibular efferent neurons and catecholaminergic cell groups in the reticular formation of the adult pigeon. Abst. of the Third Midwinter Research Meeting-Association for Research in Otolaryngology. St. Petersburg, FL: Jan. 21-23, 1980: p. 19.

9. Eden, A.R.; Correia, M.J.; Steinkuller, P.G. The distribution of horseradish peroxidase-labeled proprioceptive neurons from individual extraocular muscles in the adult pigeon. Soc. Neurosci. Abst. 6: 479; 1980.

10. Landolt, J.P.; Correia, M.J. Neurodynamic response analysis of anterior semicircular canal afferents in the pigeon. J. Neurophysiol. 43: 1746-1770; 1980.

11. Perachio, A.A.; Correia, M.J. Transfer characteristics of anterior semicircular canal afferents in the anesthetized gerbil. Soc. Neurosci. Abst. 6: 558; 1980.

12. Correia, M.J., Landolt, J.P.; Ni, M.-D., Eden, A.R.; Rae, J.L. A species comparison of linear and nonlinear transfer characteristics of primary afferents innervating the semicircular canal. IN: The Vestibular System: Function and Morphology, T. Gualtierotti, ed. New York, Springer-Verlag; 1981: 280-316.

13. Correia, M.J.; Perachio, A.A.; Eden, A.R. Space motion sickness: neural mechanisms of sensory conflict. 34th Annual Conference on Engineering in Medicne and Biology (ACEMB) Abst. 1981: p. 237.

14. Eden, A.R.; Correia, M.J. Vestibular efferent neurons and catecholamine cell groups in the reticular formation of the pigeon. Neurosci. Lett. 25: 239-242; 1981.

15. Eden, A.R.; Correia, M.J. Improved fixation of the pigeon brain by transcardiac carotid catheterization. Physiol. Behav. 27: 947-949; 1981.

16. Eden, A.R.; Correia, M.J.; Westlund, K.N.; Coulter, J.D. An autoradiographic & HRP study of the vestibulocollic reflex in the pigeon. Abst. of the Fourth Midwinter Research Meeting-Association for Research in Otolaryngology. St. Petersburg, FL: Jan. 19-21, 1981: pp. 34-35.

17. Perachio, A.A.; Correia, M.J.; Clegg, T. Responses of semicircular canal and otolith afferents to linear acceleration. Soc. Neurosci. Abst. 7: 148; 1981.

18. Clegg, T.; Perachio, A.A.; Correia, M.J. Tilt responses of semicircular canal primary afferents. Otolaryngol. Head Neck Surg. 90: 103-107; 1982.

19. Correia, M.J.; Eden, A.R.; Westlund, K.N.; Coulter, J.D. Organization of ascending auditory pathways in the pigeon (Columba livia) as determined by autoradiographic methods. Brain Res. 234: 205-212; 1982.

20. Eden, A.R.; Correia, M.J.; Steinkuller, P.G. Medullary proprioceptive neurons from extraocular muscles in the pigeon identified with horseradish peroxidase. Brain Res. 237: 15-21; 1982.

21. Eden, A.R.; Correia, M.J. Identification of multiple groups of efferent vestibular neurons in the adult pigeon using horseradish peroxidase and DAPI. Brain Res. 248: 201-208; 1982.

22. Eden, A.R.; Correia, M.J. An autoradiographic and HRP study of vestibulocollic pathways in the pigeon. J. Comp. Neurol. 211: 432-440; 1982.

23. Perachio, A.A.; Correia, M.J. Evidence that single vestibular primary afferents respond to both angular and linear acceleration. Abst. of the Eighth Extraordinary Meeting of the Barany Society, Basle, Switzerland, June 22-25, 1982.

24. Anastasio, T.J.; Correia, M.J.; Perachio, A.A. Spontaneous activity and driven responses of semicircular canal primary afferent neurons in the alert pigeon. Soc. Neurosci. Abst. 9: 525; 1983.

25. Correia, M.J.; Eden, A.R.; Westlund, K.N.; Coulter, J.D. A study of some of the ascending and descending vestibular pathways in the pigeon (Columba livia) using anterograde transneuronal autoradiography. Brain Res. 278: 53-61; 1983.

26. Perachio, A.A; Correia, M.J. Responses of semicircular canal and otolith afferents to small angle static head tilts in the gerbil. Brain Res. 280: 287-298; 1983.

27. Perachio, A.A.; Correia, M.J. Design for a slender shaft glass micropipette. J. Neurosci. Meth. 9: 287-293; 1983.

28. Perachio, A.A.; Correia, M.J.; Kevetter, G.A. Functional and morphological characteristics of gravity-sensitive primary canal afferents. Soc. Neurosci. Abst. 9: 739; 1983.

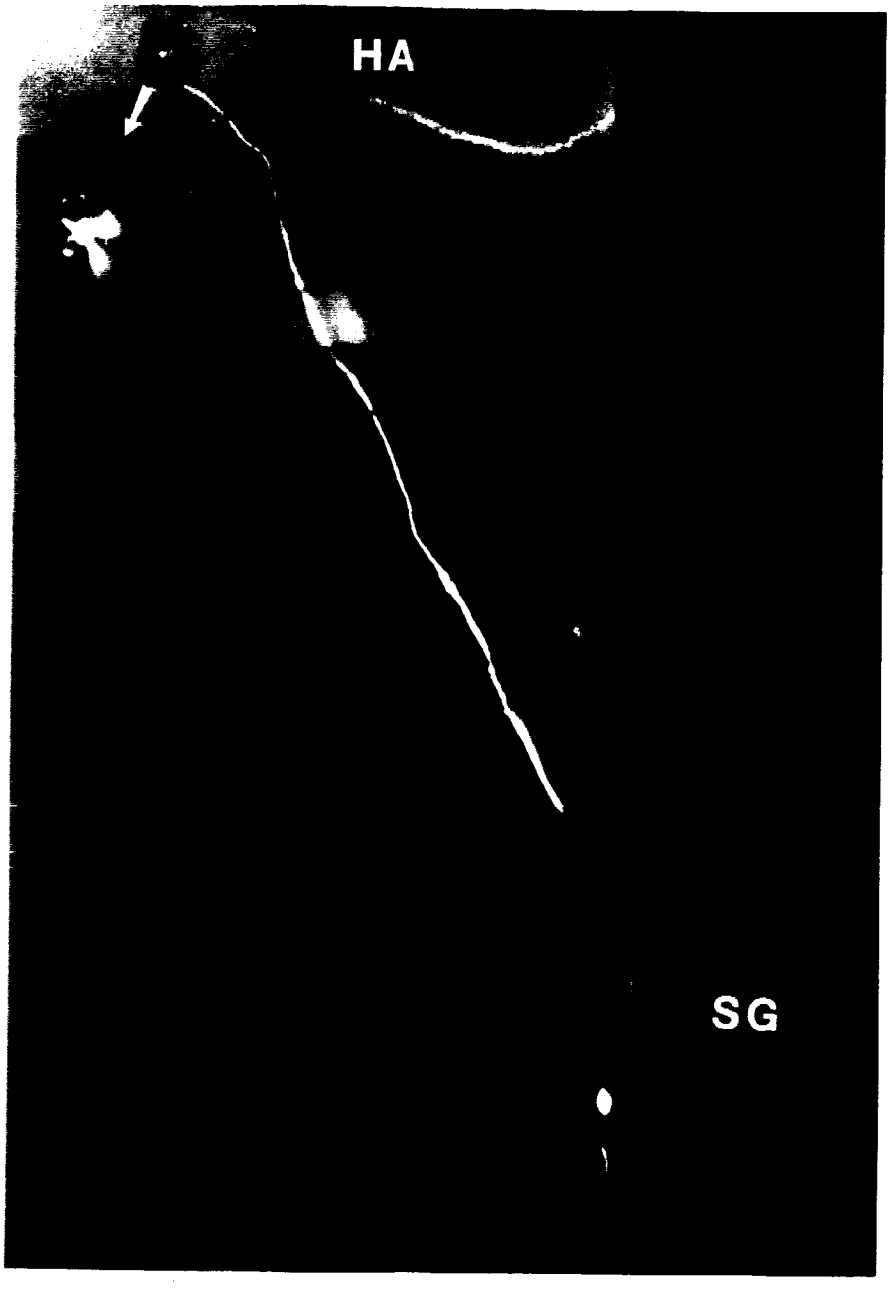

Fig. 1

TABLE I

Distribution of number of type I hair cells/calyx for three pigeons whose anterior ampullary neuroepithelium was sectioned in either the horizontal (H), transverse (T), or longitudinal (L) plane.

#/Calyx	H-Plane Σ	H-Plane %	T-Plane Σ	T-Plane %	L-Plane Σ	L-Plane %	Grouped % L-Plane
1	304	28.3	205	21.7	318	28.3	28.3
2	215	20.0	215	22.8	265	23.6	
3	208	19.3	190	20.1	214	19.1	63.9
4	132	12.3	140	14.8	137	12.2	
5	92	8.6	90	9.5	101	9.0	
6	53	4.9	48	5.1	43	3.8	
7	32	3.0	27	2.9	29	2.6	
8	20	1.9	14	1.5	8	0.7	
9	9	0.8	8	0.8	5	0.4	7.7
10	7	0.7	5	0.5	1	0.1	
11	2	0.2	1	0.1	0	0.0	
12	1	0.0	0	0.0	1	0.1	
Σ	1075**	100.0	943*	99.8	1122	99.9	
# type I HC	3233		2937		3135		

*3 sections not recovered

**1 section not recovered

III. PROGRESS REPORT - APRIL 1, 1981/November 30, 1983 (2 yrs, 7 mos)

Listed below are journal articles, abstracts, and as yet unpublished work which have been sponsored in part by this grant. Following each citation is a brief summary paragraph which describes the primary finding or findings of the communication. Also presented and underlined, are findings which relate to the rationale or methods of the renewal proposal. Selected communications are appended.

A. Articles in Refereed Journals

1. Eden, A.R.; Correia, M.J. Vestibular efferent neurons and catecholamine cell groups in the reticular formation of the pigeon. Neurosci. Letts. 25: 239-242; 1981.

Sections of the pigeon brainstem were treated with glyoxylic acid (GA) following endolymphatic injection of HRP. HRP-labeled efferent cells in the nucleus reticularis pontis caudalis were examined for both fluorescense and HRP reaction product. The absence of fluorescense of HRP-labeled vestibular efferent neurons in the reticular formation appears to preclude the existence of a direct central (nor) adrenergic component projecting to the vestibular end organ in the pigeon. However, close intermingling of HRP-labeled vestibular efferent neurons and GA-induced fluorescent neurons within the nucleus reticularis pontis caudalis suggest that there may be an indirect central adrenergic influence on the labyrinth, perhaps mediated by vestibular efferent neurons.

2. Eden, A.R.; Correia, M.J. Improved fixation of the pigeon brain by transcardiac carotid catheterization. Physiol. Behav. 27: 947-949; 1981.

A technique was developed for selective and controlled fixation of the brain and upper spinal cord in the pigeon by in vivo transcardiac bilateral carotid catheterization and pump perfusion. This method yields a blood-free and well fixed labyrinth, brain, and upper spinal cord. We were previously unable to achieve such good fixation in the pigeon using standard mammalian intracardiac perfusion techniques.

3. Correia, M.J.; Eden, A.R.; Westlund, K.N.; Coulter, J.D. Organization of ascending auditory pathways in the pigeon (Columba livia) as determined by autoradiographic methods. Brain Res. 234-212; 1982.

A mixture of tritiated proline and fucose was injected and contained within the labyrinthine endolymphatic space in white king pigeons. Using standard autoradiographic techniques, transneuronal labeling of ascending auditory pathways was noted to the level of the mesencephalon. Clear labeling was noted in the ipsilateral and contralateral superior olive, lateral lemniscus and dorsal part of the lateral mesencephalic nucleus. These results suggest that, in general, the ascending auditory pathways in the pigeon are more similar to those

described for mammals than previously thought.

4. Eden, A.R.; Correia, M.J.; Steinkuller, P.G. Medullary proprioceptive neurons from extraocular muscles in the pigeon identified with horseradish peroxidase. Brain Res. 237: 15-21; 1982.

Horseradish peroxidase was injected along the central axis in one of the six extraocular muscles in each of eighteen pigeons. HRP-labeled proprioceptive neurons were located in the ipsilateral nucleus descendens nervi trigemini (TTD) for all muscle injections. The HRP-labeled neurons in the pigeon TTD following extraocular muscle (EOM) injections suggest that at least part of the afferent (proprioceptive) innervation of the pigeon EOM courses via the trigeminal opthalamic division directly to the ipsilateral TTD, coursing through the semilunar ganglion but in keeping with the topographic pattern of the distribution of the trigeminal rami.

5. Clegg, T.; Perachio, A.A.; Correia, M.J. Tilt responses of semicircular canal primary afferents. Otolaryngol. Head Neck Surg. 90: 103-107; 1982.

Preliminary observations - Fifty-four vestibular primary afferents were identified and tested with the head in either the standard position (horizontal SC's in the earth's horizontal plane) or pitched ± 10 degrees or rolled ± 10 degrees. Recordings were made in a whole brain animal. Animals were anesthetized with a combination of urethane and ketamine. Among all lateral and anterior SC afferents in the test sample, 30% exhibited a significant tilt response (change of at least 10% in MFR re standard position). Of the 8 lateral SC afferents tested, 100% showed a decrease in firing rate of 10% or greater when the nose was pitched up 10 degrees; seventy-five percent showed an increase in firing rate when the nose was pitched down 10 degrees. These responses were reproducable with replication of the tilt paradigm.

6. Eden, A.R.; Correia, M.J. Identification of multiple groups of efferent vestibular neurons in the adult pigeon using horseradish peroxidase and DAPI. Brain Res. 248:201-208; 1982.

Horseradish peroxidase was injected and confined within the endolymphatic space of one labyrinth in 9 adult pigeons. In 9 additional pigeons DAPI was also injected and confined within the endolymphatic space in one labyrinth. Five different groups of HRP-labeled vestibular efferent neurons were identified. Three groups were located within the confines of the ipsilateral vestibular nuclear complex (in the lateral, tangential, and descending nucleus), and two groups (each bilateral) were located in the reticular formation. DAPI-labeled cells were noted in 3 of the 5 locations (tangential nucleus and both reticular groups) which in other animals contained HRP-labeled cells. The finding of vestibular efferent neurons in the vestibular nuclei remains a controversial issue.

7. Eden, A.R.; Correia, M.J. An autoradiographic and HRP study of vestibulocollic pathways in the pigeon.

J. Comp. Neurol. 211: 432-1982.

The right biventer cervicis and complexus neck muscles were divided into rostral and caudal halves in 10 animals and HRP was injected into one-half of one of the two muscles in each experiment. Tritiated proline and fucose was injected into the left labyrinthine endolymph in 5 animals. Brains of animals which had received HRP injections were processed using the tetramethylbenzidine (TMB) blue reaction process. Sections of the brains' of the 5 animals which received endolymphatic injections of tritiated proline and fucose were processed using standard autoradiographic methods. Three groups of HRP-labeled motoneurons were identified in the ipsilateral ventral horn of the upper cervical spinal cord: a ventromedial group and a ventrolateral group within lamina VIII innervating the biventer cervicis and the more rostral part of the complexus muscle and a dorsolateral group within lamina VII innervating the caudal part of the complexus muscle. Labeled motoneurons were also observed in the ipsilateral medulla adjacent to the medial longitudinal fasciculus in a location previously identified as the hypoglossal nucleus. The same clusters of motoneurons identified in the brainstem and spinal cord which were observed to be HRP-labeled were also overlayed by silver grains after autoradiographic processing.

8. Correia, M.J.; Eden, A.R.; Westlund, K.N.; Coulter, J.D. Ascending and descending vestibular pathways in the pigeon (Columba livia) as demonstrated by anterograde transsynaptic autoradiography. Brain Res. (in press, 1983).

A mixture of tritiated proline and fucose was injected into the endolymph of one of the membranous labyrinths in each of 5 white king pigeons. The labyrinth was resealed and the animal was allowed to survive for 15 days. Brain and upper parts of the spinal cords were sectioned and processed by standard autoradiographic procedures. Structures related to ascending and descending vestibular pathways were labeled to the level of the mesencephalon and the cervical spinal cord. Structures which were heavily labeled and which are associated with the ascending vestibular pathways included all of the ipsilateral vestibular nuclei, but none of the contralateral vestibular nuclei, the contralateral medial longitudinal fasciculus, the contralateral abducens and trochlear nucleus as well as two parts of the oculomotor nucleus - the dorsolateral part and the ventromedial part. Less heavily labeled ipsilateral vestibulo-ocular-related-structures included the medial longitudinal fasiculus, abducens nucleus, and the vennrolateral edge of the trochlear nucleus. The dorsomedial part of the oculomotor nucleus was heavily labeled on the side ipsilateral to the injected labyrinth. The medullary core of most folia but primarily the medullary core and granular areas of folia IX and X of the cerebellum were labeled. Contralateral structures associated with descending vestibulospinal pathways which were heavily labeled were the medial longitudinal fasciculus, terminal fields around a column of motoneurons in the brainstem, the ventral funiculus, and terminal fields around motoneuron clusters in lamina VII and VIII of the upper spinal cord. A correlation was noted to exist between those components of the vestibulo-ocular and vestibulospinal pathways which were heavily labeled and those which have been shown to be excitatory in mammalian electrophysiological studies.

9. Perachio, A.A.; Correia, M.J. Responses of semicircular canal and otolith afferents to small angle static head tilts in the gerbil. Brain Res. (in press, 1983).

Single unit activity was recorded from SC primary afferents in anesthetized or decerebrated gerbils. In decerebrated preparations, canal afferents exhibited significantly faster discharge activity (average = 87.8 impulses per sec) than that of canal afferents in anesthetized preparations (average = 66.2 impulses per sec) when the head was held so as to position the lateral SC's coplanar with the earth's horizontal plane (standard position). A comparison was made between the MFR in the standard position and following tilt of the animal 10 degrees about either its left/right or fore/aft head axes. A change in activity, from that recorded in the standard position, of 10% or greater was considered significant. Significant changes in the tilt response in anesthetized animals was observed in both anterior (23/47, 48%) and lateral (22/31, 71%) canal afferents. In decerebrate preparations using tilts about the left/right head axes, comparable effects were measured in (19/36, 53%) anterior and (17/30, 57%) lateral canal afferents. Neurons with irregular firing activity were more likely to change their average discharge rate with static tilt.

10. Perachio, A.A.; Correia, M.J. Design for a slender shaft glass micropipette. J. Neurosci. Meth. (in press, 1983).

Methods for construction of long slender shaft glass micropipettes are described. These pipettes are comparable in diameter to metal microelectrodes that have been used to record from small targets located deep within the brain. The advantages of slender glass micropipettes over metal microelectrodes are that: 1) they can be reliably produced, 2) dyes can be iontophoretically injected from them, and 3) both extra- and intracellular recordings are feasible.

B. Abstracts of Results not yet Published

1. Correia, M.J.; Perachio, A.A.; Eden, A.R. Space motion sickness: neural mechanisms of sensory conflict. Abstracts of the ACEMB Symposium, Shamrock Hilton Hotel, Houston, Texas, Sept. 21-23, 1981: p.237, 22.10.

A thesis was put forward that space motion sickness could be the result of either: a) intralabyrinthine neural conflict; b) neural conflict between labyrinthine signals and those from other sensory systems (e.g. vision, proprioception etc.) or 3) an inappropriate mode of response from one of the labyrinthine receptors. To support the last supposition, data were presented which showed that a certain percentage of semicircular canal primary afferents were gravity sensitive, signal head tilt, and therefore, may signal a response of the SC's to weightlessness.

2. Kemmerer, C.E.; Correia, M.J.; Perachio, A.A. An analog alternative to the digital anti-alias filter used to pre-process neuronal spike train data for Fourier analysis. First Southern Biomedical Conference, Shreveport, LA, June 7-8, 1982.

An analog method of anti-alaising action potential trains was developed and tested against the traditional digital method developed by French and Holden (1971a, b). The new method permits on-line processing of an action potential train resulting from alias free application of the fast Fourier transform. When amplitude ratio and phase relationships between stimulus velocity and semicircular canal afferent single unit responses were compared, using our method and the French-Holden method, mean output/input and phase differences were 1.4 dB and 0.6 degrees, respectively.

3. Anastasio, T.J.; Correia, M.J.; Perachio, A.A. Spontaneous activity and driven responses of semicircular canal primary afferent neurons in the alert pigeon. Soc. Neurosci. Abstr. 9: 525; 1983.

Spontaneous and driven responses from a sample of 124 semicircular canal (SC) primary afferents were studied in a chronic, alert pigeon preparation and compared to responses previously obtained from a barbiturate anesthetized pigeon preparation. In the alert preparation, the spontaneous mean firing rate (n = 124) was found to be 168 impulses/sec. In contrast, the spontaneous MFR reported for a sample of 124 horizontal canal primary afferents from a barbiturate anesthetized pigeon preparation was 92 impulses/sec. (Lifschitz, W.S. Brain Res. 63: 43-57; 1973). In the alert pigeon, the spontaneous MFR is biased upward by 82.6%.

Four alert pigeons were subjected to two sets of sum of sinusoidal rotations over the bandwidth 0.029-6.152 Hz. Best-fit transfer functions were determined for 10 intermediate and 5 irregular SC primary afferents.

$$\text{int.} - H(s) = Gs^{1.14}(9.9s + 1)^{-1}(0.01s + 1)$$
$$\text{irr.} - H(s) = Gs^{1.10}(9.2s + 1)^{-1}(0.02s + 1)$$

The best-fit transfer function for 14 anterior ampullary afferents in the anesthetized pigeon across CV classes over the bandwidth 0.01-2.0 Hz was found to be (Landolt, J.P. and Correia, M.J. J. Neurophysiol. 43: 1749-1770; 1980)

$$H(s) = Gs^{1.24}(10.2s + 1)^{-1}$$

4. Perachio, A.A.; Correia, M.J.; Kevetter, G.A. Functional and morphological characteristics of gravity-sensitive primary canal afferents. Soc. Neurosci. Abstr. 9: 739; 1983.

In the anesthetized gerbil, a large percentage of physiologically identified lateral (71%) and anterior (48%) canal afferents respond to static changes in head tilt. In the decerebrated gerbil, significant changes in firing rate (> 10%) were also measured when the head was tilted + 10 degrees about the pitch (left/right head) axis. Afferents ($\bar{n}$ = 50) were also injected with HRP. As previously reported for the human and cat Scarpa's ganglion neurons (Kitamura and Kimura,

1982; Chat and Sans, 1979) multipolar neurons have been identified with branching axonal or peripheral (dendritic) processes. These results suggest a possible mechanism for converging inputs from different labyrinthine receptors or for feedback from central efferent axons on to vestibular ganglion cells.

C. Unpublished Results and Pilot Data

1. Analysis of primary afferent responses in the unanesthetized pigeon (Anastasio, Correia, and Perachio, in preparation).

Spontaneous activity was recorded from 120 semicircular canal (SC) primary afferents in 8 alert white king pigeons. Eighteen canal afferents in four alert pigeons were tested subsequently using angular rotation. During testing, each animal was blindfolded and restrained in a gimbaled test apparatus. Part of this apparatus was the U-frame of a stereotaxic holder (Fig. 1).

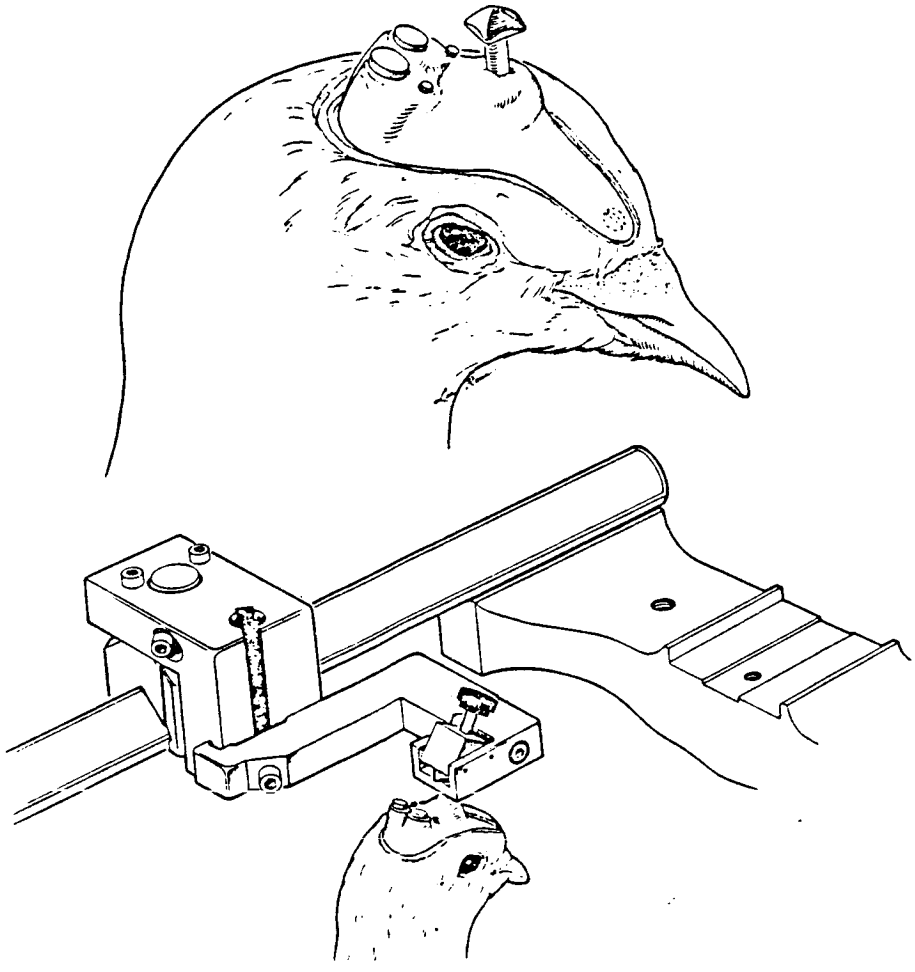

Figure 1

A schematic illustration of the method used to couple the alert pigeon preparation to the stereotaxic apparatus. This coupling occurs when a chronically implanted head bolt is secured to a modified carrier which is attached to one stereotaxic arm. Also shown in this figure are capped recording wells. At the time of the experiment, the caps are removed and a microelectrode is lowered through the well to intersect postganglionic vestibular primary afferents (histologically verified) as they course toward the brainstem.

The bird's head was coupled to the frame by an L-shaped bracket. The bracket was fastened to one arm of the stereotaxic U-frame by way of a stereotaxic carrier base and to the bird by clamping onto a stud which was chronically implanted on the bird's head (see insert Fig. 1). The stud was implanted so that when the bird's head was held by the L-shaped bracket, the horizontal SC's were in the stereotaxic horizontal plane and the bird's mid-sagittal head plane was coplanar with the mid-sagittal vertical plane of the stereotaxic U-frame. The head stud was chronically implanted on the pigeons skull by the following procedure. Slots were cut into the skull behind the eyes and two stainless steel #256 screws, whose heads had been machined flat, were inverted, inserted into the slots between the dura and the cranium and secured with nylon nuts. Near the front of the skull and at the base of the beak, a third #256 stainless steel screw was screwed into a naturally occurring triangular pocket of bone. These three screws were attached to the head stud using dental acrylic. Two holes (4 mm in diameter) were trephined into the skull at stereotaxic coordinates which were known to correspond to the entry point of a microelectrode tipped 10 degrees forward which would intersect the vestibular nerve in its medial course between Scarpa's ganglion and the vestibular nuclei. Pre-machined nylon tubes were tilted 10 degrees forward, placed over the holes in the cranium, and secured to the head stud and the anchoring screws by dental acrylic. It was determined empirically that the microelectrode had to track through the brain at a 10 degrees forward angle to miss a deep intracranial artery in the brain between the brain surface and the vestibular nerve. The nylon tubes were capped between recording sessions.

Single unit recordings were made using slender (0.2 mm) glass microelectrodes (Perachio and Correia, in press, 1983a) carried inside a stainless steel guide tube (26 gauge). The guide tube, with the micropipette inside, was lowered to a position 2 mm above the vestibular nerve and the micropipette was then advanced toward the nerve with a hydraulic microdrive. The micropipettes, filled with either 2 or 3 M NaCl, routinely had tip diameters ranging beween 1 and 2 um and impedance values between 6 and 12 Mohms (measured at 1 KHz).

The gimballed superstructure which held the animal was mounted on the platform of a Contraves-Goertz model #823 rate table. In the "standard position," the pigeon's horizontal SC's were coplanar with the earth's horizontal plane of rotation. The animal could be manually rotated or statically tilted to any angle between $\pm$ 90 degrees in either pitch or roll. Once an afferent was physiologically identified (Blanks and Precht, 1976; Perachio and Correia, 1983b) by a series of pitches, rolls, and yaws as an anterior, posterior, or horizontal ampullary afferent, it was tested. To test the vertical ampullary afferents, the animal was rolled 90 degrees, placing the sagittal head plane in the plane of rotation, and rotated about an earth vertical axis. To test the horizontal SC's the animal was yawed about an earth vertical axis. Rotational stimuli included two single sinusoidal rotations and two bandwidths of sum of sinusoidal rotations. The low and high frequency single sinusoidal rotation stimuli were at 0.147 and 1.465 Hz, respectively. The low and high bandwidth sum of sinusoidal rotational stimuli ranged from 0.029-0.615 Hz and 0.293-6.152 Hz, respectively. The reference signals for these rotational stimuli were produced by a programmable ROM function generator (Kemmerer et al., unpublished method). Tachometer output

served as the rotational stimulus signal with which the responses of SC primary afferents were compared. Peak velocity of each frequency was pre-programmed to be 20 deg/sec. A linear accelerometer (Entran EGC 240-SD) was mounted on the animal holder (off-center) and tests were made of phase error of the tachometer signal re the tangential linear acceleration signal. Phase errors ranged from 3.98 degrees. at 0.029 Hz to -1.38 degrees at 6.15 Hz.

Spontaneous activity was gathered from horizontal canal units with the animal in the standard position. Spontaneous activity was gathered from vertical canal units with the animal in the standard position or rolled 90 degrees (right ear down). Neural activity was amplified by conventional electronics and tape recorded for off-line analysis. The bandwidth of the amplification and recording system was 100 Hz-10 kHz.

All data were analyzed off-line using a DEC PDP 11/20 minicomputer. The mean, standard deviation (SD), coefficients of variation (CV), skewness (B1), and kurtosis (B2) (Pearson and Hartley, 1976) were calculated using 1024 interspike intervals (ISI's) (measured with 10 us resolution) from a segment of spontaneous activity. Responses to rotation were analyzed using two methods. In the first method, cyclic histograms of binned impulse frequency were formed. Either a single sign or sum of sinusoids were fit through the histogram using a least-square algorithm. Phase relations and amplitude ratios were calculated between the digitized tachometer signal and the best-fit curve to the cyclic histogram response. The second method consisted of using an analog filter to convert the modulated AP train into a smoothly modulated DC voltage (Kemmerer et al., 1981). Amplitude ratio and phase relationships were calculated between this signal and the tachometer signal using cross spectral Fourier techniques (Ni et al., 1978). No significant difference was found between the amplitude ratios and phase values using either method (Mann Whitney U statistic, $P > 0.05$). The results presented below used the cyclic histogram method of analysis. Transfer functions were fit to the AR and phase values using a nonlinear least squares method (Brassard et al., 1974).

Additionally, 26 units were tested using the tilt paradigm described in Perachio and Correia (1983b). Activity was recorded with the pigeon in the standard position and then pitched $\pm$ 10 degrees or $\pm$ 30 degrees. A segment of 1024 intervals was analyzed following 30 sec of tilt in one of these positions. Mean firing and other first order statistics of activity gathered under each of these static tilt conditions were compared with activity gathered while the animal was in the standard position (horizontal SC's coplanar with the earth's horizontal plane).

Analysis of spontaneous discharge was performed on 120 SC primary afferent neurons from eight alert pigeons. Of these, there were 31 horizontal, 82 anterior, and 7 posterior afferents. No significant difference was observed, when comparisons were made between spontaneous activity, mean ISI for the following SC combinations: anterior versus horizontal ($t = 0.28$, $df = 111$, $P > 0.7$); anterior versus posterior ($t = 1.05$, $df = 87$, $P > 0.2$); horizontal versus posterior ($t = 1.06$, $df = 36$, $P > 0.1$). Spontaneous activity was gathered from 21 of the 82 anterior afferents while the animal was maintained in a 90 deg roll right posi-

tion. No significant difference ($t = 0.82$, $df = 80$, $P > 0.4$) between mean ISI was noted for spontaneous activity gathered in this tilted position when compared to that gathered when the animal was tested in the standard position. The tilted anterior afferent's spontaneous data were pooled with that gathered in the standard position. This pooled data were then combined with that gathered from horizontal and posterior afferents and a histogram of the distribution of spontaneous MFR's (the reciprocal of mean ISI's) for the alert pigeon preparation is presented in Fig. 2A.

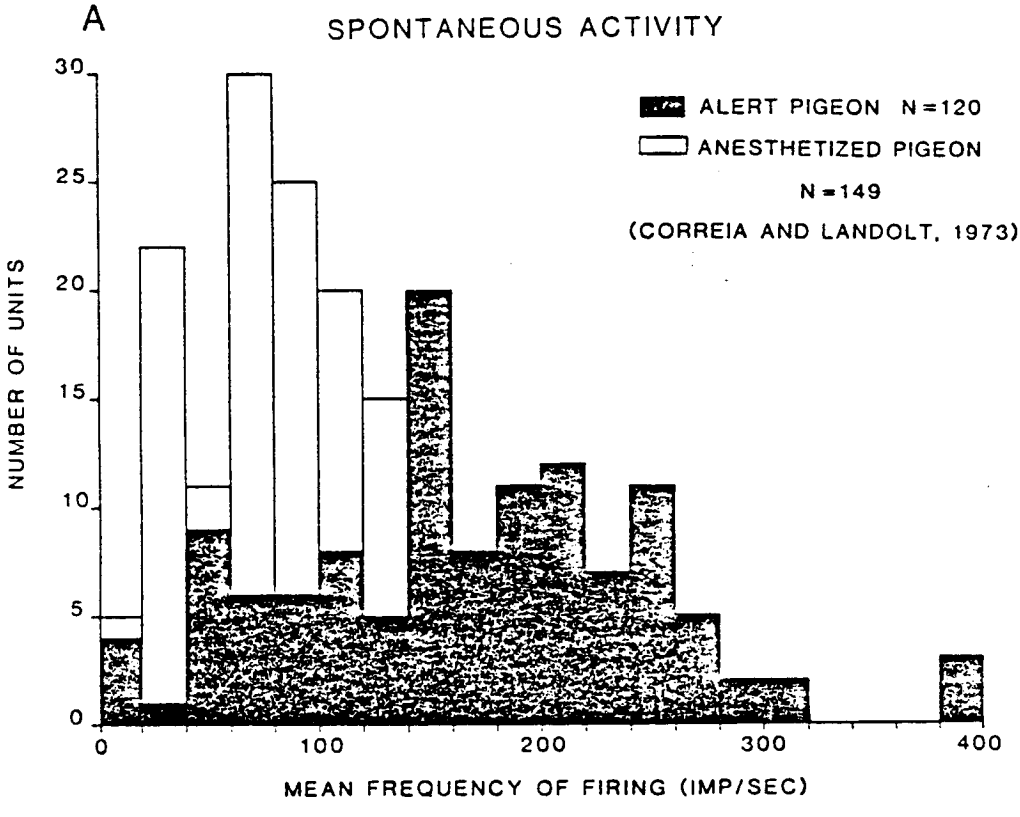

Figure 2A

A histogram of mean frequency of firing (imp/sec) for 120 primary afferents in the alert pigeon preparation (shaded). These data overlay a distribution of mean frequency of firing (imp/sec) for 149 vestibular primary afferents obtained from a barbiturate anesthetized pigeon preparation (unshaded). In this figure it can be seen that the mean frequency of firing is clearly higher in the alert pigeon preparation.

From this figure it can be seen that the mode MFR fell in bin 140-160 imp/sec. The mean of the MFR was determined to be 167.6 imp/sec $\pm$ 7.3 (SEM). The median MFR was 161.4 imp/sec. Individual MFR values varied

from 8 to 396 imp/sec. For comparison, also presented in Fig. 2A is a distribution of spontaneous MFR's from a sample of 149 anterior SC afferents from barbiturate anesthetized pigeons (Correia and Landolt, 1973). Spontaneous discharge was gathered from anterior ampullary afferents using metal microelectrodes with the pigeons rolled 90 degrees from the standard position. The spontaneous MFR for the anterior ampullary afferents was 93.3 imp/sec $\pm$ 5.3 (SEM). Lifschitz (1973), using glass micropipettes studied the spontaneous activity of 124 horizontal ampullary afferents in the barbiturate anesthetized pigeon tested in the standard position. He found the mean MFR to be 92 imp/sec. The mean MFR for the alert preparation data shown in Fig. 2A, was compared with the mean MFR for the barbiturate anesthetized data also shown in Fig. 2A. The alert mean MFR was significantly faster than the mean MFR for the anesthetized data ($t = 11.82$, $df = 267$, $P < 0.005$, one tailed test).

Figure 2B presents the distribution of CV's of SC primary afferents. Coefficients of variation ranged from 0.06 to 1.40. Arrows indicate arbitrary divisions of the distribution in the three categories of "regularity of firing." An afferent was considered to be regular if its CV was less than 0.1; as irregular if its CV was greater than or equal to 0.4; and as intermediate if its CV value was greater than or equal to 0.1 and less than 0.4. Using this division, 35/120 (29%) were classified as regular; 37/120 (31%) were classified as irregular; 48/120 (40%) were classified as intermediate. Lifschitz (1973) studied the CV distribution of 122 horizontal SC afferents from the barbiturate anesthetized pigeon preparation; 36/122 (29%) had CV's < 0.1; 46/122 (38%) had $0.1 <$ CV's ≤ 0.4; and 40/122 (33%) had CV's > 0.4. A distribution of these data are also presented in Fig. 2B.

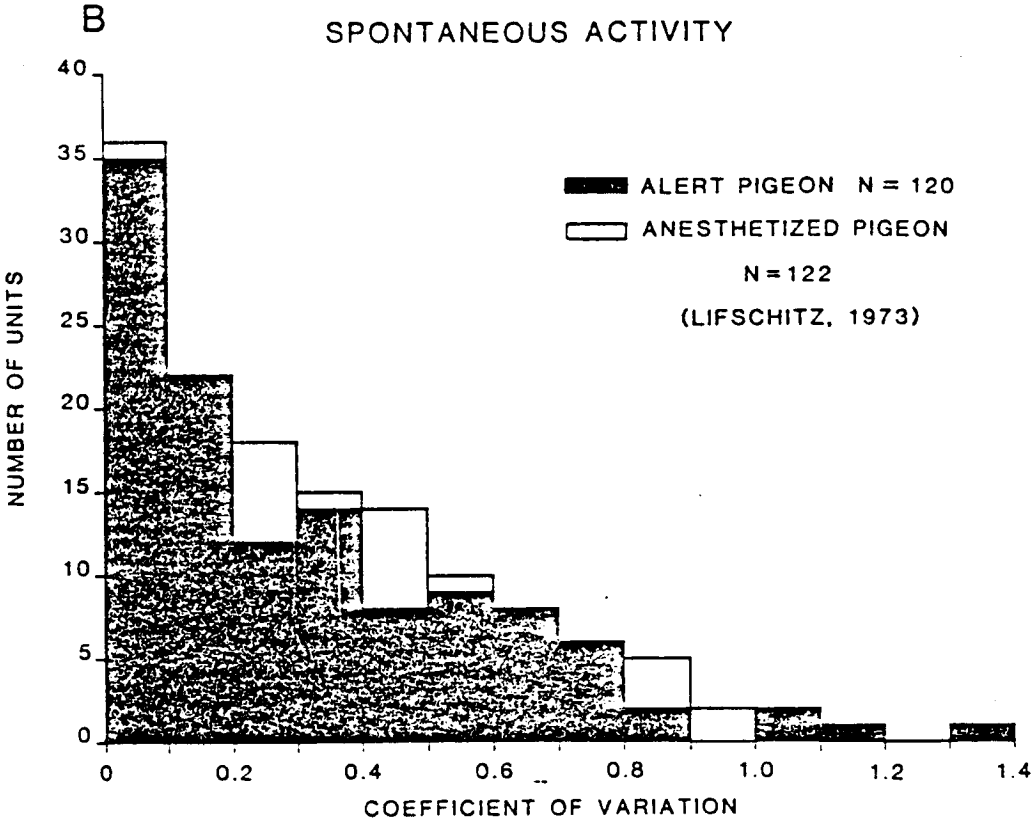

Figure 2B

A distribution of coefficient of variation for spontaneous activity in 120 vestibular primary afferents in the alert pigeon (shaded). This distribution overlays a distribution of coefficient of variation for 122 vestibular primary afferents in the anesthetized pigeon preparation (unshaded). Since the mean firing rate in the alert pigeon preparation is clearly higher than that of the anesthetized pigeon preparation (Fig. 2A) but the coefficient of variation is the same (Fig. 2B), the standard deviation (SD) must decrease proportionally with the increase in mean frequency of firing.

A scatter plot of mean ISI against SD (based on 1024 intervals) for 120 ampullary afferents from the unanesthetized pigeon is plotted in Fig. 2C. Also presented in this figure is the best-fit power function and 99% tolerance limits (Wiesberg and Batey, 1960). A best-fit power function provided a significantly better fit to these data than a best-fit straight line ($t = 8.60$, $df = 118$, $P < 0.01$; Williams and Klut

test). The equation and correlation coefficient (r) for the power function fit was: $SD = 0.049\ (ISI)^{1.769}$; r = 0.86. Correia and Landolt (1978) regressed mean ISI against SD for 51 anterior ampullary afferents in the anesthetized pigeon. The best-fit power function which fit those data was described by the equation: $SD = 0.072\ ISI^{(1.527 \pm 0.157)}$; r = 0.81.

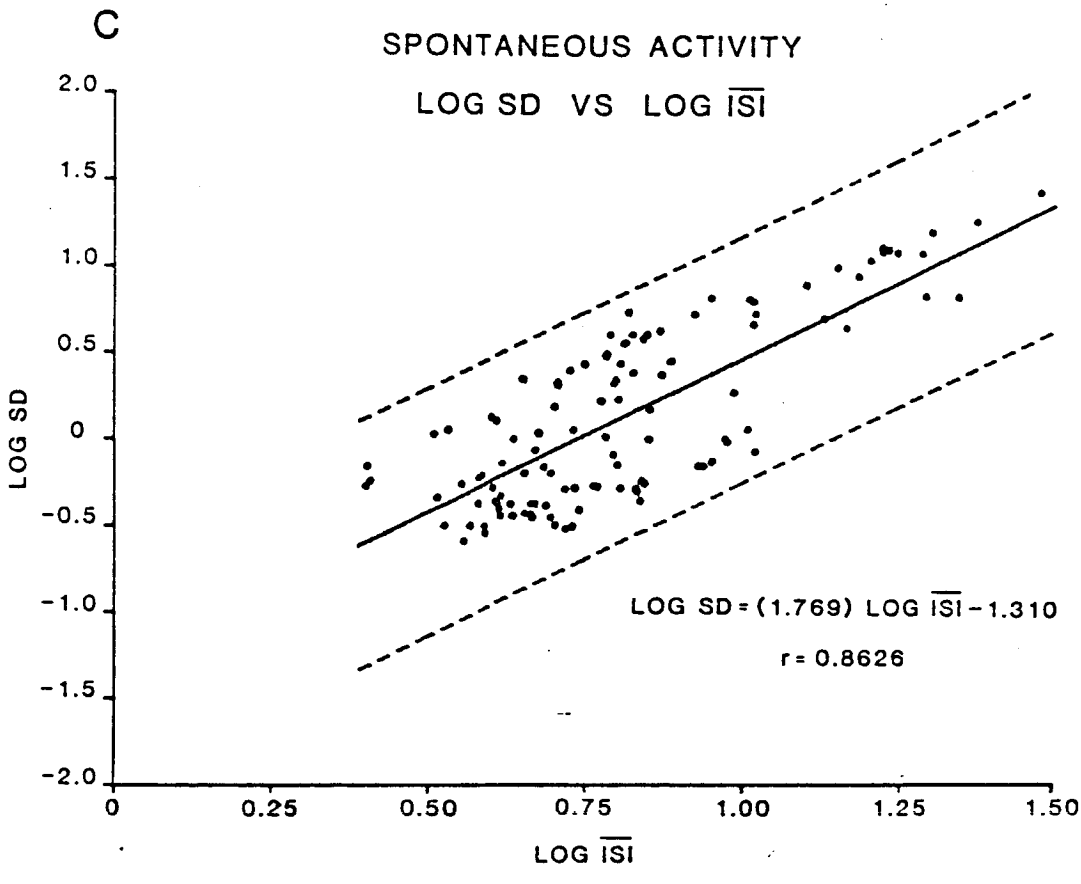

Figure 2C

A plot of the relation of standard deviation and mean interspike interval (reciprocal of mean frequency of firing) for the alert pigeon preparation. The power function relationship between standard deviation and mean interspike interval is illustrated by the straight line regression of log SD versus log mean interspike interval. The parameters of the equation shown in this figure and the correlation coefficient of the best-fit straight linear regression line are very similar to those determined for these variables in the barbiturate anesthetized pigeon (Correia and Landolt, 1978). The dashed lines in this figure represents 99% tolerancce limits on the regressed data.

Figure 2D is a scatter plot of the coefficient of skewness (B1) against the coefficient of excess (B2-3) (coefficient of kurtosis (B2) -3.0).

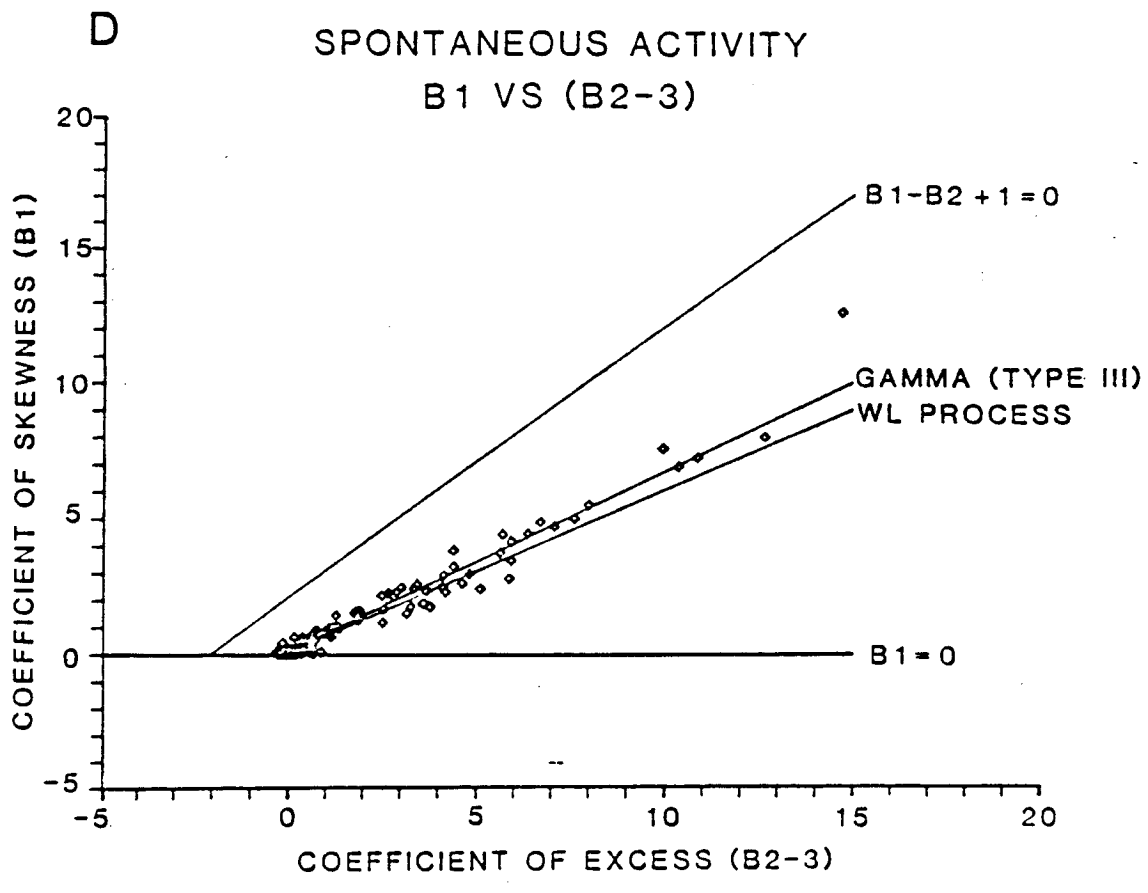

Figure 2D

A linear-linear plot of the coefficient of skewness (B1) versus the coefficient of excess (coefficient of kurtosis (B2)-3). These data represent points derived from 120 vestibular primary afferents in the alert pigeon preparation. It can be seen in this figure that a large number of points are concentrated near coordinates (0,0). These coordinates correspond to those which are associated with the normal distribution. However, it can also be noted that the remaining points align themselves along a straight line which have been identified with the family of probability density functions associated with the gamma and Wiener-Levy processes.

It can be seen that the values of B1 plotted against B2-3 align themselves along a straight line. Also it can be seen that a large percentage of values are clustered around coordinates (0,0). Pearson and Hartley (1970) have shown that these coordinates are those of a normal distribu-

tion probability density function. Two families of probability density function (pdf) distributions are described by straight lines in the B1 vs. B2-3 plot which are close to the straight line of points which we have plotted in Fig. 2D. These pdf's are the family of gamma distributions and the family of distributions describing the first passage times of particles undergoing Brownian motion as they pass through an absorbent barrier (the Wiener-Levy process). Correia and Landolt (1978) plotted B1 vs. B2-3 for anesthetized pigeon primary afferent spontaneous discharge. They noted the same pattern as shown in Fig. 2D but the points were more scattered. However, this difference could be due to measurement resolution. Correia and Landolt (1978) measured the ISI's using 1 ms resolution; the data in Fig. 2D was gathered measuring ISI's with 10us resolution.

In summary, it appears that the major difference between spontaneous discharge on SC primary afferents in the alert pigeon preparation when compared with the barbiturate anesthetized pigeon preparation is an 83% increase in the MFR for the alert (unanesthetized) pigeon preparation.

Figures 3A and B present Bode plots of the driven responses from 10 intermediate and 5 irregular SC primary afferents.

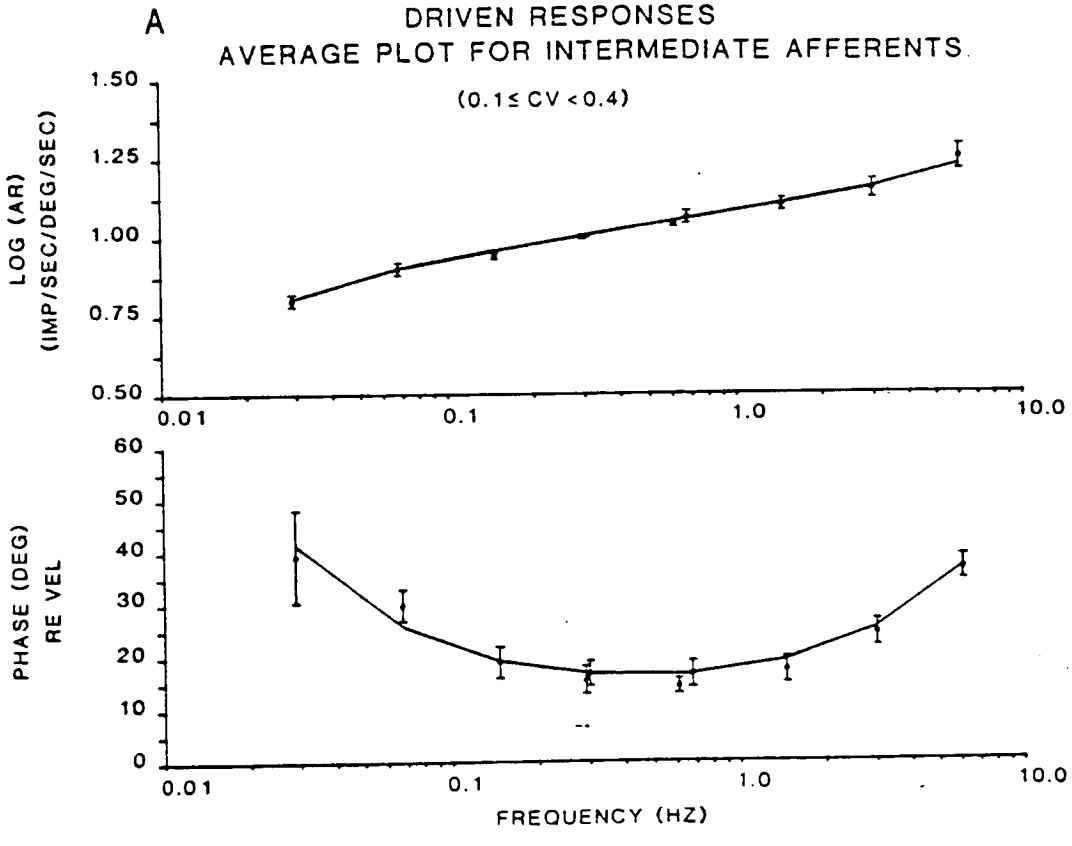

Figure 3A

A Bode plot of mean log AR and phase re velocity over the bandwidth from 0.029 Hz to 6.152 Hz. Units included in the average plot in this figure had coefficients of variation for their spontaneous activity which ranged between 0.1 and 0.4.

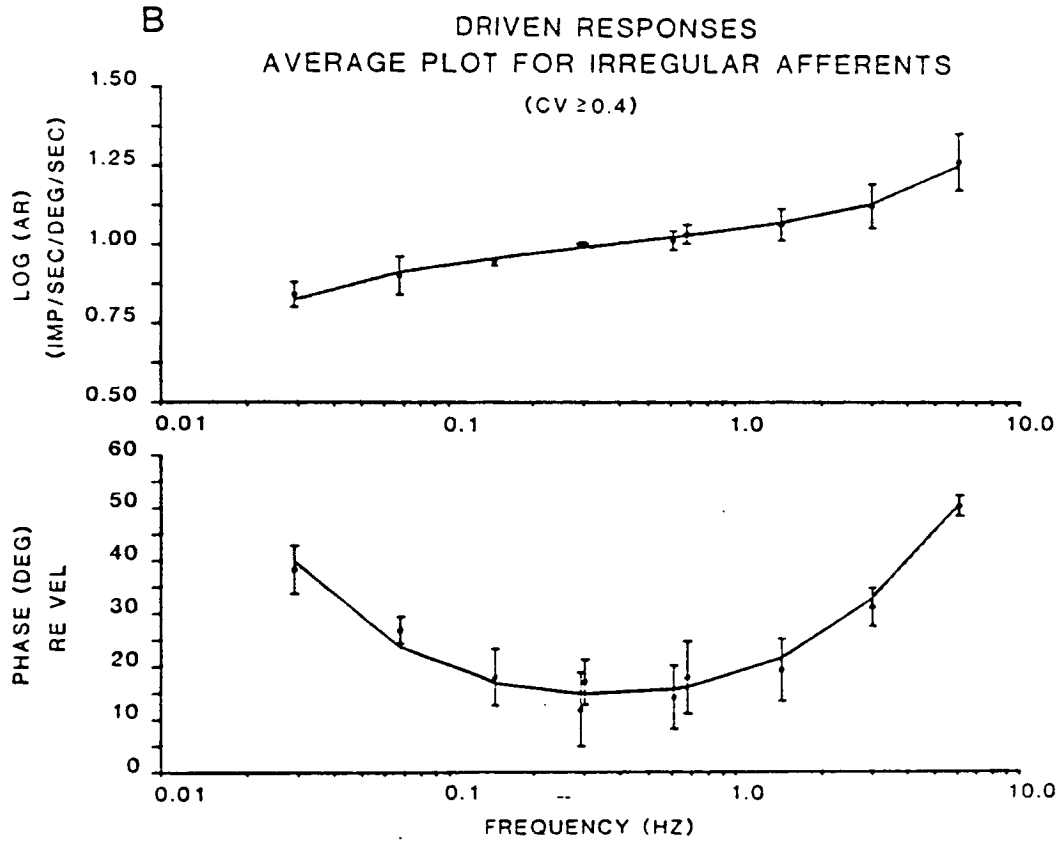

Figure 3B

A Bode plot (with same axes as Fig. 3A) of average data for vestibular primary afferents in the alert pigeon preparation whose coefficient of variation of their spontaneous discharge was > 0.4. As expected, these data show a greater gain enhancement and phase advance at higher frequencies than those illustrated in Fig. 3A.

Best-fit transfer functions based on the data in Figs. 3A and B and associated mean square errors (MSE's) are:

$$\text{int.} - H(s) = Gs^{1.14}(9.9s + 1)^{-1}(0.01s + 1), \quad MSE = 0.11;$$

$$\text{irr.} - H(s) = Gs^{1.10}(9.2s + 1)^{-1}(0.02s + 1), \quad MSE = 0.12.$$

By comparison, Landolt and Correia (1980) determined the mean best-fit transfer function for 14 ampullary afferents in the barbiturate anesthetized pigeon across CV classes over the bandwidth 0.01 to 2.0 Hz. That equation is presented below:

$$H(s) = Gs^{1.24}(10.2s + 1)^{-1}.$$

Although the number of units tested for both the anesthetized and alert pigeon preparation is small, the following suggestions can be made. The so-called "cupula long-time constant" (see review - Correia et al., 1981) is not different for the alert pigeon preparation when compared to the barbiturate anesthetized pigeon preparation (9 sec vis-a-vis 10 sec). As for squirrel monkey (for example, Fernandez and Goldberg, 1971), at high frequencies, a gain enhancement and phase advance exists for intermediate and irregular units. In the pigeon, this operator appears to take effect over the bandwidth 2-6 Hz. Sensory adaptation (see, for example, Correia et al., 1981; Schneider and Anderson, 1974) appears to be less in the alert pigeon preparation when compared with the mean value derived from the best-fit for anterior ampullary afferents in the anesthetized pigeon (Landolt and Correia, 1980). The part of the fractional exponent of s in the transfer function which has been related to adaptation was 0.24 (mean across CV categories) for anesthetized pigeon and 0.14 for intermediate units; 0.10 for irregular units in the alert pigeon..

Gain was compared at 0.292 Hz from equations presented above. It was determined that at 0.292 Hz gain for the anesthetized pigeon was 2.9 imp/sec/deg/sec and for the unanesthetized pigeon 3.1 imp/sec/deg/sec.

Table 1 summarizes the tilt responses of SC primary afferents in the unanesthetized pigeon preparation.

Table 1
TILT SENSITIVITY OF SEMICIRCULAR CANAL PRIMARY AFFERENTS IN ALERT PIGEONS

Afferent type	Degree of tilt	Number of units tested	Number of tilt sensitive units	% of tilt sensitive unit
lateral	10	15	8	53.3%
lateral	30	9	6	66.7%
anterior	10	11	5	45.5%
anterior	30	4	4	100.0%

Units were tested during head pitch tilts of ± 10 degrees and/or zero degree tilt position and in at least one other head tilt position. Units were considered tilt sensitive if their discharge rate in a 10 degree or 30 degree tilt position differed by 10% or more from their discharge rate in the zero degree tilt position.

It can be seen from this table that 26 ampullary afferents (15 horizontal, 11 anterior) were tested at ± 10 degrees and ± 30 degrees pitch tilt. For ± 10 degrees pitch tilt 8/15 horizontal and 5/11 anterior afferents had MFR's which differed from those in the standard position by least 10%. This result extends the findings of Perachio and Correia (1983b) who, using similar methods, have demonstrated the same tilt response in the anesthetized and decerebrate gerbil.

2. Development of a method for a chronic implantable bipolar stimulating electrode in the labyrinth of an unanesthetized pigeon (Hoddeson, Cooper, and Correia, unpublished observations).

Ten pigeons were used to develop a method to produce a chronic implantable bipolar stimulating electrode within the pigeon's bony labyrinth. On the day of surgery, each animal was deeply anesthetized with a combination of nembutal and ketamine. The bony labyrinth

was exposed using a post auricular approach (Correia et al., 1973). An attempt was made to remove a minimum number of bony air cells and yet clearly visualize the labyrinthine structures that was the target site of the stimulating electrode. Electrodes were successfully implanted proximal to the lateral and posterior ampulla as well as over the vestibule. Once the labyrinthine target site was visualized, two stainless steel tubes (26 gauge) are each positioned by a micromanipulator just over (1/2 mm) but not touching the bony labyrintine structure. The bony skull defect was then reconstructed with dental acrylic so as to hold each guide tube (separated by 1/2 mm) in place. After the second guide tube was secured in place and the entire skull reconstructed, the skin flap which was reflected during the first phase of the surgery, was replaced over the reconstructed skull and the two guide tubes were exteriorized through the skin. Prior to this surgery, each animal had received the head holding device implant shown in Fig. 1. The method of guide tube implants just described, avoids any bone erosion or foreign body reaction since the stainless steel guide tubes do not touch any part of the animal's labyrinth or skull bone. Our animals appear to tolerate this implant well and two pigeons have surived for five months without any observable adverse affects of having the guide tube implants. On the day of the experiment, two prefabricated stimulating electrodes were lowered through the guide tubes to touch the bony labyrinth. These stimulating electrodes consisted of teflon-coated silver wire (0.10 mils thick). The insulation had been removed from 0.2 mm of the end of the silver wire and this surface had been silver-silver chlorided. The opposite ends of the wire had been soldered into a small plug which was attached to the head restraint device using dental acrylic. The resistance through the stimulating electrodes was measured as they were lowered through the guide tubes. We concluded that we had made contact with the bony labyrinth when: a) resistance values were no longer infinite but reached a typical value of about 10,000 ohms and b) after traveling through the guide tube a premeasured distance we could feel pressure against the wire after proper electrical mechanical contact was assured. The electrodes were then tacked into the guide tubes with dental cement. Using these electrodes we have been able to orthodromically drive neurons in the lateral vestibular nucleus and produce nystagmic responses from the alert pigeon using electrical pulse trains and DC polarizing currents. At the end of the experiment, the stimulating electrodes were removed from the guide tubes. For subsequent experiments, the procedure was repeated, that is, a new set of stimulating electrodes were reinstalled through the guide tubes to touch the membranous labyrinth and the stimulating paradigm was repeated.

3. Single unit neural responses in the lateral vestibular nucleus to intracardiac injection of scopolamine (Hoddeson and Correia, unpublished observations).

Six pigeons were selected and implanted with head holders and recording wells (Fig. 1). Three of these pigeons received indwelling

labyrinthine stimulating electrodes and two then received indwelling venus catheters. The catheters consisted of silastic tubing 0.020 x 0.037 in. The tubing was inserted through the medial wing vein and advanced toward the heart. The catheter was advanced 7 cm and stopped when blood pulsation could be visualized in the catheter. Subsequent postmortem examination of on one pigeon indicated that the catheter had been positioned in the animal's right atrium. The catheter, attached to a capped syringe needle was then sutured to the pigeon's wing and the pigeon was returned to its cage. After several days, each pigeon with an indwelling venus catheter, and an indwelling labyrinthine stimulating electrode (as described in last section), was installed into a stereotaxic apparatus. Single unit recordings were obtained from neurons in the lateral vestibular nucleus of the alert pigeon using the methods described in section II.C.1. These neurons were physiologically characterized as responding to yaw angular rotations and tilt. Then DC current steps were applied to the labyrinth (Lifschitz, 1973). This electrical stimulation produced an increase or decrease in firing rate depending upon the polarity of stimulation.

A typical single unit response from a lateral vestibular neuron responsive to yaw acceleration (type I) is shown in Fig. 4A.

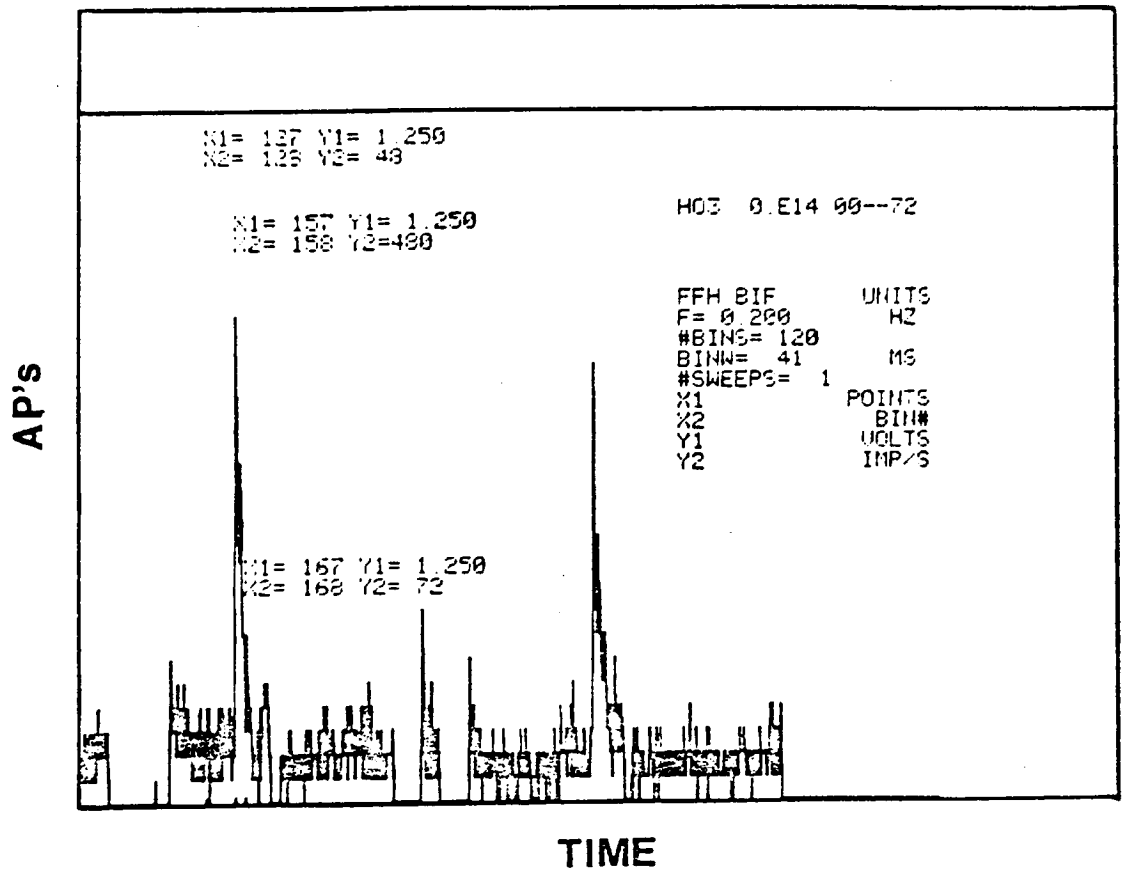

Figure 4A

A photograph of a hard copy of a video terminal display of a frequency of firing histogram of a single lateral vestibular nucleus neuron's response to step-current-electrical stimulation of the labyrinth in the alert pigeon. A comparison of the Y2 values indicates that electrical stimulation increased the firing rate from a spontaneous level of 48 imp/sec to 480 imp/sec. Although constant step current stimulation was provided, the mean firing rate fell to within one-half of its peak value in the next 0.241 sec.

The frequency of firing histogram illustrates that application of the step polarization current was followed by an increase in activity which immediately decayed even through stimulation was still applied. The experimental paradigm was repeated for the same unit but 10 min. after 0.173 mg of scopolamine had been administered intraveinously.

Figure 4B presents the frequency of firing histogram for the same neuron as presented in Fig. 4A during electrical stimulation but following drug injection.

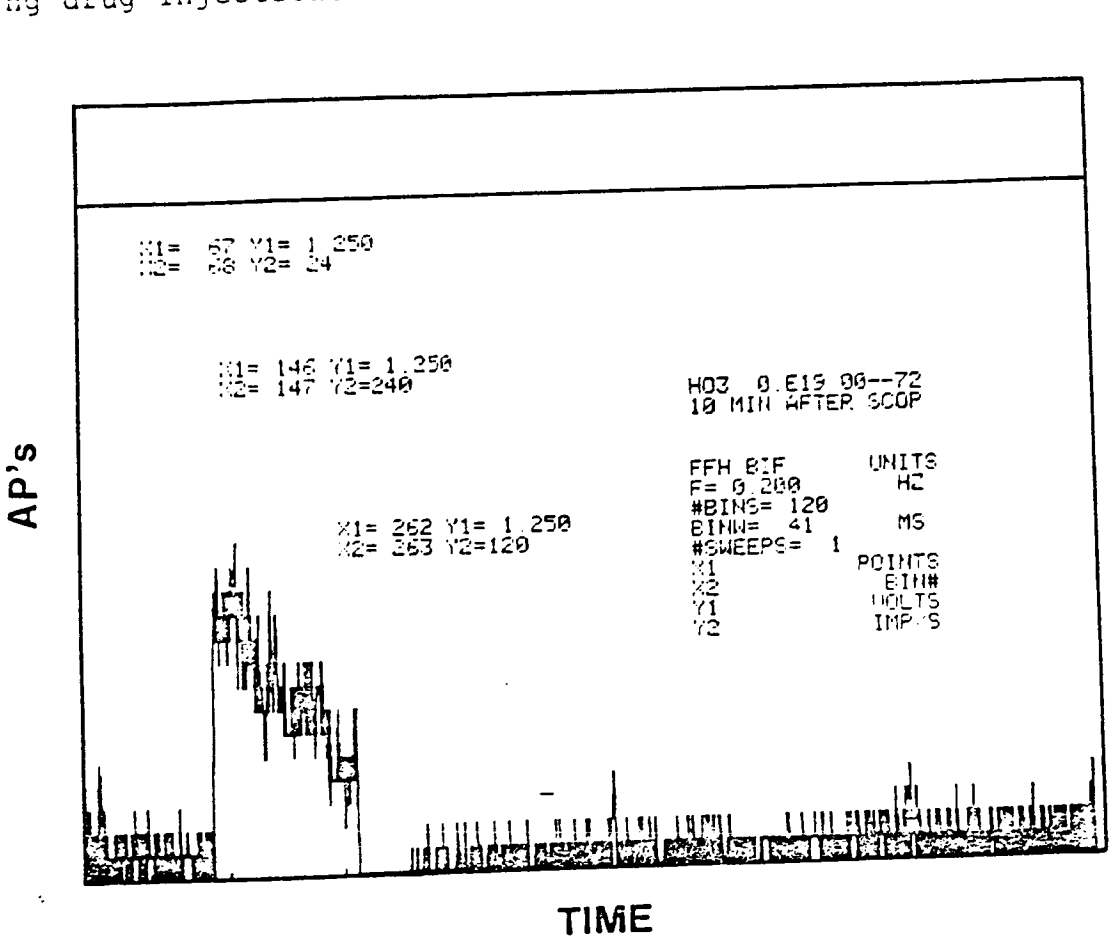

Figure 4B

A frequency of firing histogram for the same lateral vestibular nucleus neuron depicted in Fig. 4A, except that this frequency of firing histogram was produced 10 minutes after intracardiac injection of 0.173 mg of scopolamine. The spontaneous firing rate is reduced to 24 imp/sec. This spontaneous rate is also increased 10 fold by current-step-electrical stimulation of the labyrinth. However, in contrast to the data presented in Fig. 4A, frequency of firing during constant electrical stimulation did not decrease to one-half amplitude until 4.64 sec. This decay rate is 19 times that noted for the same neuron in the pre-scopolamine-injection condition.

Prior to injection of scopolamine, the binned frequency of firing decayed to half value in 241 ms after the step current was applied to the labyrinth. Ten minutes following injection of the scopolamine, the time to half amplitude was lengthened to 4.64 sec-a change of 19 times. Since

electrical stimulation of the labyrinth presumably bypasses the mechanical part of the cupula-endolymph system, it would seem that this preliminary pilot data suggests that scopolamine either affects the nature of convergence of neurons onto vestibular nuclei cells or modifies the process involved in sensory adaptation of the end organ receptor itself. In a later section, we will propose to examine this phenomenon (first at the level of the primary afferents) in a more detailed and controlled set of experiments.

4. Scanning and TEM of Scarpa's ganglion and the vestibular neuroepithelium of the pigeon (Rae, Eden, Landolt, and Correia - unpublished observations).

We (Landolt et al., 1975) examined the morphology and geometry of neural surfaces and structures associated with the vestibular apparatus of the pigeon. We used scanning electron microscopy (SEM) and examined among other things, Scarpa's ganglion (SG). We noted that in SG (Fig. 5 below - Fig. 8A, Landolt et al., 1975) thin fibers of unknown origin which eminated from an axon and a cell body and which terminated as pods (P) on other cell bodies.

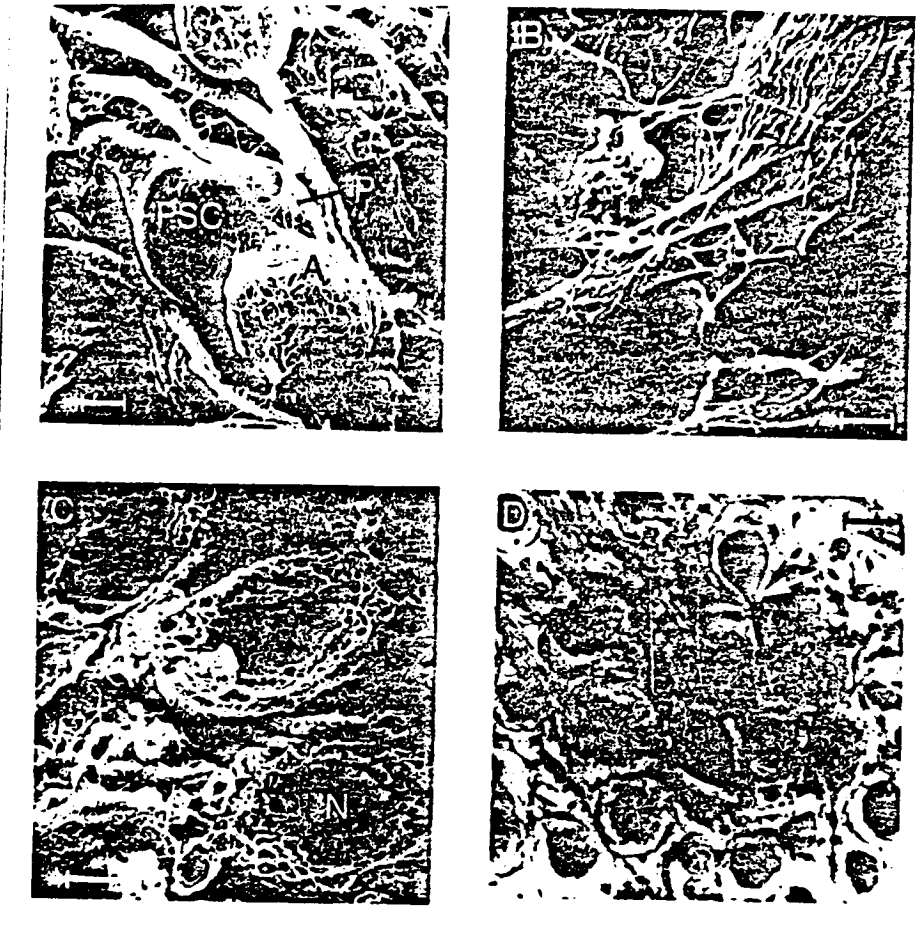

Figure 5

A collage of photomicrographs of the pigeon's vestibular ganglion. Figures 5A-C are SEM photomicrographs; Figure 5D is a light photomicrograph. In these figures it can be seen that although cells appear to be myelinated (Fig. 5C) pod-like attachments (P) can be observed on ganglionic cell bodies (Fig. 5A).

These structures suggested to us that there might be synaptic processes in SG. However, using freeze-fracture techniques and SEM, it appeared to us that the majority of the cells in SG were myelinated. To try to understand if there could some mechanism whereby synaptic contact could occur in SG between myelinated cell bodies, we extended these studies using TEM.

Figure 6 shows a low power TEM photomicrograph of a myelinated SG cell body and Fig. 7 shows a high power TEM photomicrograph of an axonal process apparently inside the mylin sheath of a cell body with an interposing thick membrane reminiscent of chemical synaptic processes but with no synaptic vesicles.

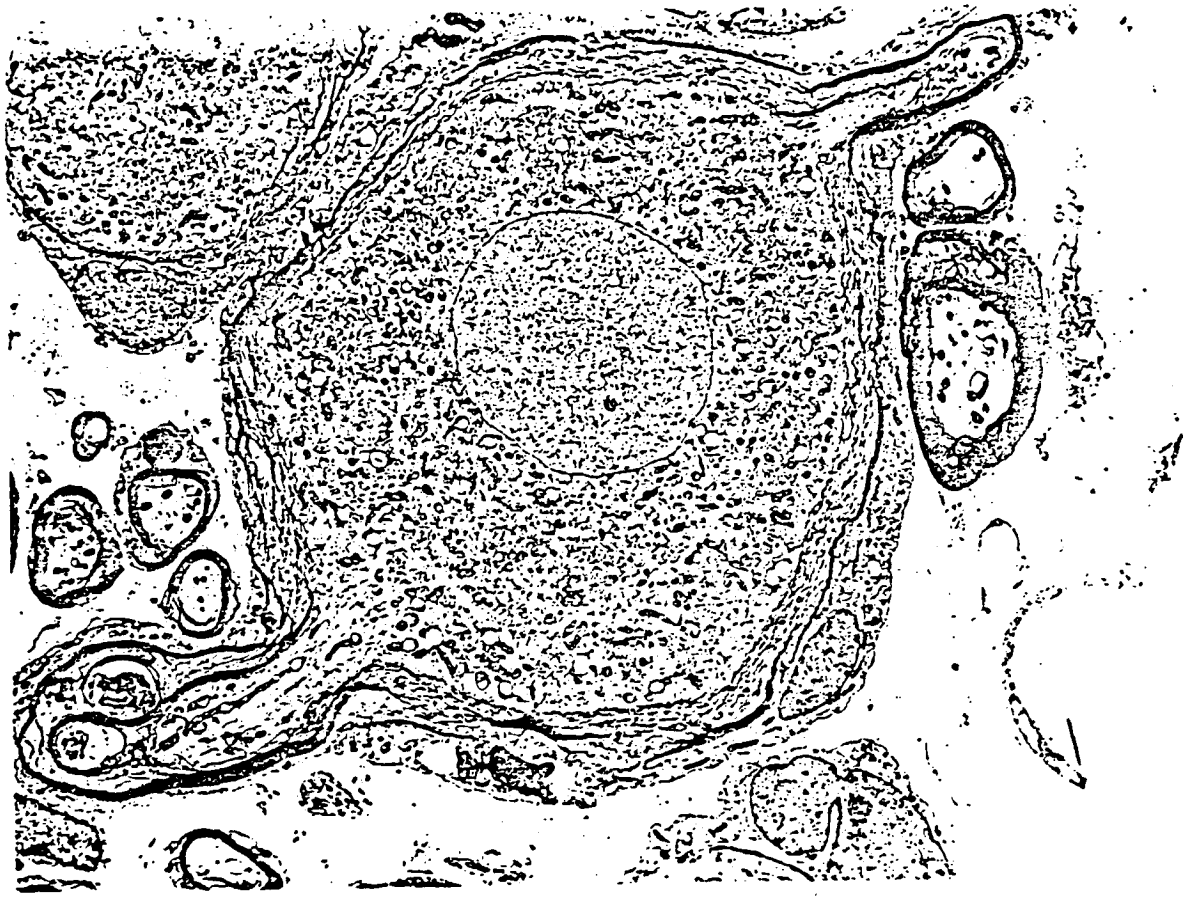

Figure 6

A TEM photomicrograph of a bipolar ganglion cell in the pigeon's vestibular ganglion. Myelin can be seen surrounding the cell body and its two axons. No synpatic processes were noted proximal to this cell.

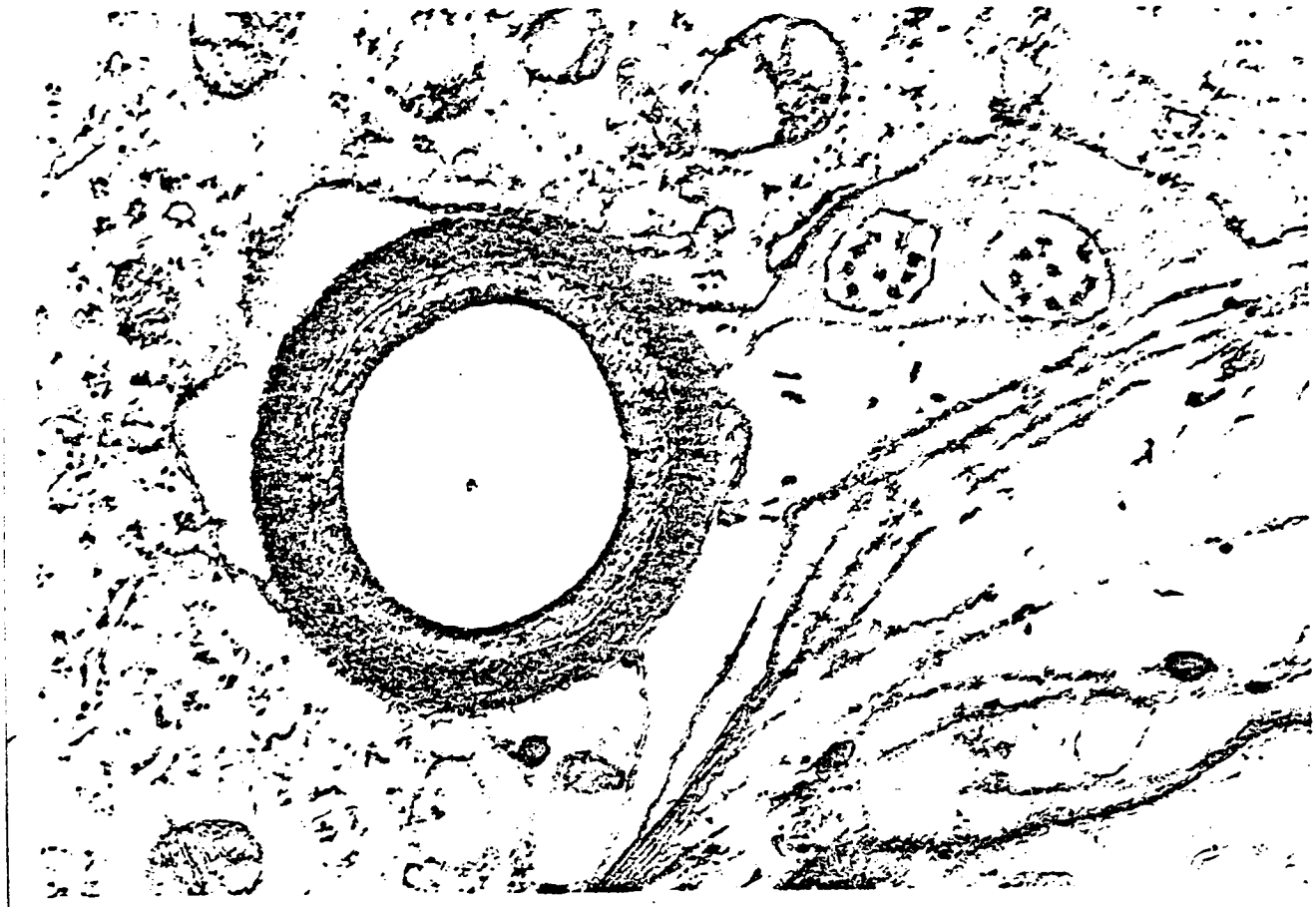

Figure 7

A high power TEM photomicrograph showing an axon which passes inside the myelin sheath of an adjacent vestibular ganglion cell. The axon extrudes a process which contains unidentified bodies but which makes contact with the soma of the adjacent ganglion cell, in part, through a thickened membrane.

We did not pursue these investigations since we assumed that all of the pigeon SG cell bodies were myelinated and we could find few precedents for synapses onto myelinated cell bodies. We wish to reopen these investigations in light of recent interesting findings. Kitamura and Kimura (1983) have shown that in one human, the majority of SG cells are unmyelinated and a certain percentage of them are multipolar and make synaptic contact with other cells in SG. There is an accumulating literature which suggests that multipolar cells may exist in SG in species other than man (cat - Chat and Sans, 1979; gerbil - Perachio et al., 1983).

For several years, we have also been studying the sensory neuroepithelium of the pigeon's crista ampullaris. We have been studying the distribution and number of type I hair cells contained in a given

calyx. Figure 8A presents a low power TEM photomicrograph of a cross section through an epon embedded crista ampullaris of the pigeon.

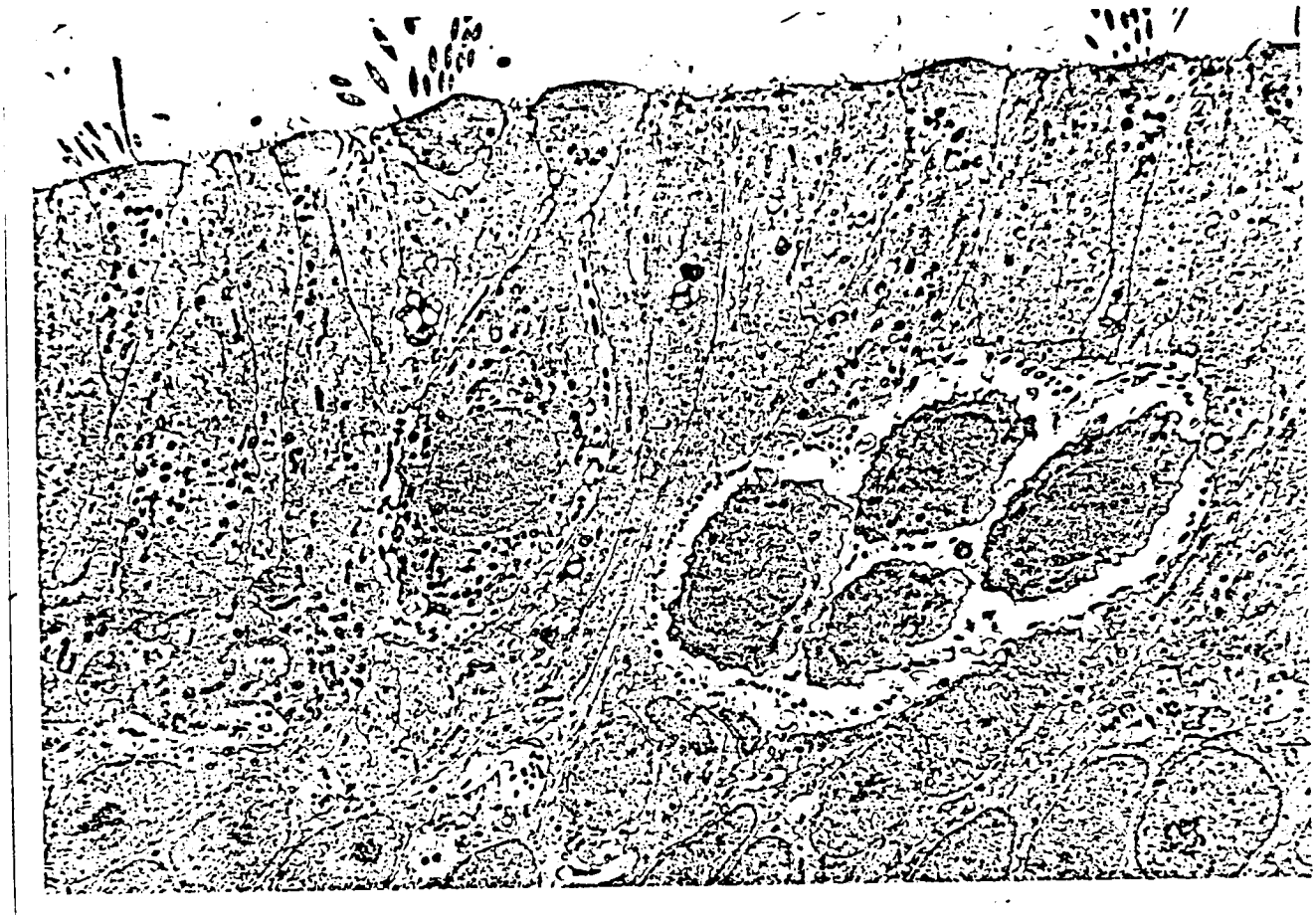

Figure 8A

A TEM photomicrograph through the crista ampullaris of the pigeon. This photomicrograph illustrates the variation of hair cells seen in a given region in the sensory neuroepithelium. In this figure, a type II hair cell, a single type I hair cell, and 4 hair cells contained within a single type I nerve calyx can be identified. Also, boutons containing dense spherical synaptic vescicles can be noted proximal to each of these three types of hair cells.

It can be seen from this figure and Fig. 8B (a photomicrograph of the crista using interference light microscopy) that in the pigeon, multiple hair cells are contained within a single neural calyx.

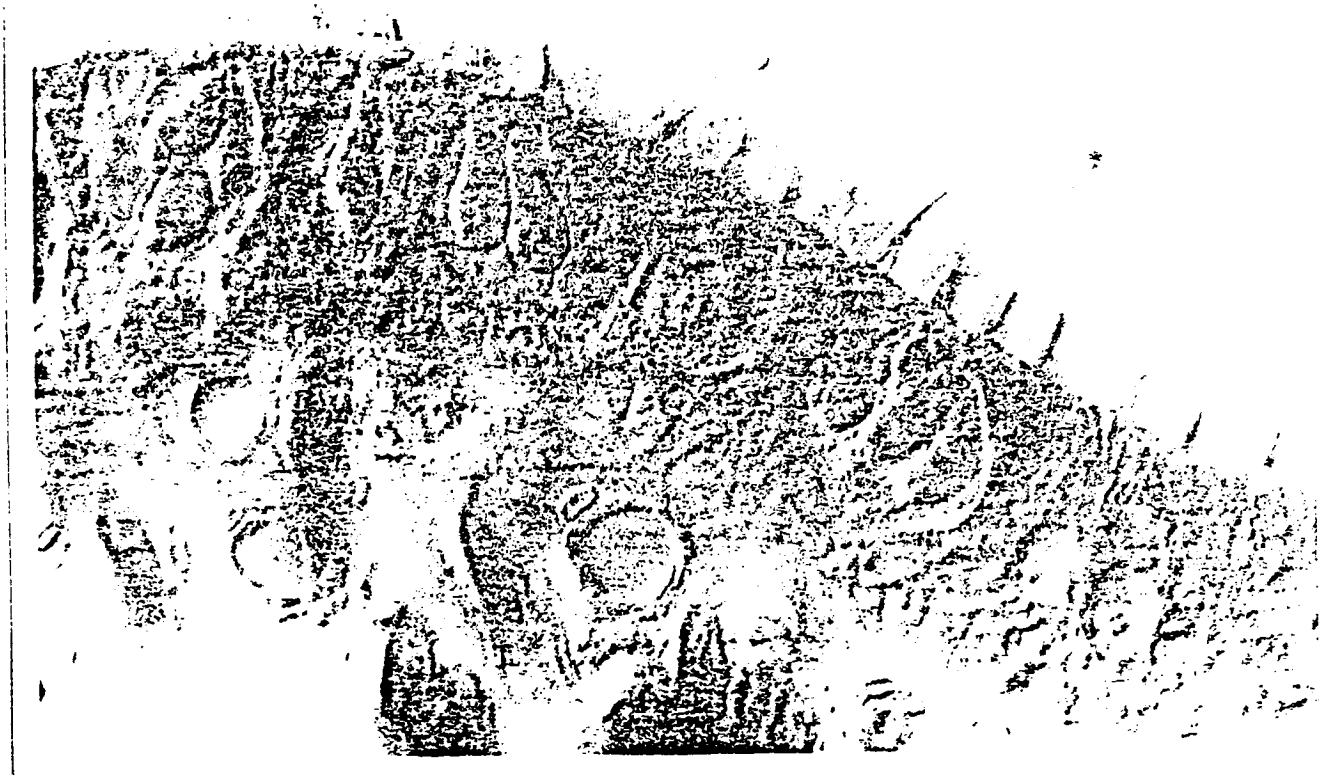

Figure 8B

An interference light microscopy photomicrograph of the slope of the crista ampullaris of the lateral ampulla in the pigeon. This figure illustrates the variable number of hair cells which can be contained in a single type I nerve calyx.

We have preliminary evidence, that in the pigeon, these multiple hair cells in a single calyx are differentially distributed on the cristae. They are primarily distributed on the slopes at the bases of the cristae, while single type I hair cells (Fig. 8C) are distributed with type II hair cells on the apeces of the cristae.

Figure 8C

A TEM photomicrograph of a single type I hair cell. Arrows point to afferent (light chalice-shaped structure) and efferent (dark vesiculated structure) terminals within the vestibular neuroepithelium of the pigeon.

In a later section we will propose to continue these studies as an adjunct to a series of neurophysiological studies investigating postsynaptic potentials within the vestibular neuroepithelium

D. Progress Expected During the Period from December 1, 1983-March 31, 1984

This time period represents the final portion of the third year of this current grant period. During this time, experiments initiated in the second and third years will be completed. Preliminary results from these experiments were presented in Section II.C.1. During the final four months of the grant period, more single unit data will be gathered from the alert pigeon preparation. Specifically, efforts will be focused on obtaining driven responses from regularly firing horizontal ampullary afferents in the alert pigeon using procedures detailed in Section II.C.1. Bode plots will be determined for the regularly firing afferents and a mean transfer function will be fit to these data. It is anticipated that the long-time constant for this transfer function will be approximately 9 seconds as was the case for the intermediate and irregular afferent transfer functions presented in Figs. 3A and 3B. Furthermore, based on previous work with anesthetized animals (Fernandez and Goldberg, 1971; Schneider and Anderson, 1974; Landolt and Correia, 1980) it is anticipated that the transfer function will not contain the zero operator which has been ascribed to cupula velocity sensitivity (Fernandez and Goldberg, 1971). Finally, it is anticipated that the coefficient (k) of the adaptation operator (s^k) in the transfer function will be smaller than those we determined for irregularly firing (k = 0.10) and intermediate firing (k = 0.14) afferents. If this expectation is true, then it will be noted that the mean coefficient of the adaptation operator for the sample of afferents from the alert pigeon is but half as large (less adaptation) as the mean coefficient (across CV class) we found in the barbiturate anesthetized pigeon (Landolt and Correia, 1980; k = 0.24) .

Also during the remaining time period in the third year of this grant, pdf's will be fit to ISI histograms for selected units along the straight line regressing B1 and B2-3 (Fig. 2D). Candidate pdf's which will be fit (Brassard et al., 1975, 1977) are: the normal, log normal, gamma, and first passage time of the Wiener-Levy process. Goodness of fit of probability density function will be determined by lowest MSE. The probability density function which best represents most of the selected units will be determined. We (Correia and Landolt, 1978) have used this method in the past to make inferences about the nature of synaptic events occurring in the sensory neuroepithelium as they relate to the production of spontaneous discharge on vestibular primary afferents. The rationale for this approach will be developed in the next section where we propose to test the inferences which we (Correia and Landolt, 1978) have made by actual measurement of synaptic events in the pigeon's sensory neuroepithelium.

IV. PROGRESS - 1979/1980

A. CURRENT PRESENTATIONS AND PUBLICATIONS RELATED TO CONTRACT

1. Correia, M.J.; Eden, A.R.; Westlund, K.N.; Coulter, J.D. Autoradiographic demonstration of auditory and vestibular pathways in the pigeon by means of anterograde transneural transport. Neurosci. Abstr. 5:18; 1979.
2. Landolt, J.P.; Correia, M.J. Transfer characteristics of primary-afferent semicircular canal units in the pigeon. Neurosci. Absts. 5:691; 1979.
3. Eden, A.R.; Correia, M.J. Horseradish peroxidase identification of four separate groups of vestibular efferent neurons in the adult pigeon. Neurosci. Abstr. 5:690; 1979.
4. Landolt, J.P.; Correia, M.J. Neurodynamic response analysis of anterior semicircular canal afferents in the pigeon (J. Neurophysiol. (in press 1980).
5. Correia, M.J.; Landolt, J.P.; Ni, M.-D.; Eden, A.R.; Rae, J.L. A species comparison of linear and nonlinear transfer characteristics of primary afferents innervating the semicircular canal. Vestibular Function and Morphology. Springer-Verlag; (in press) 1980.

B. OUTLINE OF ACCOMPLISHMENTS (January 1, 1979 - January 1, 1980)

1. Defined four discrete clusters of efferent vestibular neurons in the pigeon's medulla oblongata at the level of the vestibular nuclei using retrograde transport of horseradish peroxidase.

2. Determined ascending and descending auditory and vestibular pathways in the pigeon using transsynaptic transneural anterograde transport methods.

3. Completed a frequency and time domain analysis of primary afferent data from the pigeon.

4. Developed a computer program to analyze neurophysiological single unit responses to trapezoidal, white noise, and sinusoidal stimuli.

5. Developed procedures for chronic recording of action potentials from primary afferents in an awake gerbil preparation.

C. DETAILED DESCRIPTION OF ACCOMPLISHMENTS (January 1, 1979 - January 1, 1980)

1. Defined four areas of efferent vestibular neurons in the pigeon medulla oblongata at the level of the vestibular nuclei.

Objectives

The objectives for this area of research during the past year were to: (a) continue to refine a procedure which permits uptake of horseradish peroxidase (HRP) by efferent vestibular terminals in the vestibular and auditory sensory neuroepithelium without risking uptake by other axonal fibers related to structures which make contact with the perilymphatic space and (b) use the above procedure to determine the location, extent, and existence of efferent vestibular neurons.

Progress

To meet objective (a) listed above, we have developed a procedure for injection of HRP into the endolymphatic space without leakage into the contiguous perilymphatic space. The details of this procedure are outlined in Fig. 1. In essence, as illustrated in this figure, a micropipette is glued into the transected end of the anterior semicircular duct and HRP is injected through the micropipette into the endolymphatic liquid where it mixes with the liquid and circulates throughout the endolymphatic space. Following injection, the cut ends of the semicircular ducts are cauterized shut and the animal is permitted to survive. During the following 24 hours, either through a break-

down within the sensory neuroepithelium or through absorption, the efferent and afferent vestibular sensory terminals take up the HRP. This method differs from previous methods (e.g., Gacek and Lyon, 1974; Goldberg and Fernandez, 1977) since we have verified that when using this method, HRP does not come in contact with neural structures which are bathed by perilymph. Using this methodology we have conducted two series of experiments during the past year. The results of the first series will be reported in this section and the second will be reported in the next section.

HRP was injected and confined for 16 to 21 hours in the endolymphatic space of one labyrinth in five adult pigeons. Amounts of 0.5 µl of 50% HRP were delivered through a micropipette glued into the transected anterior semicircular duct every 10 to 15 minutes until a total of 7 to 10 µl was injected. The brain and labyrinths were fixed by bilateral transcardiac intracarotid cautherization. HRP was reacted by the tetramethylbenzidine blue reaction process. Twenty to fourty micron frozen sections were made of the brain and the following observations, which are summarized in Figs. 2 and 3, were noted. Fig. 2 shows a camera lucida drawing of a transverse section of the brain and illustrates the clusters of labeled neurons. As may be noted in Fig. 2 some of these cell groups are within the vestibular nuclei while others are within the reticular formation. The cell groups within the reticular formation appear to be large multipolar neurons which appear to be distributed equally bilaterally (mean $\pm$ SD number of cells each side: 49 $\pm$ 25). The majority of these cells were found to be clustered close together in the nucleus reticularis pontis caudalis immediatelly ventro-latero-caudal to the abducens nucleus. A second cluster of labeled similar size multipolar neurons was also noted within the same nucleus but adjacent and medial to the nucleus paragigantocellularis

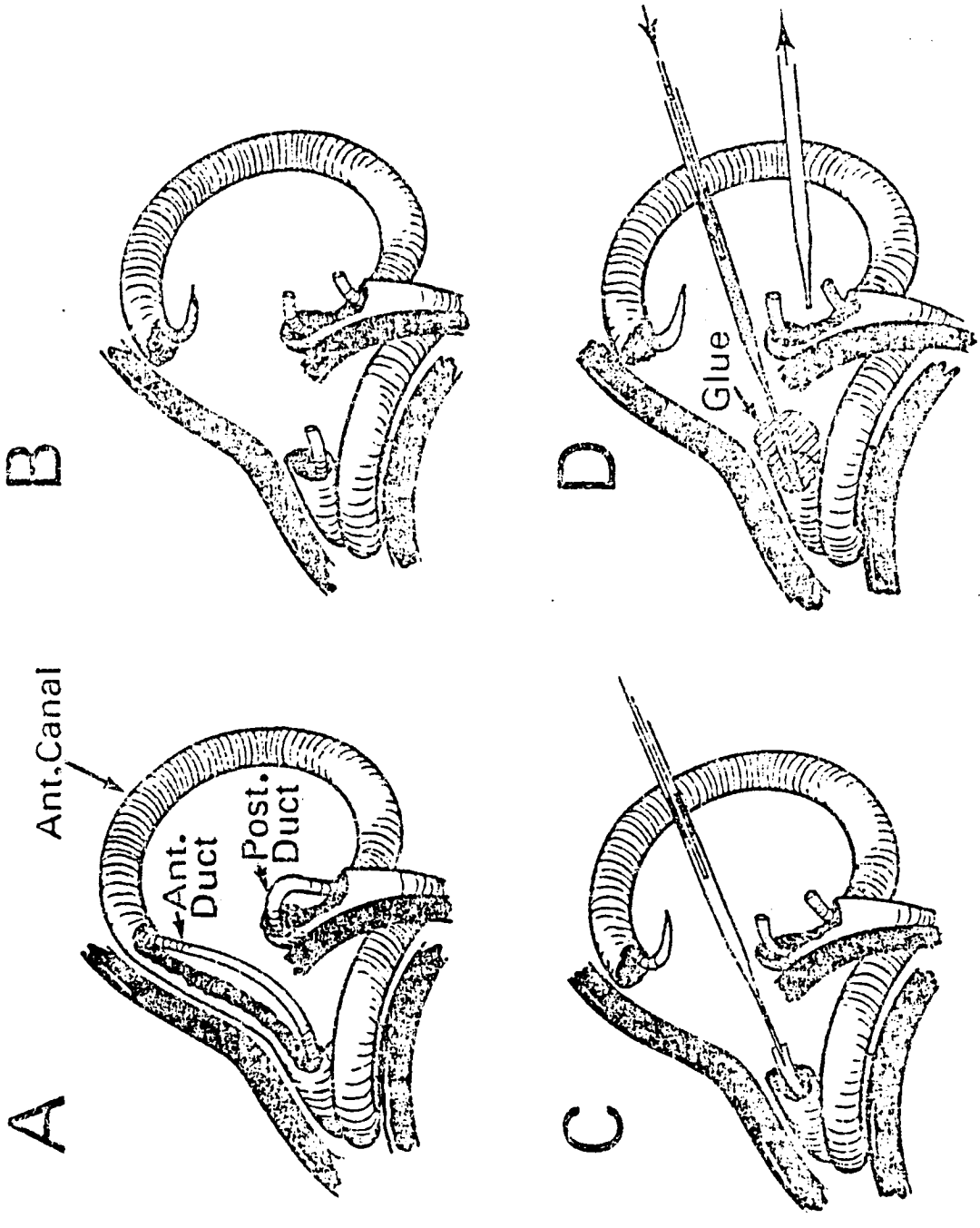

Figure 1

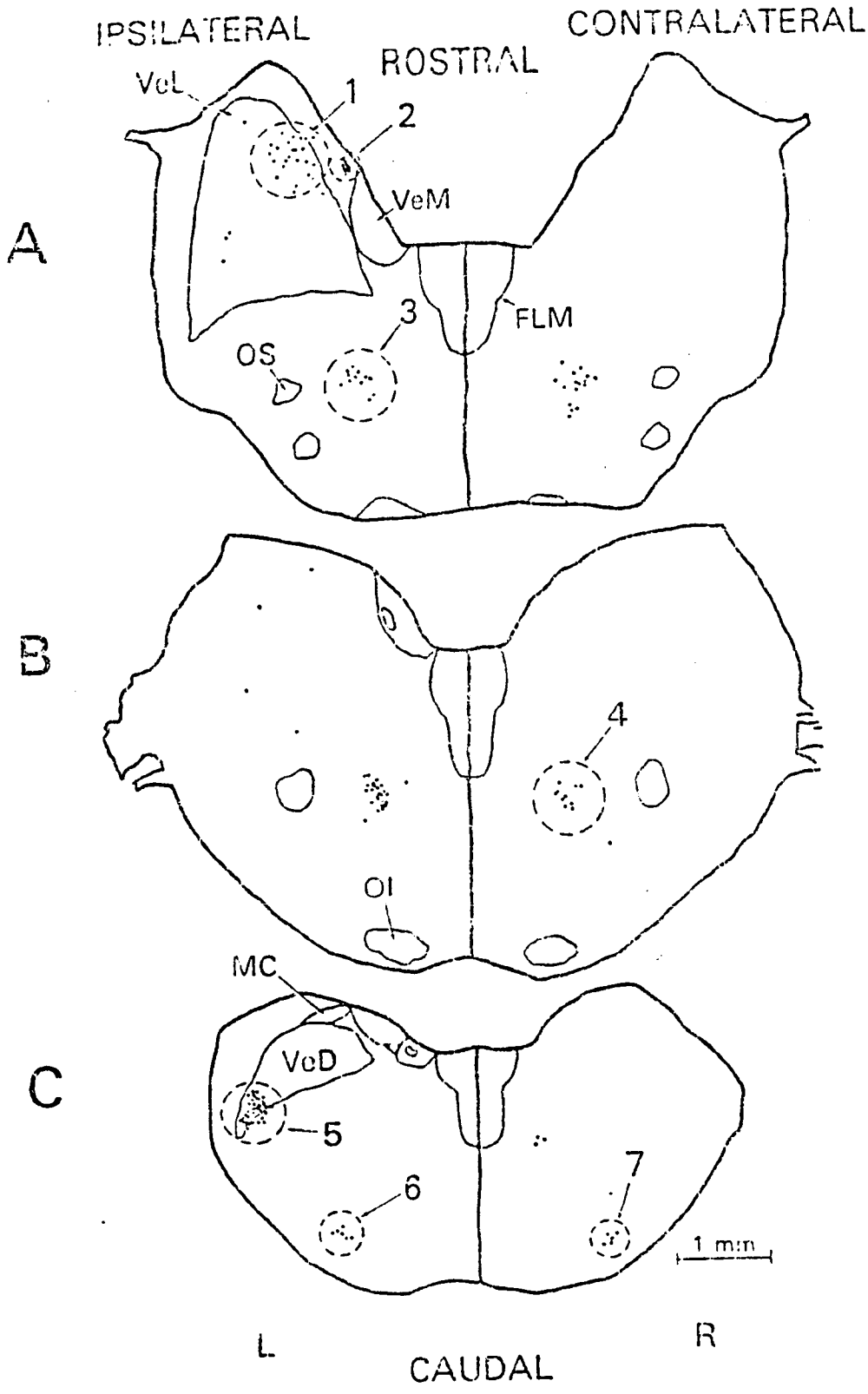
IPSILATERAL
CONTRALATERAL
ROSTRAL
VeL
1
2
VeM
A
3
FLM
OS
B
4
OI
MC
VeD
C
5
6
7
1 min
L
R
CAUDAL

Figure 2

lateralis and ventro-latero-caudal to the first group of labeled cells. These cell groups are identified in Fig. 2 as areas 3 and 6 respectively. Within the ipsilateral vestibular nucleus complex, labeled efferent neurons (mean ± SD number of cells: 77 ± 25) were also noted to cluster in distinct groups in the majority of the animals we tested. A group of medium size bipolar cells were located within the tangential vestibular nucleus (region 5, Fig. 2) adjacent to and intermingled with larger multipolar labeled neurons in the latero-caudal part of the inferior (descending) vestibular nucleus (region 5, Fig. 2). A second group of large multipolar labeled neurons (possibly Deiters cells), interspersed with labeled medium sized round and triangular cells were noted to cluster in the medial pole of the lateral vestibular nucleus (VeL) adjacent to the nucleus laminaris (region 1, Fig. 2). Another group of small labeled neurons were also noted in the ipsilateral nucleus laminaris (region 2, Fig. 2). These neurons may represent cochlear efferent neurons. Fig. 3 shows sagittal plane sections of the relationship of these regions which are presented for the transverse plane in Fig. 2.

It appears from the data presented in Figs. 2 and 3, that in the pigeon there is not one discrete group of cells which comprise the cell bodies for the efferent vestibular system but rather there are distinct groups of cells which are distributed throughout certain of the vestibular nuclei and regions of the medullary retucular formation.

These data are different from those presented for the squirrel monkey (Goldberg and Fernandez, 1977) and for the cat (Gacek and Lyon, 1974). However, they are generally in agreement with those presented for the guinea pig and rabbit (Rossi and Cortesina, 1965). As did we, Rossi and Cortesina (1965) found multiple clusters of efferent vestibular neurons. The finding that only

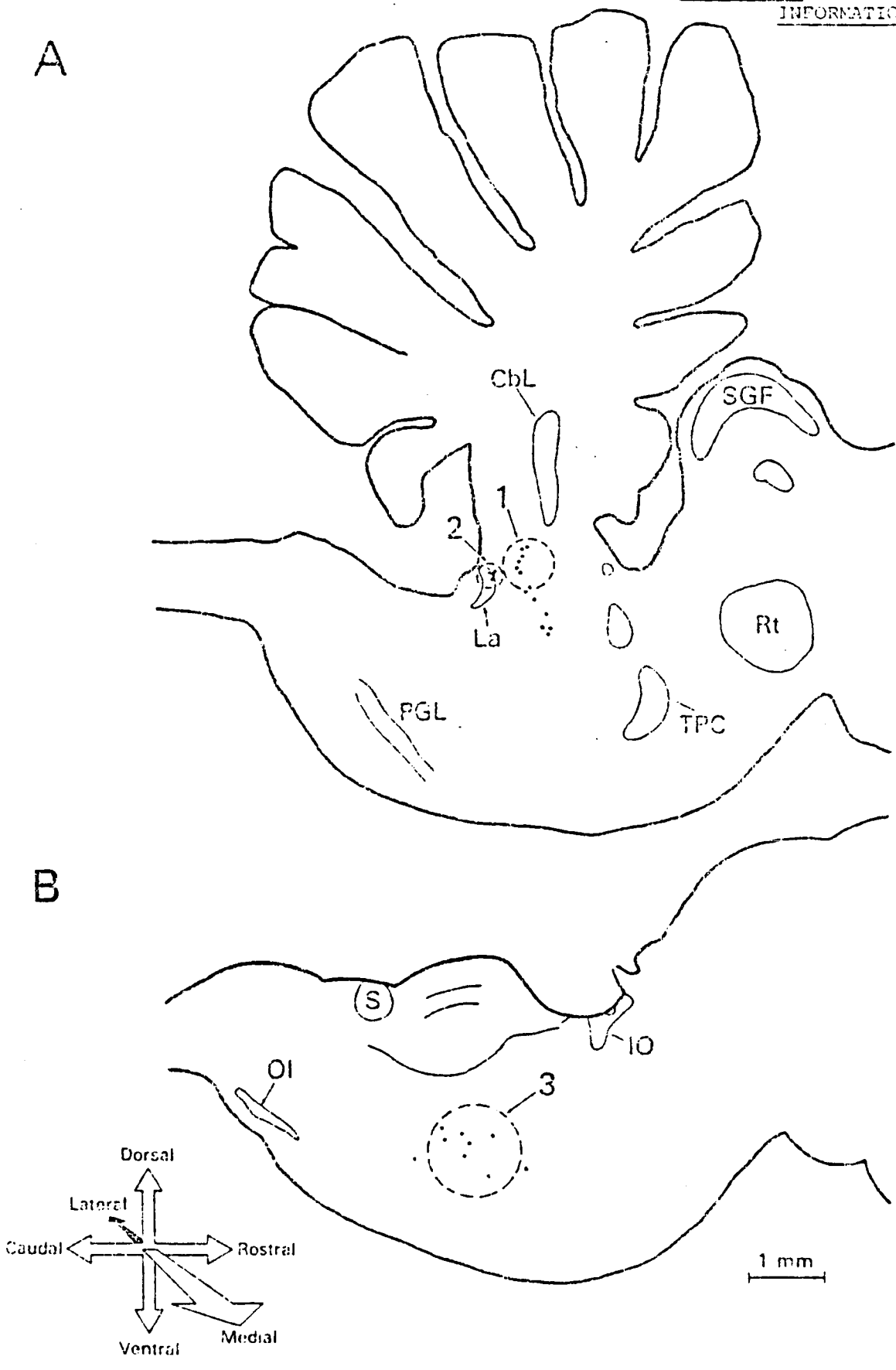
A
CbL
SGF
1
2
La
Rt
PGL
TPC
B
S
IO
OI
3
Dorsal
Lateral
Caudal
Rostral
Medial
Ventral
1 mm

Figure 3

one cluster of efferent vestibular neurons apparently exists for the monkey and cat could be a) because of species differences or b) because of technique differences. Rossi and Cortesina (1965) used a variety of techniques to delineate the different clusters of efferent vestibular neurons in the guinea pig and rabbit. We contained HRP within the endolymph for long periods of time. Goldberg and Fernandez (1977) and Gacek and Lyon (1974) injected HRP into the perilymphatic space.

Future Plans

During the next year of this contract we will attempt to determine if electrical stimulation of each of the regions we have identified as sites of efferent neuron clusters have any effect on single unit discharge from vestibular primary afferents in the pigeon. Moreover, we will attempt to use additional histological procedures to determine if some of the clusters of cell bodies which we have identified have peripheral processes which are cholinergic. Goldberg and Fernandez (1977) argued that since efferent terminals on the neuroepithelium are cholinergic, these processes and somas should be sensitive to acetylcholinesterase incubation. The specific details of each of these areas of research will be presented in the subsequent section—RESEARCH PROPOSAL (1980 - 1981).

2. Determined ascending and descending auditory and vestibular pathways in the pigeon using transsynaptic transneural anterograde transport methods.

Objectives

The objectives for the past year for this area of research were (a) to contain radioactive substances in the endolymphatic space for long periods of time to permit transsynaptic anterograde transport to take place and (b) use autoradiographic techniques to find first-, second-, and possibly third-order projections of the cochlea and the vestibular apparatus.

Progress

Using the same procedure illustrated in Fig. 1, we injected an equal parts mixture of L-[^{3}H] proline and 1-[6-^{3}H] fucose (50 μCi/μl) into the endolymphatic space of the left membranous labyrinth in five white king pigeons. A total of one μl of the above solution was injected into the anterior semicircular canal over a period of one hour. Following injection, the cut ends of the ducts were sealed by cauterization and the animal was allowed to survive for 15 days. The brain, spinal cord, and labyrinths were fixed with 10% buffered formalin delivered by bilateral transcardiac intracarotid catheterization. Serial paraffin sections (15 microns) were prepared by standard autoradiographic techniques. Fig. 4 is a darkfield photomicrograph of a transverse section through the brain of one of the pigeons at the level of the cochlear branch of the eighth cranial nerve. Auditory structures which were heavily labeled and which can be noted to be lighter than surrounding structures in this photomicrograph are the left cochlear nerve (NVIIc), the left angular nucleus (An), and the left magnocellular nucleus (MC). Rostral auditory structures which labeled due to transsynaptic transport included the ipsilateral and contralateral superior olive, the ipsilateral and contralateral lateral lemniscus, and the contralateral nucleus mesencephali lateralis parsdorsalis (MLD), the analog of the mammalian inferior colliculus. While other structures such as the cochlear nuclei, the lateral lemniscus, and the MLD have been demonstrated previously using anatomical degeneration studies, our observation of labeling in the avian superior olive has not heretofore to our knowledge, been reported. Other new findings resulted from this experimentation and one of them is illustrated in Fig. 5. It can be seen in Fig. 5 that a symmetry exists with regard to labeling within the avian oculomotor nucleus. Specifically, we observed that on the side ipsilateral to

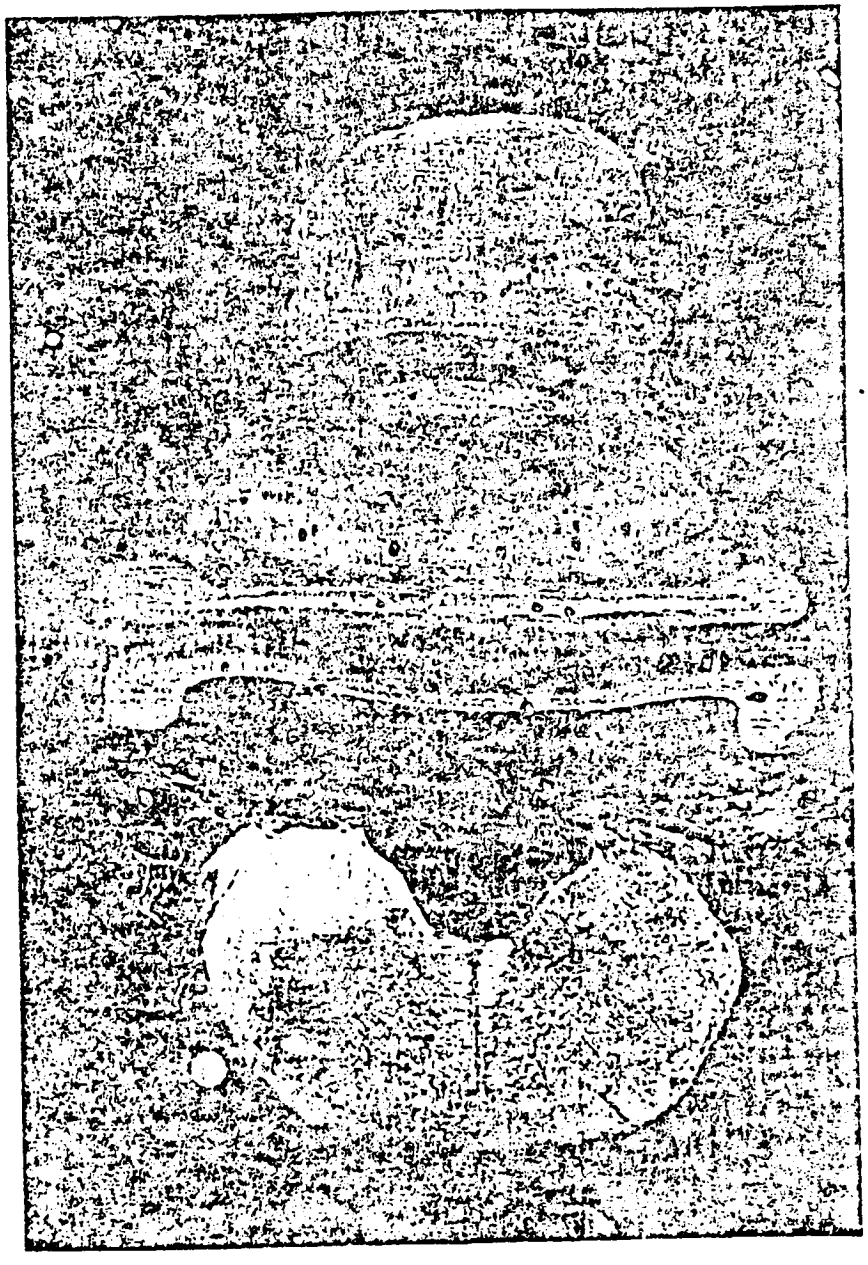

Figure 4

Figure 5

the site of injection, the dorso-medial component of the oculomotor nucleus was heavily labeled; however, the ventro-medial and dorso-lateral components were not. On the other hand, contralateral to the injection site, the ventro-medial and dorso-lateral components were heavily labeled and the dorso-medial component was not. Thus, a clear topographic projection within the oculomotor nucleus apparently exists for each labyrinth. Other auditory and vestibular structures which were identified but which do not represent new contributions to knowledge were as follows: Auditory structures - auditory structures ipsilateral to the side of injection which were labeled were; cochlear nerve, angular nucleus, magnocellular nucleus, lateral lemniscus, and ventral nucleus of the lateral lemniscus. Labeled structures contralateral to the side of injection included the lateral lemniscus and ventral nucleus of the lateral lemniscus. Vestibular structures - vestibular structures ipsilateral to the side of injection which were heavily labeled were: the vestibular nerve, all six vestibular nuclei, and the cerebello-vestibular lateral process. Less heavily labeled ipsilateral structures included: the medial longitudinal fasciculus, terminations on motorneurons in the medial and lateral part of the ventral grey of the spinal cord and the abducens, oculomotor, and trochlear nuclei. Contralateral vestibular structures which were heavily labeled were: the medial longitudinal fasciculus, terminations on motoneurons in the medial and lateral part of the ventral grey of the spinal cord and the oculomotor, trochlear, and abducens nuclei.

Future Plans

As in the case of retrograde transport of HRP, anterograde transport of tritiated proline and fucose provided new and important information. However, this information is confounded by the fact that using the methodology

illustrated in fig. 1, both auditory and vestibular afferent and efferent terminals pick up the labeling material because these terminals share common endolymphatic space.

To deal with this situation during the next year we will execute the following set of experiments. We will repeat the experiments that we have conducted during the past year, that is, injecting HRP and a mixture of proline and fucose into the endolymphatic space of one of the labyrinths in the pigeon. However, the injection will not be made until all of the nerve branches innervating all of the end organs except the one of interest have been sectioned. That is, we will, for example, determine which of the projections that we have identified for both the vestibular and cochlear end organs are part of the vestibular system by first sectioning the cochlear nerve in an animal; let the animal survive from four to six weeks and then inject the labeling substance into the endolymphatic space. We reason that 4 to 6 weeks following a neurectomy there will be degeneration of the nerve fibers in the cut branches and these fibers will not transport the labeling substance to the brain. In future years we will selectively section each of the component branches of the vestibular nerve to determine the central nervous system projections of both vestibular and auditory afferents. Using HRP, the blue reaction product tetramethylbenzidine procedure, and tritiated proline and fucose, we should be able to use anterograde and retrograde transport to identify higher order projections from each of the labyrinthine end organs as well as the cochlea.

3. Completed a frequency and time domain analysis of primary afferent data from the pigeon.

Objectives

Our goals in this area of research were two-fold: (a) to empirically characterize the dynamic response of the pigeon's semicircular canal primary

afferent system; and (b) to develop a meaningful mathematical model to explain the response dynamics we observed.

Progress

We have recently completed a thorough analysis of single unit data from pigeon vestibular primary afferents (see attached manuscript—Appendix 1.) in which we attempted to characterize both the linear and nonlinear transfer characteristics of single unit data. We used both sinusoidal and pulse angular acceleration stimuli and concentrated our analysis primarily on anterior semicurcular canal afferents. We found that intensity function plots of peak first harmonic neural response plotted against peak sinusoidal angular acceleration produced two types of relationships: one was a linear relationship and the second was a nonlinear relationship. Those units which demonstrated a nonlinear relationship for their intensity function were fit well by a power law function. The exponent of the function varied as frequency varied and it became closer and closer to unity with increasing values of frequency. In general we found the mean $\pm$ SEM for the coefficient of the power function to be 1.086 $\pm$ 0.095 for the units we thoroughly investigated. The data from all of the units we investigated fit the transfer function, $G'(s) = Cs^k/(\tau_L s+1)$, where C is a gain constant, $0 \leq k \leq 1$, and τ_L, a time constant for the single pole, can be considered to be the long-time constant of a classical torsion pendulum model. The value of τ_L varied from 4.45 seconds to 18.61 seconds (mean $\pm$ SEM = 10.24 $\pm$ 1.20 seconds). The value of k varied from 0.017 to 0.66. We found that there was a relationship between the degree of regularity of the resting discharge for a given afferent and the parameter k. Specifically, the larger the coefficient of variation (CV) the larger the value of the corresponding k. When we analyzed data resulting from time domain stimulation using acceleration

pulses and modeled the responses with the Laplace transform of the equation just presented, we found that there was a relationship between the value of k and the amount of adaptation that a unit showed during various durations of pulse angular accelerations. We observed that the larger the value of k, the more adaptation a unit exhibited. The fact is illustrated in Fig. 9 which is contained in the accompanying manuscript (Appendix 1.). We drew several conclusions based on our theoretical and empiricaly analyses of the data. Specifically, we concluded that the term s^k which is contained in the transfer function for pigeon data generally is applicable to the description of adaptation phenomena for most species (see Correia et al., 1980). Moreover, we concluded that the term s^k can be mathematically decomposed into an expression containing a series of polynomials in s in the numerator and the denominator. The first term of this expansion $k^o\tau_1 s/(\tau_1 s+1)$ has previously been shown to describe the so-called adaptation properties in the dynamics of the semicircular canals. For the pigeon we found that mean ($\pm$ SEM) τ_1 = 77.18 ($\pm$ 13.06) seconds. We suggest that the s^k operator describes a general biological relaxation phenomenon which is inherent in time varying neuroelectric Na^+/K^+ transport processes such as occur in the vestibular neuroepithelium. The components of these processes are summed with the receptor potential in the hair cell to produce an adaptation phenomenon. Furthermore, we suggest that the term s^k, by virtue of the fact that it can incorporate primary, secondary, and tertiary adaptation phenomenon and since it has been found to characterize adaptation phenomenon in other sensory receptors in other species (for example see, Thorson and Biederman-Thorson, 1973), is more than just a mathematical convenience but is a powerful descriptor of adaptation processes within sensory neuroepithelia.

Future Plans

In both our time domain and frequency domain analyses of primary afferent data in the pigeon, obvious nonlinearities were observed for some of the units. We suspect that these nonlinearities may be contributed by: (a) nonlinearities inherent in the receptor potential from hair cells within the vestibular neuroepithelial system, (b) nonlinearities contributed by the generator potential within the sensory neuroepithelium, and (c) nonlinerities contributed by the fact that primary afferent discharge is undefined for negative firing frequencies. We will attempt to explore these nonlinearities in future years by first characterizing the types of nonlinearities that occur during prolonged pulse acceleration as well as during repeated sinusoidal stimulation. There are several models which represent a cascade of systems, some linear and some nonlinear (for example see, Segal and Outerbridge, 1979). These models make specific predictions as to the output of primary afferent responses for a variety of stimuli. We will attempt to test these model's predictions for two species, the gerbil and the pigeon.

4. Developed a computer program to analyze neurophysiological single unit response to trapezoidal, white noise, and sinusoidal stimuli.

Objectives

(a) To develop a program to acquire time of events (TOEs) of each of a series of action potentials, bin inter-event intervals, or determine instantaneous firing frequency. (b) To develop a program to calculate and display either a cycle histogram, a poststimulus time histogram, or a continuous record of frequency of firing as well as a digitized representation of the driving stimulus signal. (c) To develop a program to store on magentic tape, in real-time, TOEs as they are being acquired and displayed. (d) To develop a program to least square fit a sine wave through both the digitized stimulus signal and a cycle histogram and determine the amplitude ratio and phase relationship between the two.

Progress

All of the objectives described above were met and a computer program was written whose tutorial is presented in Appendix 2. Sample runs illustrating the capabilities of the program are also presented. The program has been thoroughly tested, debugged and is currently being used in the neurphysiological experiments in our laboratory. Source listings of the program are available on request.

Future Plans

Since we have the capability of storing time of events (TOEs) on magnetic tape in real-time, we have provided ourselves with considerable flexibility for off-line processing of these data. Two goals loom in the immediate future regarding development of programs to utilize the time of event data which are stored on magnetic tape acquired by the program DNIP. First, we wish to be able to analyze these data with the program LSA (Ni et al., 1978) following filtration by the French and Holden (1971) algorithm. Specifically, we will acquire time of event and stimulus data for either white noise or sum of sinusoid stimuli. We then will apply the French and Holden (1971) anti-alaising filtering algorithm to these data and subject the resulting waveform to programs (LSA—Ni et al., 1978) which we have already written for Fourier analysis of two continuous waveforms to obtain the amplitude ratio, phase, and coherence function. Moreover, in the future, we will evaluate the possibility of incorporating TOE data resulting from this program with a series of programs which have been developed at Rockefeller University. These programs perform linear and nonlinear systems analysis of TOEs of action potential modulation produced by stimuli which represent the sum of sinusoidal stimuli.

1. Developed procedures for chronic recording of action potentials from primary afferents in an awake gerbil preparation.

Objectives

(a) To develop a procedure for recording from vestibular primary afferents in an unanesthetized gerbil which: (1) requires minimum surgery, (2) requires minimum setup time, and (c) produces a high yield of single unit data.

Progress

We have made considerable progress in the last several months in achieving the objectives outlined above. We have been able to confirm that by simply making a hole 2 to 3 mm in diameter at stereotaxic positions A-PO, L3, 10 degrees tilt, that we can record from an anesthetized preparation in a stereotaxic frame and obtain a "good" yield of vestibular primary afferents. This procedure obviates: (a) having to remove any of the brain prior to the recording session, (b) producing any thermal gradients across the labyrinth due to the opening of air space in the internal meatus, and (c) having to cover the nerve microelectrode interface with agar to diminish brain pulsations. In fact, we have not found it necessary even to use a fluid filled chamber to identify, isolate, and record from vestibular afferents using the above procedure. Although we have isolated the gerbil's cortex by a precollicular decortication procedure, we have not embarked upon studies using an unanesthetized preparation because of humane reasons. Specifically, we have not had time yet to develop a painless head holding procedure. However, we anticipate no problems since Dr. Perachio has considerable experience with these devices in other species. We probably will develop a chronically implanted head holding method which involves attaching dental acrylic to the skull and in which is encased a rectangular tube (placed with the animal's head in a stereotaxic frame) which will be mated with a head holding device. We will use the acrylic for two

purposes, (1) it will serve to solidify the skull of the gerbil and (2) it will serve to humanely hold the animals head without having to use earbars and consequently enable us to record from an unanesthetized preparation.

Future Plans

In the next several months we will develop the gerbil head holder as well as a body restraint device. These two developments will allow us to record from both the central nervous system neurons and primary afferent neurons in the awake gerbil. Using this animal model we will attempt to characterize anterior and posterior ampullary afferents and thereby extend work initially begun by Schneider and Anderson (1976) for lateral ampullary afferents. Moreover, we will generalize the procedures which we have developed for the gerbil to the pigeon so that we can implement the major thrust of our research effort for the next year which is, the electrophysiological analysis of the influence of stimulation of efferent vestibular neurons on vestibular afferent activity. These studies represent the major set of experiments which comprise our research proposal for the upcoming year and they will now be detailed.

V. PROGRESS - 1978/1979

A. CURRENT PRESENTATIONS AND PUBLICATIONS RELATED TO CONTRACT

1. Correia, M.J. and Guedry, F.E.: The vestibular system: basic biophysical and physiological mechanisms. IN: Handbook of Behavioral Neurobiology, Vol. 1 Sensory Integration, R.B. Masterton, ed. Plenum Press, N.Y. 1978:311-351.

2. Landolt, J.P. and Correia, M.J.: Neuromathematical concepts of point process theory. IEEE Trans. Biomed. Eng. BME-25:1-12 (1978).

3. Ni, M.-D., Correia, M.J., Rae, J.L., and Koblasz, A.J.: A real-time, mini-computer program for calculation of frequency function and coherence function by digital Fourier methods. Proceedings of the International Symposium on Mini and Microcomputers. IEEE Catalog #77CH1347-4C; 1978:2-5-212.

4. Landolt, J.P. and Correia, M.J.: Neurodynamic response analysis of anterior semicircular canal afferents in the pigeon (submitted, 1979).

5. Correia, M.J. Landolt, J.P., Eden, A.R., Ni, M.-D., and Rae, J.L.: A species comparison of the linear and non-linear transfer characteristics of the semicircular canal primary afferent system. Proceedings of the Society for Neuroscience Satellite Symposium on Vestibular Function and Morphology. Pittsburgh, PA, Oct.-Nov., 1978 (in preparation, 1979).

B. OUTLINE OF ACCOMPLISHMENTS (April 1, 1978 - January 1, 1979)

1. Analyzed the spontaneous and driven response from the pigeon's vestibular primary afferents and determined a transfer function which describes the mean amplitude ratio and phase response over the frequency range from 0.01-15.0 Hz.

2. Compared the transfer characteristics of the vestibular primary afferent system in the bird with several species. Intensity functions (stimulus - response function) and frequency response functions were calculated for the semicircular canal primary afferent system of the frog, gerbil, pigeon, guitar-fish, squirrel monkey, and rhesus monkey. These functions were compared and some conclusions were drawn.

3. Horseradish peroxidase (HRP) was injected into (and contained within) the endolymphatic spaces of the inner ears of 10 pigeons. Efferent neurons and afferent fiber tracts were identified and their location delineated.

4. Thick sectioned, epon embedded labyrinths were analyzed to describe the distribution of types of hair cells, stereocilia length, and afferent/efferent innervation patterns in various regions of the cristae ampullares.

C. DETAILED DESCRIPTION OF ACCOMPLISHMENTS (April 1, 1978 - January 1, 1979)

1. Analyzed the spontaneous and driven responses from the pigeon's vestibular primary afferents and determined a transfer function which describes the mean amplitude ratio and phase response over the frequency range from 0.01-16.0 Hz.

The following observations which are applicable to most species and to the pigeon in particular, and which are described in more detail in Landolt and Correia (1979) and Correia et al. (1979), were made during the last year of this contract. (a) Nonlinear distortion of average instantaneous frequency of ampullary afferent discharge has three forms: (1) sine wave asymmetry — a unidirectional rate asymmetry in which the portion of the sine wave response corresponding to a decreasing rate of discharge is steeper than the portion of the response corresponding to an increasing rate of discharge. (2) Complete and partial rectification of the neural response - this nonlinearity has been documented for the primary ampullary afferent system of several species. Moreover, partial rectification has been discovered by Taglietti et al. (1977) for the generator potential in Rana esculenta (response corresponding to peak sinusoidal oscillation of $119.2^{o}/s^{2}$ in Fig. 1).

FIG. 1

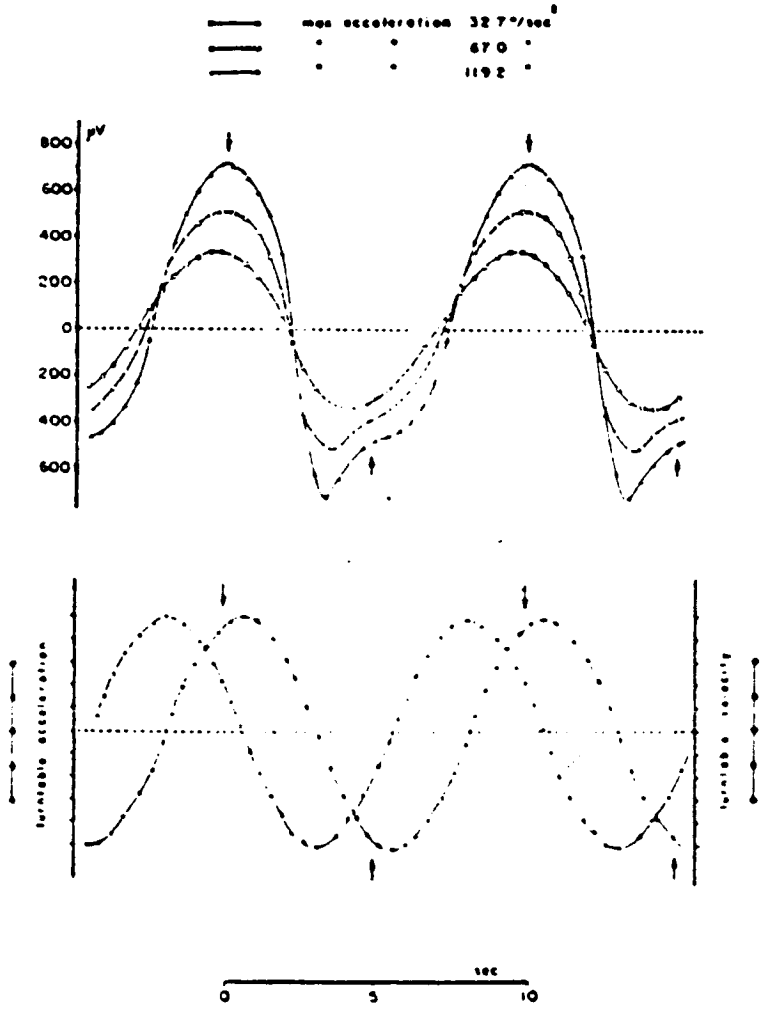

(after Taglietti et al., 1977)

(3) Harmonic distortion - for the pigeon, the coefficient of harmonic distortion,

$$CD = \sum_{n=2}^{10} \frac{\sqrt{a_n^2 + b_n^2}}{a_1 + b_1}$$ (a_n and b_n are Fourier series real and imaginary

coefficients, respectively) varies with frequency and stimulus amplitude. The higher the frequency and the smaller the stimulus, the greater the magnitude of the distortion coefficient. (4) Nonlinear intensity function - for the pigeon, one of two classes of ampullary afferent units showed a nonlinear intensity function which varied with frequency. Figure 2B summarizes the mean (N=15) first harmonic response to five levels of peak angular acceleration at two frequencies of oscillation (f = 0.2 Hz and 0.02 Hz).

FIG. 2

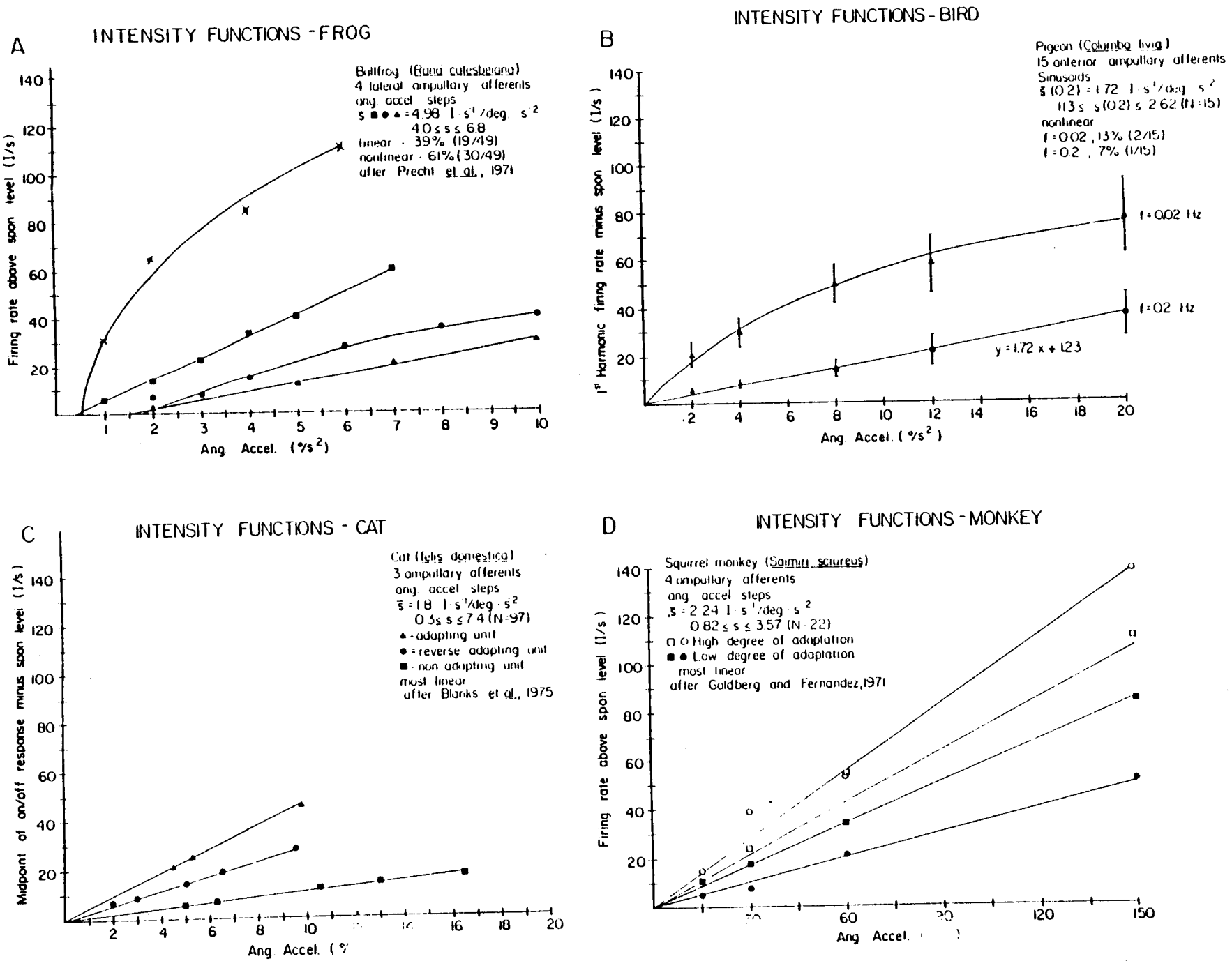

The mean response is clearly nonlinear over the stimulus intensity range for an oscillation frequency of 0.02 Hz. At a frequency of f = 0.2 Hz, only 1 of 15 units demonstrated any nonlinearity and the mean response is best fit by the regression equation $Y = 1.72X + 1.23$. This regression line indicates a sensitivity of 1.72 impulses per second/degree per second^2 and a threshold value of 1.23 impulses per second.

We have not been able to unequivocally isolate and describe the type of nonlinearity which is present in the intensity functions described above. Both Steven's power function and the Weber-Fechner law appear to apply and be indistinguishable. For example, Table I contains data (9 units - 27 intensity functions) which enable a comparison between linear regression line correlations (after appropriate logarithmic-logarithmic transformations have been made) for the Weber-Fechner equation (r_c^w) and the Steven's power law equation (r_c^s).

TABLE I

Properties of Power Function

Response, $r_{1m} = a\,\alpha_m^b$

Unit	f (Hz)	a (imp·s^{-1})/(deg·s^{-2})^b	b	r_c^s	r_c^w	Unit	f (Hz)	a (imp·s^{-1})/(deg·s^{-2})^b	b	r_c^s	r_c^w
92770	0.01	2.949	0.746	0.992**	0.986*	91169	0.01	1.510	0.913	0.979*	0.963*
	0.02	3.214	0.609	0.985**	0.981**		0.05	1.015	0.970	0.990**	0.937*
	0.05	2.467	0.788	0.999**	0.974**						
	0.10	2.162	0.750	0.993**	0.950*	Mean		1.263	0.941	0.985	0.940
	0.20	1.340	0.978	0.991**	0.965**	±SEM		±0.247	±0.029	±0.005	±0.013
	0.50	0.865	0.992	0.989**	0.954*						
						91069	0.05	2.997	0.600	0.923*	0.935*
Mean		2.166	0.811	0.991	0.968		0.10	2.718	0.546	0.985**	0.960**
±SEM		±0.373	±0.061	±0.002	±0.006						
						Mean		2.858	0.573	0.953	0.948
4670	0.01	3.275	0.695	0.991**	0.952*	±SEM		±0.140	±0.027	±0.030	±0.012
	0.02	3.247	0.667	0.993**	0.979**						
	0.05	2.272	0.911	0.922*	0.961**	91070	0.02	0.843	0.917	0.994**	0.960**
	0.10	1.714	0.923	0.992**	0.946*		0.05	0.380	0.800	0.965**	0.884*
Mean		2.627	0.779	0.993	0.959	Mean		0.611	0.859	0.980	0.922
±SEM		±0.383	±0.068	±0.001	±0.007	±SEM		±0.231	±0.059	±0.015	±0.038
102269	0.01	2.354	0.899	0.951*	0.986*	51370	0.01	1.090	0.787	0.997**	0.972*
	0.02	2.467	0.779	0.957*	0.988**		0.02	0.953	0.803	1.000**	0.982**
	0.05	1.950	0.891	0.990**	0.987**						
	0.10	1.890	0.867	0.994**	0.987**	Mean		1.021	0.795	0.999	0.977
						±SEM		±0.069	±0.008	±0.001	±0.005
Mean		2.165	0.859	0.973	0.987						
±SEM		±0.143	±0.027	±0.011	±0.000	1870	0.02	0.961	0.806	0.998**	0.967**
						81970	0.10	1.574	0.877	0.984**	0.922*
72970	0.02	0.415	1.262	0.979**	0.985**						
	0.05	0.476	1.062	0.997**	0.947*						
	0.10	0.431	0.935	0.995**	0.969**						
Mean		0.441	1.086	0.990	0.967	Average mean		1.574	0.841	0.985	0.956
±SEM		±0.018	±0.095	±0.006	±0.011	±SEM		±0.268	±0.041	±0.004	±0.007

Two-tailed tests: **P < 0.01; *P < 0.05

Average mean value for $r_c^w = 0.956$ ($\pm$ 0.007) and for $r_c^s = 0.985$ ($\pm$ 0.004). These correlation coefficients are essentially equivalent. However, because of the greater potential generality of the Steven's power function and because it has been applied to more different sensory systems, we present parameters based on this equation in Table I. The average equation which we derived was $R = 1.57\ (\pm\ 0.268) \cdot \alpha_m^{\ 0.841\ (\pm\ 0.041)}$. The exponent of α_m (peak stimulus magnitude) has an average value of 0.8. However, Table I shows that the values range from low to higher values of the coefficient b as frequency is increased. Thus the intensity functions approach linearity (b = 1.0) as frequency of oscillation is increased. This general finding is consistent with the results illustrated in Fig. 2B and indicates that for low frequencies of rotation, frequencies outside the physiological bandwidth, superposition of responses to angular accelerations over the range $2\text{-}20^\circ/s^2$ does not occur. However, superposition does occur for some units over the limited range from $2\text{-}12^\circ/s^2$ (Correia and Landolt, 1973). We chose 14 of these units which demonstrated properties consistent with a linear system and we fit numerous general forms of transfer functions to amplitude ratio and phase values using a nonlinear least squares curve fit program (Brassard et al., 1974). The simplest equation which provided a good fit was

$$H(s) = Cs^k/\tau_L s+1 \quad . \qquad \text{Eq. (1)}$$

This equation relates instantaneous frequency of action potentials to angular head acceleration. The parameters are: C ≡ gain constant, k ≡ fractional exponent, τ_L ≡ long-time constant in the torsion pendulum equation. The fractional operator, s^k, has been related to the phenomenon of neural adaptation in other sensory systems (Thorson and Biederman-Thorson, 1974). The time constant τ_L characterizes the biophysical response of the semicircular canal.

The so-called "short-time" constant, τ_s, of the torsion pendulum model of the semicircular canal was not included in Eq. (1) since this parameter has only the slightest effect over the frequency range 0.01-2.0 Hz. Fig. 3 illustrates Bode plots for two extreme types of frequency responses from two representative units.

FIG. 3

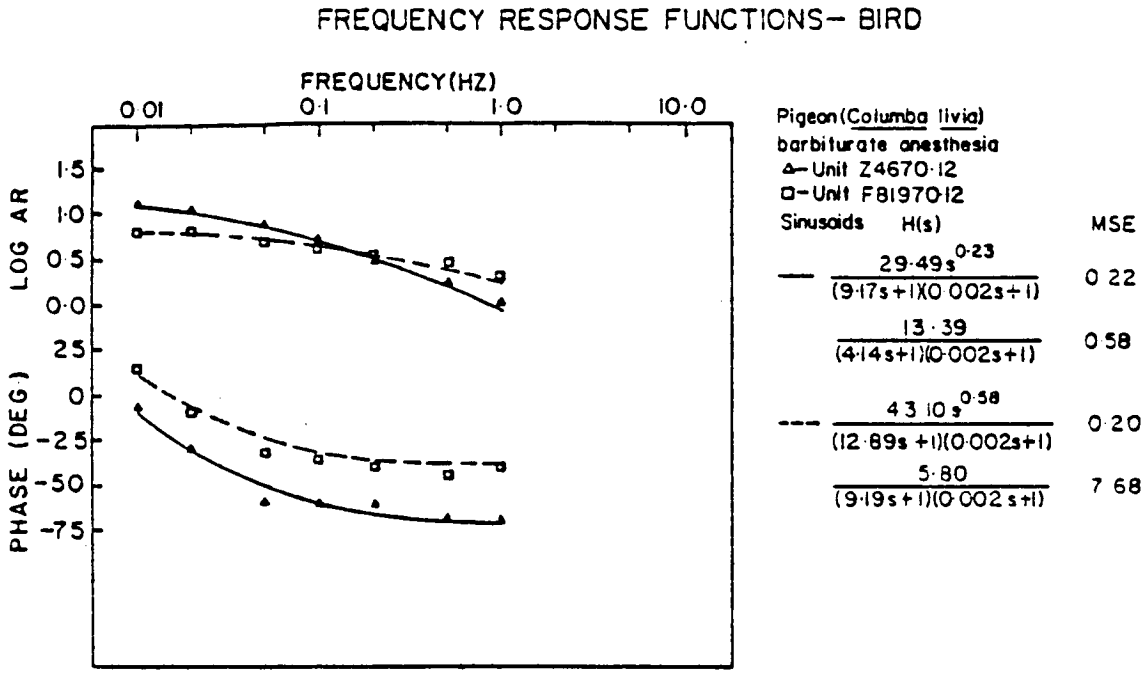

The first unit's amplitude ratio (AR) and phase values (denoted by triangles) was best fit by a transfer function whose parameter values were k = 0.23 and τ_L = 9.19. This unit typifies a neural unit which displays moderate neural adaptation. The second unit's AR and phase values (denoted by squares) showed a longer time constant (τ = 12.89) and stronger adaptation (k = 0.58). A range of values for C, K, and τ_L were determined for 14 units. These values are summarized in Table II.

TABLE II

Characteristics of transfer function, $Cs^k/(\tau_L s+1)$,

for 14 selected units

Unit	λ_m (degrees·s^{-2})	Parameters: C (impulses·s^{-1}/degrees·s^{-2})	k	τ_L (s)	Mean square error, MSE	Range of f (Hz)
81070	4	37.15	0.51	11.64	0.710	0.01-0.50
	12	43.10	0.58	12.87	0.180	0.01-2.00
	20	64.72	0.66	20.93	0.281	0.02-2.00
Mean		48.32	0.58	15.16	0.390	
±SEM		±8.38	±0.08	±2.91	±0.163	
102269	4	74.95	0.49	19.29	0.382	0.01-0.20
	8	43.13	0.46	12.78	0.370	0.01-2.00
	12	66.34	0.57	22.17	0.192	0.01-2.00
	20	51.41	0.57	20.21	0.168	0.02-2.00
Mean		59.11	0.52	18.61	0.278	
±SEM		±7.23	±0.06	±2.03	±0.057	
92270	4	37.11	0.35	8.00	1.614	0.01-0.50
	8	28.93	0.26	8.25	0.775	0.01-2.00
	12	29.30	0.35	8.20	0.399	0.01-2.00
	20	26.06	0.34	9.43	0.425	0.02-0.50
Mean		30.35	0.33	8.47	0.803	
±SEM		±2.37	±0.02	±0.32	±0.284	
4670	2	57.27	0.29	10.38	2.393	0.01-0.50
	4	44.21	0.30	10.47	1.032	0.01-1.00
	8	26.20	0.20	7.64	0.234	0.01-5.00
	12	29.49	0.23	9.20	0.195	0.01-2.00
	20	42.13	0.35	13.77	0.276	0.02-2.00
Mean		39.86	0.27	10.29	0.926	
±SEM		±3.57	±0.03	±1.01	±0.516	
51370	8	3.06	0.11	8.95	0.031	0.01-0.50
91169	8	8.40	0.20	9.39	0.402	0.01-0.20
9870	12	6.51	0.26	11.49	0.012	0.01-0.50
122369	2	100.29	0.35	17.10	1.983	0.01-1.00
1870	12	3.17	0.080	11.01	0.011	0.01-0.20
91069	8	19.25	0.10	4.45	3.899	0.01-0.50
10369	8	30.66	0.23	12.34	3.088	0.01-0.10
101570	8	19.21	0.16	5.67	0.052	0.01-1.00
51270	8	7.19	0.20	5.08	0.147	0.01-0.50
31170	20	2.01	0.017	4.87	0.002	0.02-1.00
Average mean		26.96	0.24	10.24	0.859	
±SEM		±7.45	±0.04	±1.20	±0.334	
Median		19.23	0.22	10.09		

As can be noted from Table II, the average mean transfer function was determined to be

$$H(s) = \frac{26.96s^{0.24}}{(10.24s+1)\ (0.002s+1)} \quad . \qquad \text{Eq. (2)}$$

The value of τ_s (short-time constant of torsion pendulum) was arbitrarily set at 0.002. This value results from a biophysical analysis of the pigeon's semicircular canal by Money et al. (1971).

Figure 4 presents a plot of Eq. (2) except that the plot represents a mathematical integration of the transfer function and thus relates instantaneous action potential frequency to angular head velocity.

FIG. 4

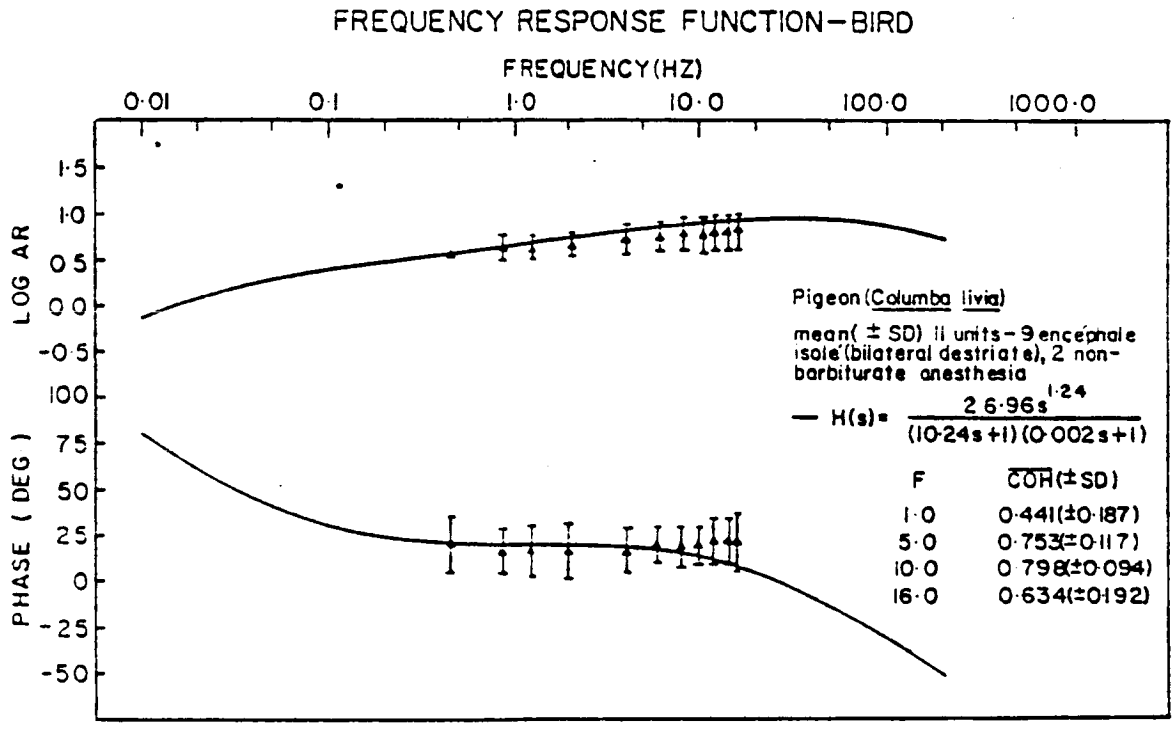

The solid lines drawn in Fig. 4 represent evaluation of Eq. (2) which is the mean transfer function obtained from analysis of 14 units from an anesthetized preparation exposed to sinusoidal rotation over a frequency range of 0.01-2.0 Hz. One of the goals of the current year's effort was to

extend the range of analysis to higher frequencies and obtain responses from an unanesthetized preparation. Average responses (± 1SD) from 11 units tested in unanesthetized preparations using Gaussian bandlimited noise (DC-20 HZ) are shown as triangles in Fig. 4. Coherence values are presented for selected frequencies as an indication of confidence in data points. It is apparent from Fig. 4 that data from unanesthetized preparations over an extended upper frequency range can be described by the transfer function (Eq. (2)) derived from data at lower frequencies using an anesthetized preparation.

Table II clearly demonstrates that there is a continuum of values for the parameters k and τ_L. Thus it appears that each ampullary afferent has its own response dynamics and adaptative properties.

We further analyzed the driven discharge data presented in Fig. 4 to see if either of the parameters τ_L or k correlated with statistical parameters associated with spontaneous discharge. An important relation appears to obtain. Coefficient of variation (C.V.) of the resting discharge of a neural unit is positively correlated (significant at the 5% level) with the neural adaptation parameter k and the best fit estimated regression line is

$\hat{CV} = 0.25\hat{k} + 0.15.$

To determine the applicability of the general transfer equation form presented in Fig. 4 and to test the validity of the parameters obtained by our frequency domain calculations, we wrote a computer program, based on an algorithm kindly provided us by Dr. A.R. Didonato, USHAVWC, Dohlgren, VA, to perform an inverse Laplace transform of the transfer function represented by Eq. (2). The time domain function which corresponds to this equation for an acceleration pulse (b seconds wide) is

(a) $0 \leq t \leq b$

$$f(t) = \frac{1}{(\tau_L - \tau_s)} \frac{1}{t^{k'}} \left\{ e^{-t/\tau_L} \gamma^*(-k', -t/\tau_L) - e^{-t/\tau_s} \gamma^*(-k', -t/\tau_s) \right\}$$

Eq. (3)

$$y(t) = f(t)$$

(b) $t > b$

$$y(t) = f(t) - f(t-b)$$

Eq. (4)

where γ^* is the incomplete gamma function and $k' = k-1$.

These equations were applied to time domain responses of neural units whose frequency domain transfer function parameter values are presented in Table II. Figures 5 and 6 present theoretical time domain curves (based on evaluation of Eqs. (3) and (4) using parameter values in Table II) to short (1.2s) and long (93.4s) duration angular acceleration pulses, respectively.

FIG. 5

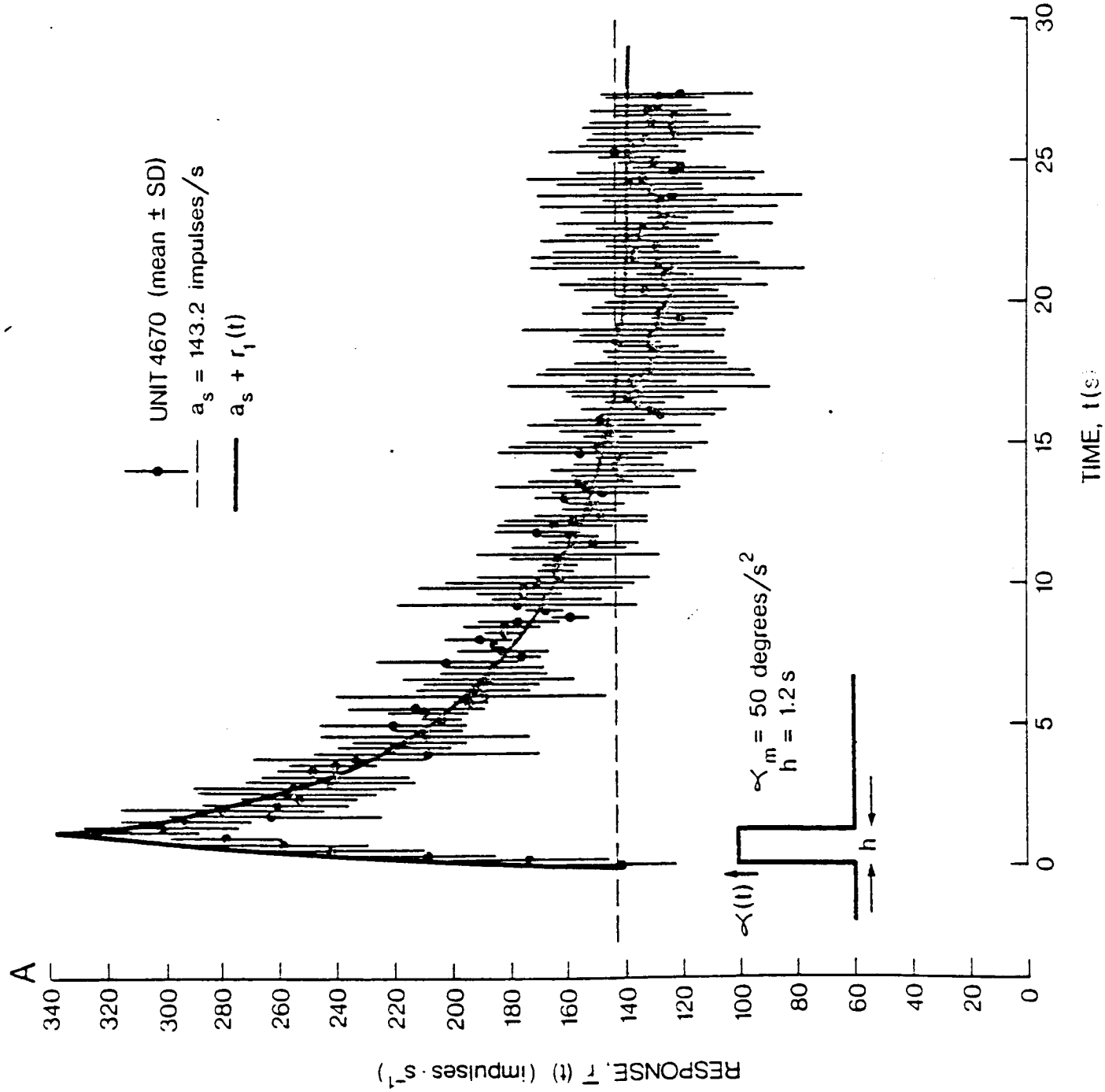

FIG. 6

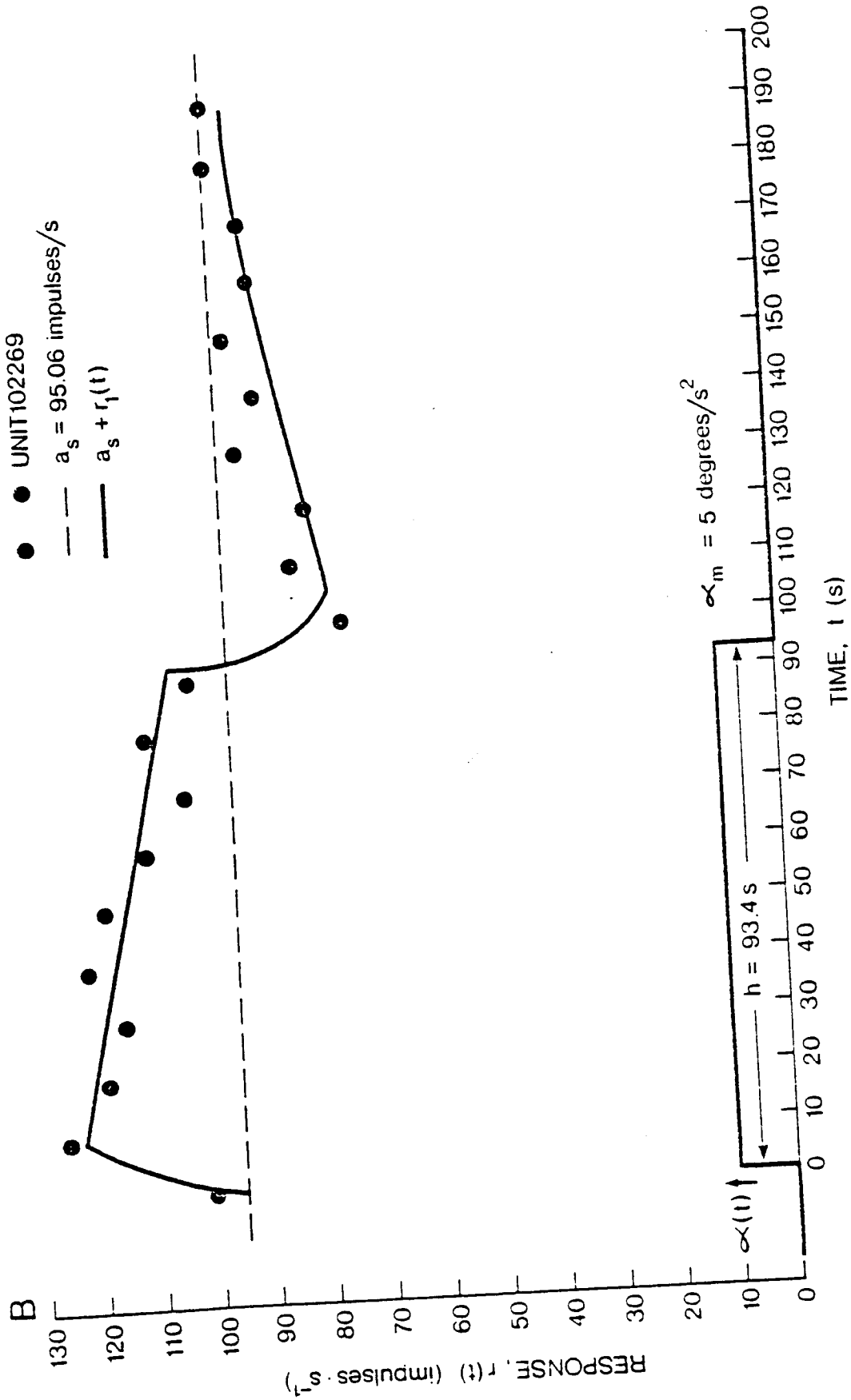
B
UNIT102269
a_s = 95.06 impulses/s
$a_s + r_1(t)$
RESPONSE, r(t) (impulses · s^{-1})
130
120
110
100
90
80
70
60
50
40
30
20
10
0
$\alpha(t)$
h = 93.4 s
α_m = 5 degrees/s^2
0 10 20 30 40 50 60 70 80 90 100 110 120 130 140 150 160 170 180 190 200
TIME, t (s)

The long duration angular acceleration pulse had a constant value of $5.0^{\circ}/s^2$ and the short duration angular acceleration pulse had a constant value of $50^{\circ}/s^2$. In Fig. 5, the theoretical curve is superimposed on mean neural responses (average of 3 replications - bars indicate plus or minus one standard deviation). In Fig. 6 the theoretical curve is superimposed on a single neural response to a long duration pulse. It is evident from these figures that the model described by Eq. (2) provides a good fit to corresponding time domain data. Moreover, perrotatory adaptation effects and postrotatory "undershoot" phenomena are described by this model.

Finally, it appears that the transfer function presented in Eq. (2), but with different constant values, is applicable to the primary afferent ampullary responses of species at each level of evolutionary development. This conclusion is based on three months work in which we fit transfer functions to frequency response function obtained from the work of several investigators using a variety of species.

2. Compared the transfer characteristics of the vestibular primary afferent system in the bird with several species; intensity functions (stimulus-response functions) and frequency response functions were calculated for the semicircular canal primary afferent system of the frog, gerbil, pigeon, guitarfish, squirrel monkey, and rhesus monkey.

Figure 2 presents four intensity functions which we obtained by analysis of data from articles by Prècht et al. (1971), Blanks et al. (1975), and Fernandez and Goldberg (1971). Figure 2B summarizes our data on the pigeon. Several interesting comparisons emerge from this figure. It appears that as one moves up the phylogenetic scale a smaller percentage of ampullary afferent responses show a nonlinear input-output relationship. For example, Precht et al. (1971), reported that in the frog, 61% (30 to 49) of the units tested showed a nonlinear relationship between stimulus and response over the range $1\text{-}10^{\circ}/s^2$. Moreover, these responses produced data, which when extrapolated back to the stimulus intensity axis, demonstrated a threshold of between $1\text{-}2^{\circ}/s^2$. By comparison, intensity functions for the squirrel monkey (Fernandez and Goldberg, 1971) which are illustrated in Fig. 2D, show the absence of a threshold and responses which are typically linear.

For all species, at least some ampullary afferents demonstrate linear response characteristics (superposition etc.). This allows us to perform a analysis of these responses. Fernandez and Goldberg (1971) were the first to provide an equation to describe ampullary afferent responses to different frequencies of rotation. A Bode plot based on their data is presented in Fig. 7.

FIG. 7

FREQUENCY RESPONSE FUNCTIONS — SQUIRREL MONKEY

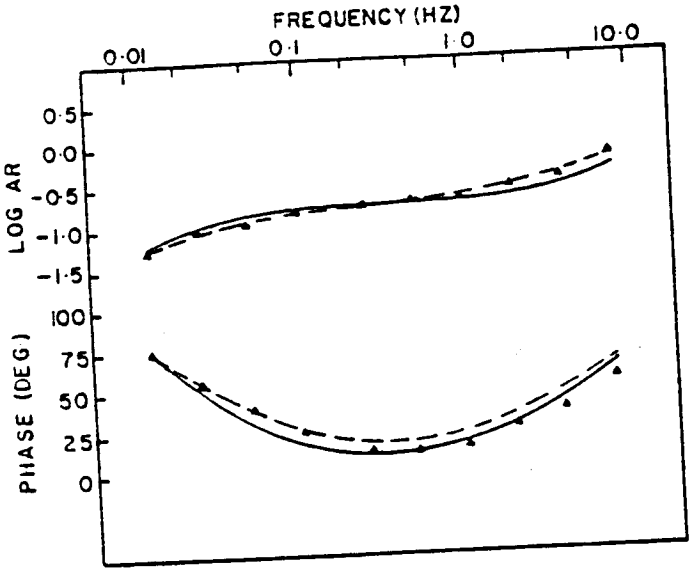

Squirrel monkey (Saimiri sciureus)
barbiturate anesthesia
mean (variable N at each frequency)
ampullary afferent response
Sinusoids
after Fernandez and Goldberg (1971)

	H(s)	MSE
—	$\frac{80s}{(80s+1)} \frac{s(0.049s+1)}{(5.7s+1)(0.003s+1)}$	0.002
---	$\frac{1.25 s^{1.16}(0.033s+1)}{(7.3s+1)(0.003s+1)}$	0.001

Both amplitude ratio and phase points are mean values based on a reasonable size but variable number of points ($6<N<56$). These investigators suggested that their frequency response function could be best described by the equation (solid line, Fig. 7):

$$H(s) = \frac{80s}{(80s+1)} \frac{s(0.49s+1)}{(5.7s+1)(0.003s+1)} \quad . \qquad \text{Eq. (5)}$$

They suggested that the term $80s/(80s+1)$ was an "adaptation operator", the terms $(5.7s+1)$ and $(0.003s+1)$ were operators corresponding to the "long- and short-time constants", respectively, of the torsion pendulum model and the term $(0.049s+1)$ corresponds to the possibility that cupula velocity information may be transduced at higher frequencies of head oscillation.

Landolt and Correia (1979) have shown that the "adaptation operator" in the above equation can be replaced by a more general operator which has been described for other sensory systems (Thorson and Biederman-Thorson, 1974). It can be shown rigorously that the operator $\tau_a s/\tau_a s+1$ is but the first in a series of terms which represent an expansion of a more general adaptation

operator, s^k. The dashed line in Fig. 7 illustrates that a transfer function containing the s^k operator produces an equivalent (possibly slightly better - cf., M.S.E. of 0.001 to M.S.E. of 0.002) fit to the Fernandez and Goldberg (1971) Bode plot data.

Figure 7 is a plot of pooled data from Fernandez and Goldberg (1971). In Figs. 8 and 9, mean plots are presented for "regular" and "irregular" units, respectively.

FIG. 8

FREQUENCY RESPONSE FUNCTIONS- SQUIRREL MONKEY

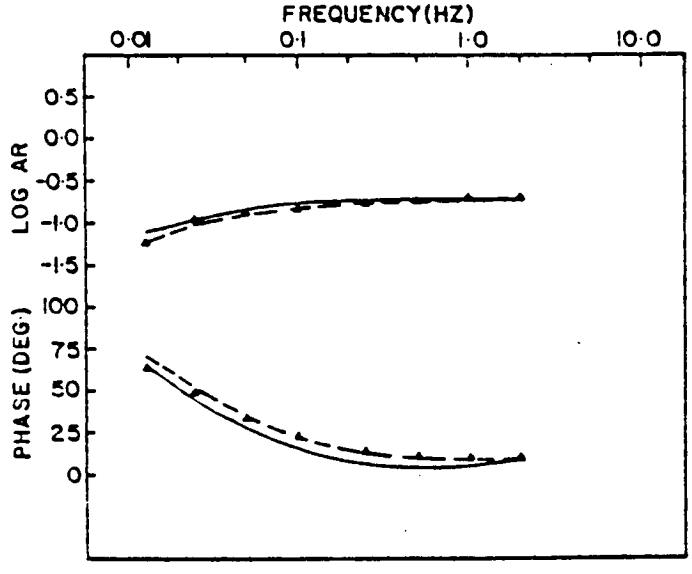

Squirrel monkey (Saimari sciureus)
barbiturate anesthesia
mean (variable N at each frequency)
Sinusoids
after Goldberg and Fernandez (1971)

"regular" units

	H(s)	MSE
—	$\frac{1{\cdot}00s(0{\cdot}017s+1)}{(5{\cdot}7s+1)(0{\cdot}003s+1)}$	0·0003
- - -	$\frac{0{\cdot}93s^{1{\cdot}06}}{(5{\cdot}6s+1)(0{\cdot}003s+1)}$	0·00006

FIG. 9

FREQUENCY RESPONSE FUNCTIONS- SQUIRREL MONKEY

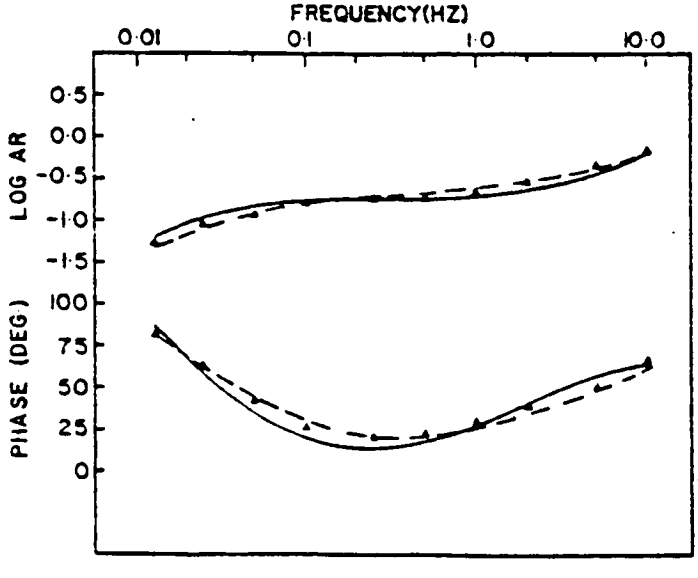

Squirrel monkey (Saimari sciureus)
barbiturate anesthesia
mean (variable N at each frequency)
Sinusoids
after Goldberg and Fernandez (1971)

"irregular" units

	H(s)	MSE
—	$\frac{33{\cdot}6s}{(33{\cdot}6s+1)}\,\frac{s(0{\cdot}08s+1)}{(5{\cdot}7s+1)(0{\cdot}003s+1)}$	0·00076
- - -	$\frac{s^{1{\cdot}16}(0{\cdot}03s+1)}{(5{\cdot}6s+1)(0{\cdot}003s+1)}$	0·00076

In Fig. 8 it can be seen that the transfer function containing the s^k operator provides a better fit (smaller M.S.E. by almost one order of magnitude) and obviates the necessity of inclusion of the zero, (0.017s+1). As pointed out earlier, a small value of k indicates little adaptation. A value of 0.06 confirms the Fernandez and Goldberg (1971) conclusion that "regular" units show slight adaptative properties. The "irregular" unit's response data (Fig. 9) does indicate more adaptation (k = 0.16) and a small but present "cupula velocity" operator (0.03s+1).

As one descends the scale in evolutionary development the transfer function of the form

$$H(s) = \frac{Cs^{k+1}}{(\tau_L s+1)\ (\tau_s+1)} \qquad \text{Eq. (6)}$$

appears to apply to other species. Figure 10 shows transfer functions of the form of Eq. (6) fit to frequency responses of "regular" (□) and "irregular" (▲) ampullary afferents in the gerbil (after Schneider and Anderson, 1976).

FIG. 10

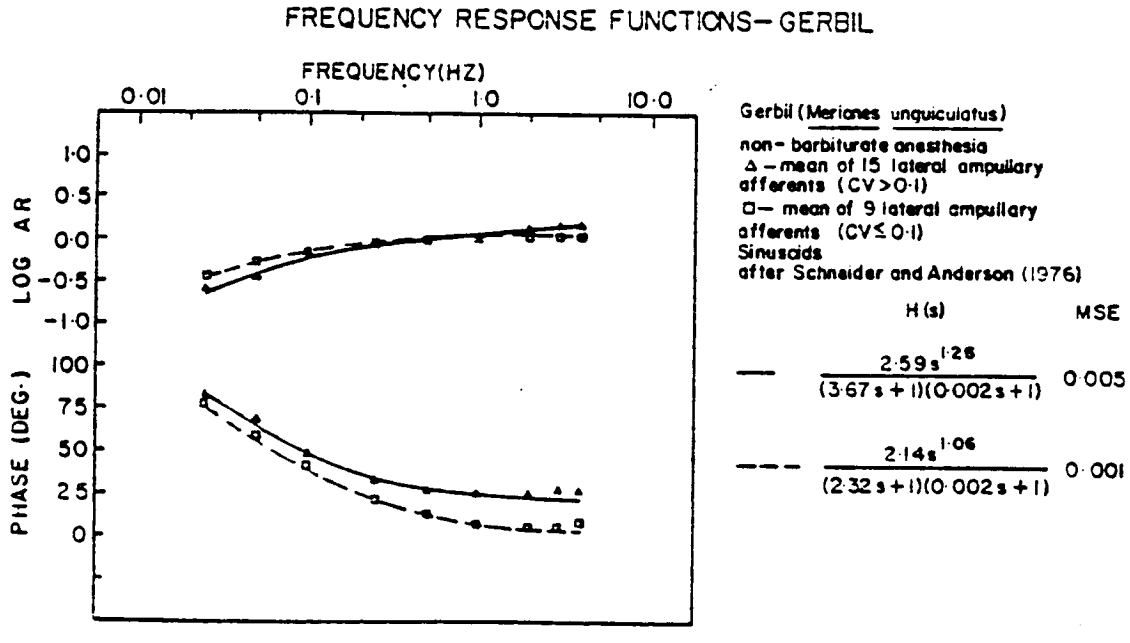

As for the squirrel monkey, "regular" neurons show less adaptation (k = 0.06) than "irregular" neurons (k = 0.26). Both types have a shorter long-time constant than that obtained for the squirrel monkey (cf., 3s for gerbil compared to 6s for monkey).

As indicated earlier, the pigeon has a mean value of k = 0.24 but k has a continuum of values which are correlated with "regularity" of discharge as quantified by the index coefficient of variation.

Lower in evolutionary development, the frequency response function for the frog also exhibits properties which are amenable to description by Eq. (6). Figure 11 shows a Bode plot which summarizes these properties.

FIG. 11

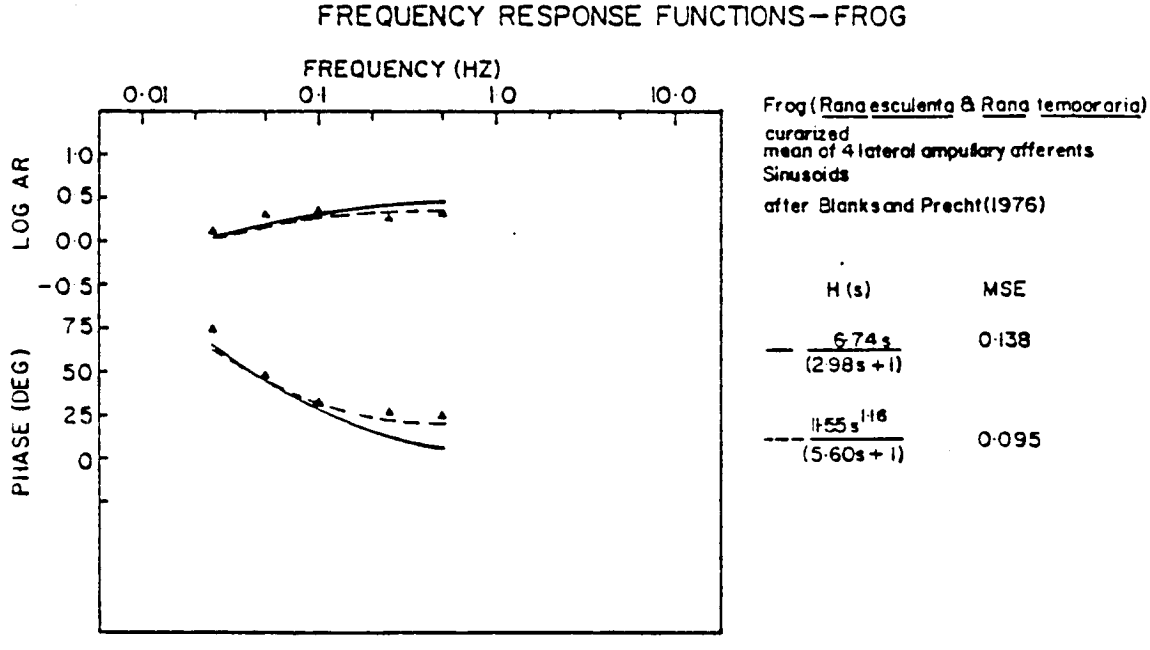

As may be noted from this plot, based on the work of Blanks and Precht (1976), the mean ampullary response has a phase lead re velocity (at 0.02 Hz) which decreases to a constant value (25°) as frequency is increased. The amplitude ratio on the other hand increases to asymptote in a region between 0.1 and 0.5 Hz. Unfortunately, Bode plots for only 4 units were presented by Blanks and Precht (1976), and no indication of regularity of response was given. Assuming these units showed no adaptation, that is k = 0, a value of τ_L = 2.98 was obtained. However, as can be seen from Fig. 11, the theoretical curve fit to the data is not good. The best fit value of k causes τ_L to assume a value of

5.6s. This value is contradicted by time domain studies which show τ_L to be around 3s (Precht et al., 1971). A more comprehensive frequency domain analysis of the ampullary afferent system of this species should be conducted.

Finally, the guitarfish ampullary afferent response has been typed into four general classes (O'Leary and Honrubia, 1976). One of the classes has been described as showing clear neural adaptation. Figure 12 is a Bode plot of this class of guitarfish ampullary afferent responses.

FIG. 12

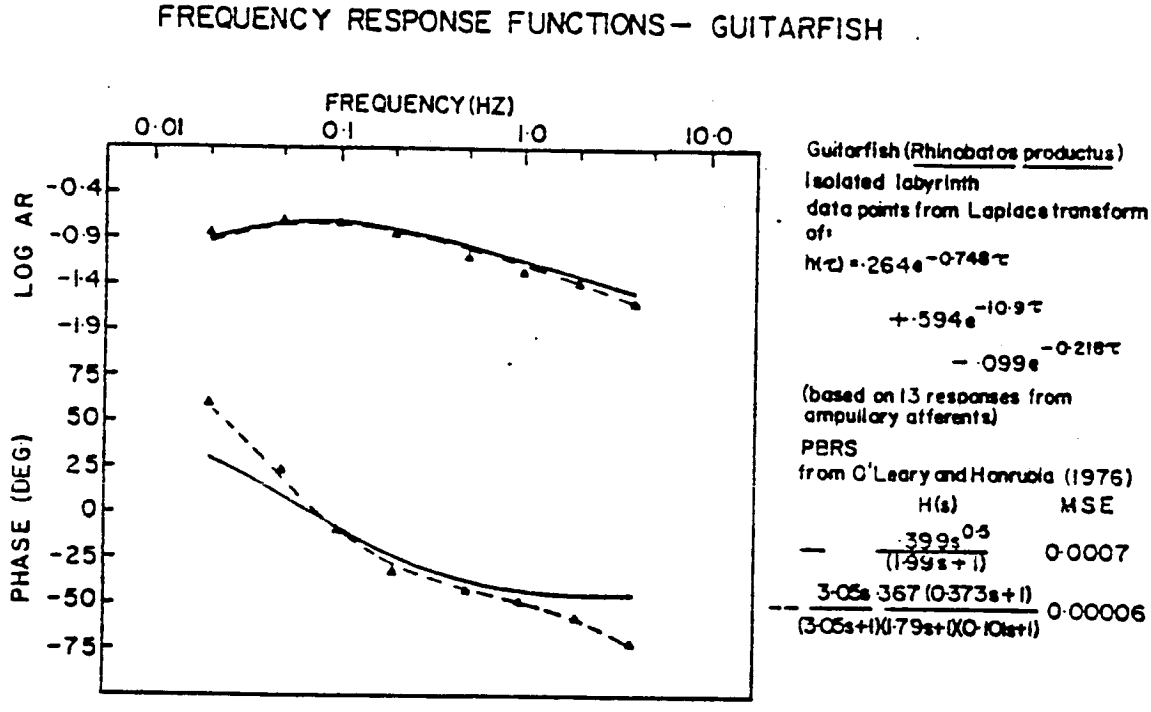

It is clear that a transfer function of the form of Eq. (6) (solid line) does not fit the amplitude ratio and phase values. However, as pointed out earlier, s^k can be represented as a series of poles and zeros when there are only several orders of adaptive processes operating in neural transduction of head velocity (Landolt and Correia, 1979). Such a series is represented in Fig. 12 as a dashed line and it is clear that this form of Eq. (6) clearly describes the guitarfish's frequency response function.

With the exception of the frog, the value of τ_L derived from best fit of frequency response functions of the form presented in Eq. (6) is quite close

to that derived from biophysical calculations (Jones and Spells, 1963). This observation suggests that if the s^k operator is not included in the transfer function, erroneous values of τ_L result.

Table III compares values of τ_L calculated from best fit of the data from ampullary afferents (with account taken of adaptation) and those derived for biophysical measurements (size, volume measurements etc.). As can be noted from the values in Table III, a clear correspondence exists for most species.

TABLE III

COMPARISON OF BIOPHYSICAL PREDICTIONS OF τ_L AND ESTIMATED VALUES OF τ_L FROM AMPULLARY AFFERENT DATA

Species	Ampullary afferent	τ_L (Biophysical)	τ_L (Primary afferent)
Squirrel monkey	Pooled (Lat. + ant. + pos.)	—	5.73 ± 0.23[1]
Cat	Lateral	5.00	(1) 3.70[2], (2) 4.95 ± 1.87[3]
Gerbil	Lateral	3.51	(1) 2.5[4], (2) 3.00*
Pigeon	Anterior	10.19	10.24[5]
Frog	Lateral	2.54	(1) 1.9[6], (2) 2.98*, (3) 3.0[7]
Guitarfish	Lateral	4.99	2.66 ± 1.22[8]

[1]Fernandez and Goldberg, 1971; [2]Blanks et al., 1975; [3]O'Leary et al., 1978; [4]Schneider and Anderson, 1976; [5]Landolt and Correia, unpublished observations; [6]Blanks and Precht, 1976; [7]Precht et al., 1971; [8]O'Leary et al., 1978. *Derived from best fit transfer function.

The data in the above table and the foregoing discussion leads to several generalizations. (1) The ampullary afferent responses of most species show the following types of nonlinearities: (a) rectification, (b) asymmetry for "excitatory" and "inhibitory" stimuli - a unidirectional rate sensitivity, (c) a decay in response ("neural adaptation") during a velocity step input followed by an "undershoot" or "overshoot" after stimulus termination, and (d) soft saturation in the intensity function particularly for animals such as the pigeon and frog. (2) Over a restricted stimulus and frequency range, the linear system response can be modeled by a transfer function which contains: an adaptation operator, s^k, poles corresponding to the torsion pendulum model - (τ_L+1) (τ_s+1), and in the case of primates an additional zero, (τ_y+1) (3) Apparently, after accounting for adaptation, τ_L deduced from ampullary

afferent discharge is close to that obtained from biophysical calculations derived from the "torsion pendulum model" and ranges from 3.0-6.0s (except for the pigeon). (4) The gain (AR) re velocity at 0.25 Hz appears to be five times greater in the frog and pigeon than in mammals which ranges from 0.50 to 1.05 $I \cdot s^{-1}/d \cdot s^{-1}$ on the average. (5) The constant k, in the term s^k, appears to decrease, on the average, as one progresses upward in phylogenetic development indicating less and less "adaptation".

3. Horseradish peroxidase (HRP) was injected into (and contained within) the endolymphatic spaces of the inner ears of 10 pigeons.

Using procedures which we have developed, we injected HRP into the pigeon's membranous labyrinth and produced the following previously unreported results: (1) we produced clear anterograde and retrograde transport to the vestibular nuclei and to efferent neurons in an adult animal. (2) We found two clusters of neurons which appear to be cells of origin of vestibular efferents. (3) We found cells in a location in the brain which corresponds to a region thought to be associated with auditory efferents.

Figure 13 shows a coronal section through a pigeon's brain. On the left-hand side of the figure, stained fiber tracts from the vestibular nerve root to the vestibular nuclei are apparent.

FIG. 13

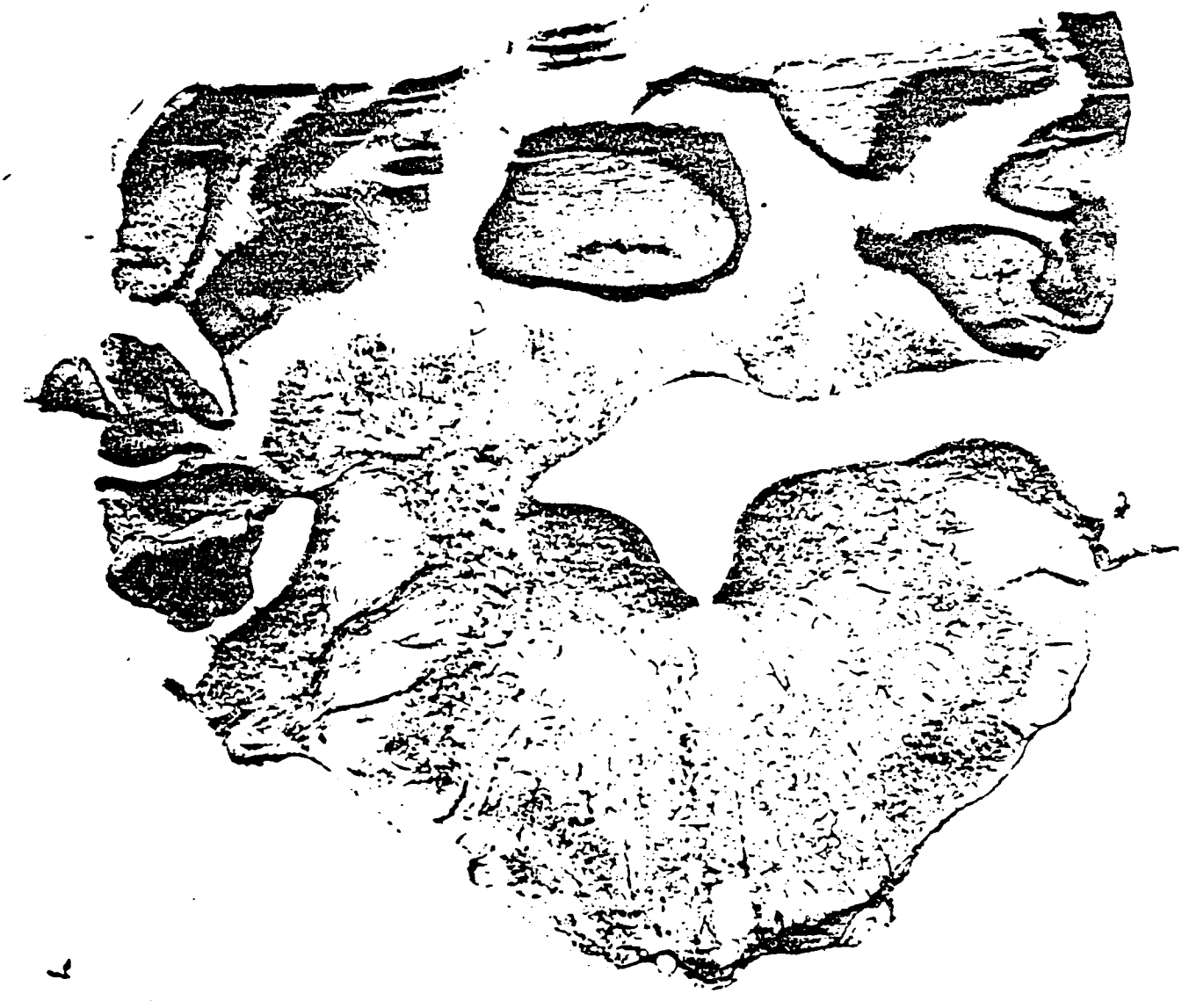

CONFIDENTIAL AND
PRIVILEGED INFORMATION

FIG. 14

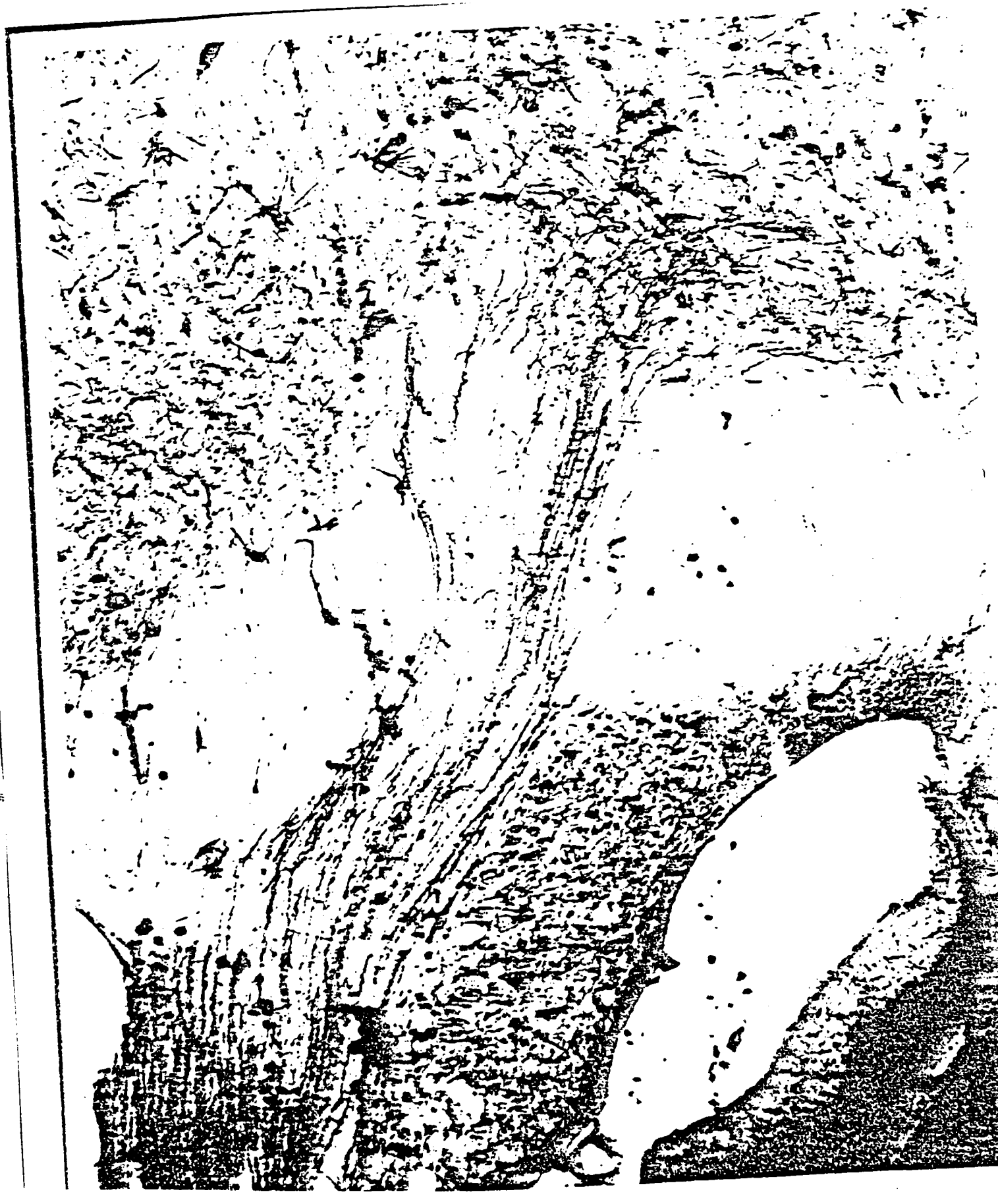

We are currently quantifying the sites of termination of these primary afferent fibers within the vestibular nuclei. We are highly encouraged that the sensitivity of our techniques produce such a high density of stained fibers (anterograde transport staining) in an adult animal. In the future we hope to estimate the percentage of stained afferents which project to each of the nuclei and examine the sites of termination of these afferents using transmission electronmicroscopy (TEM).

Figure 15 summarizes the results we have obtained from localization of efferent neurons (retrograde transport) in the pigeon's brainstem.

FIG. 15

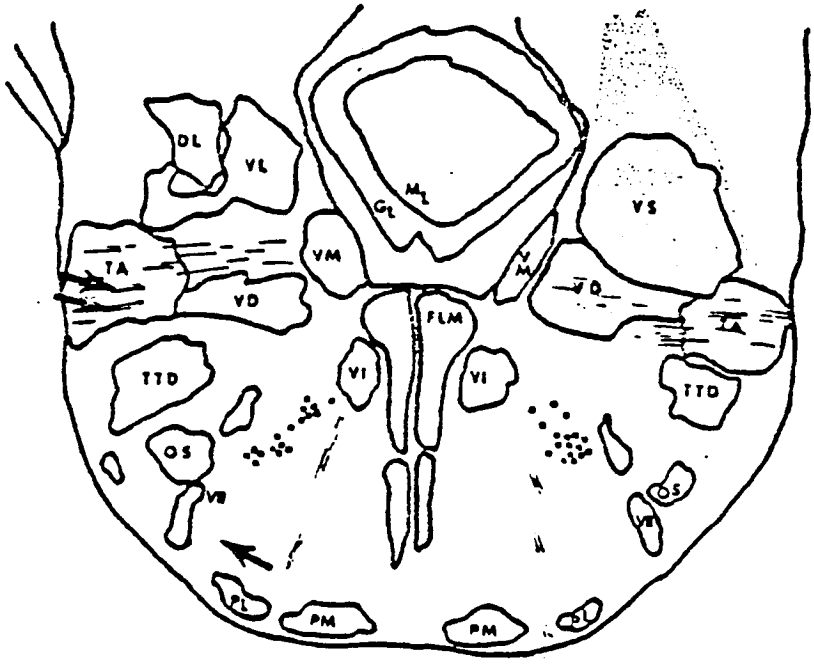

Fig. 5. Semidiagrammatic view of efferent vestibular neurons found labeled after [^{3}H]adenosine injection into the left horizontal canal crista. Cells found in this (obliquely cut) section are marked by circles, those found in neighbour sections up to 120 μm rostral or caudal to this section are shown as squares. The region exhibiting anterograde label (cf. Fig. 4) (ipsilateral vestibular nuclei) is stippled. VS, VD, VM, VL, DL, TA = nucleus vestibularis superior, descendens, medialis, ventrolateralis, dorsolateralis and tangentialis respectively; TTD = descending trigeminal nucleus and tract, OS = oliva superior; PM, PL = nucleus pontis medialis and lateralis; FLM = fasciculus longitudinalis medialis; VI = nucleus abducens; VII = nucleus facialis; GL, ML = granular and molecular layer of the lingula.

(after Schwarz et al., 1978)

We have extended the preliminary work of Schwarz et al. (1978) in that we have a sample of 10 animals compared to their 1 animal; we are carefully counting cells and determining sample statistics and we have discovered two cell clusters which they failed to report.

The small squares in Fig. 15 show one cell group of efferent vestibular neurons in the pigeon's brainstem. These cells reported by Schwarz et al. (1978) are found in a narrow region within the nucleus reticularis pontis caudalis just later-ventro-caudal to the abducens nucleus (VI). We too have found efferent cells in this region. Moreover, we have found clearly labeled cells in the region of the tangential vestibular nucleus (TA) as indicated by two arrows in Fig. 15 and in a region just inferior to the superior olive (indicated by a single arrow in Fig. 15). It is tempting to speculate that the neurons located in the TA are associated with sensory end organ activity; those in the pontine reticular formation are associated with autonomic function and those in the region of the inferior olive are saccular or auditory neurons. This latter speculation presumes that HRP was transported into the endolymphatic fluids of the cochlea. Further study will provide statistics as to the extent and receptor of origin of these efferent neurons and thereby provide factual support (or lack of support) for the just stated speculations.

4. Thick sectioned epon embedded labyrinths were analyzed to describe the distribution of types of hair cells, stereocilia length, and afferent/efferent innervation patterns in various regions of the cristae ampullares.

Figure 16 is a phase contrast photomicrograph through the anterior ampulla crista ampullaris and eminentiae cruciatae. The section is 40 microns (μ) thick and the photomicrograph is focused on one level of the specimen.

FIG. 16

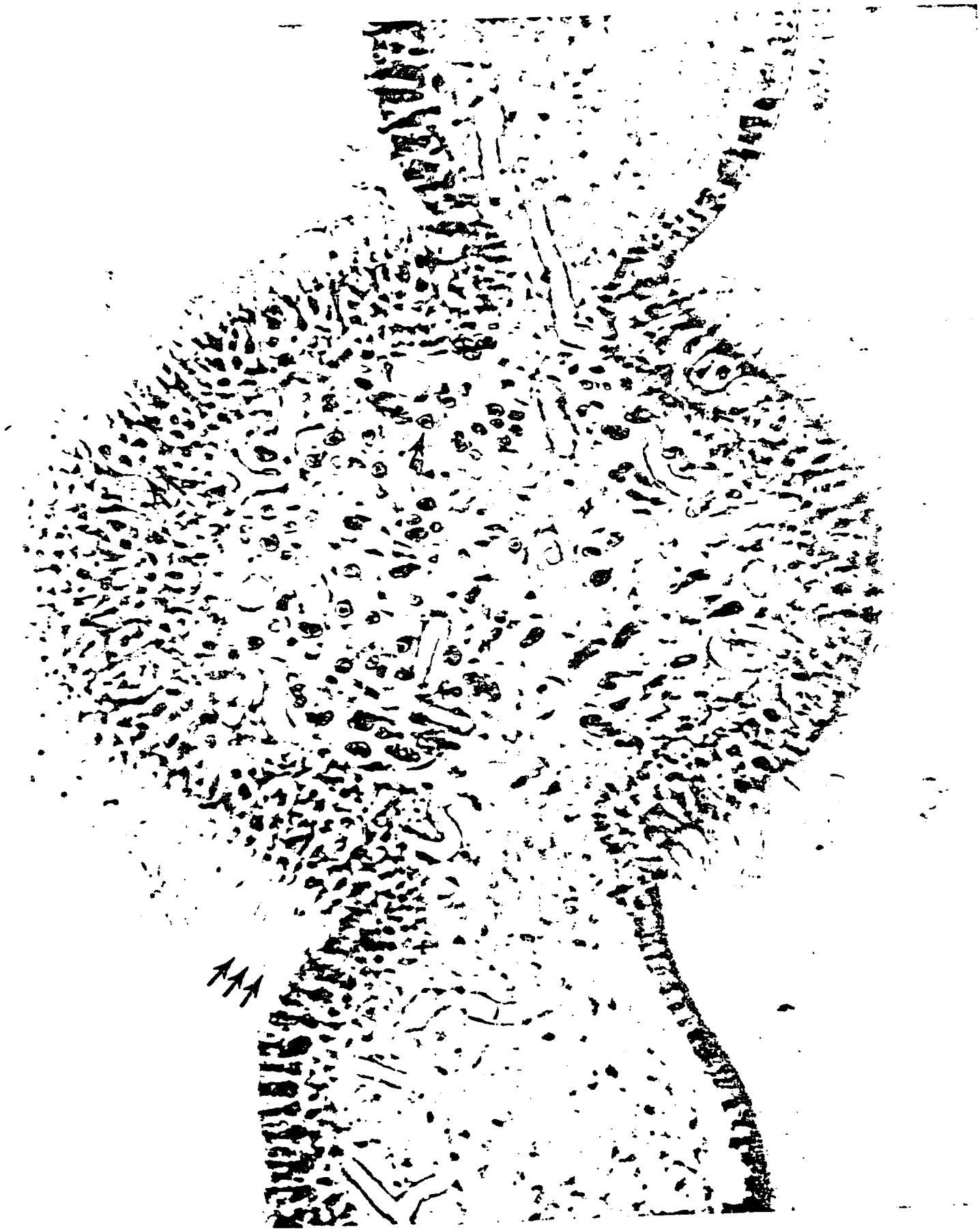

CONFIDENTIAL AND
PRIVILEGED INFORMATION

The perspective of the section is that of "looking down on the crista from above". Several features of the photomicrograph deserve comment. First, the technique which we developed during the past year to thick section epon will allow us to trace and determine cross sectional diameters of afferent fibers as they enter the crista and course upward to innervate hair cells at its bottom, top, and sides. A clearly stained myelinated afferent is indicated by a black arrow in Fig. 16. Second, since the section is 40 μ thick and since we have techniques at our disposal for ultrasectioning this section, we can re-block it and use TEM to determine the ratio of unmyelinated afferents/efferents to myelinated nerve fibers. Third, it is clear that there are multiple hair cells within the nerve chalice of the Type I hair cell (as indicated by double arrows in Fig. 16). We are currently counting these multiple hair cells and graphing their distribution on the surface of the crista. Fourth, it is clear from the photomicrograph that there are some very long kinocilia at this level of the crista (midway from base to crest). These cilia are indicated by three arrows in Fig. 16. Using special fixation procedures and thick epon sections, we hope to see if there is a difference in cilia length over different areas of the crista.

During the past year we have perfused four animals, blocked eight labyrinths, and sectioned them at different thickness (1, 10, 20, 30, and 40 μ) in three planes. Figure 16 shows a 40 micron section sliced in a plane which we have concluded is the best thickness and orientation to address the goals for our next year's research which we will now describe.

VI. PROGRESS - 1976/1978

PROGRESS REPORT
(May 1, 1976 - January 31, 1978)
NASA - 14641, REF 9BC[illegible]-07-76P

1. Linear and Non-Linear Transfer Characteristics of the Pigeon's Vestibular Primary Afferent System

Sinewave analysis of driven discharge from fibers innervating the horizontal and anterior ampullary receptors in the pigeon have yielded the following results.

Sine wave analysis - linear responses. We have determined a transfer function which relates first harmonic neural response (N=50) to sine wave angular acceleration input. This transfer function is of the form

$$H(s) = \frac{Ks^k}{(\tau_1 s+1)(\tau_2 s+1)}$$

where the parameter ranges for best iterative values are

$$3.06 \leq K \leq 66.19$$

$$0.02 \leq k \leq 0.35$$

$$4.45 \leq \tau_1 \leq 19.29$$

and τ_2 is constrained on the basis of biophysical measurements to the range

$$0.002 \leq \tau_2 \leq 0.005 \quad .$$

The so-called "long-time constant", τ_1, which has been determined empirically, has a range of values which incorporate those found by Grant and Von Buskirk (1976) in their analysis of the biophysical properties of the vestibular endorgans in the pigeon. A bode plot which shows a best-fit model to the amplitude ratio and phase of a representative neural unit is illustrated in Figs. 1a and 1b respectively.

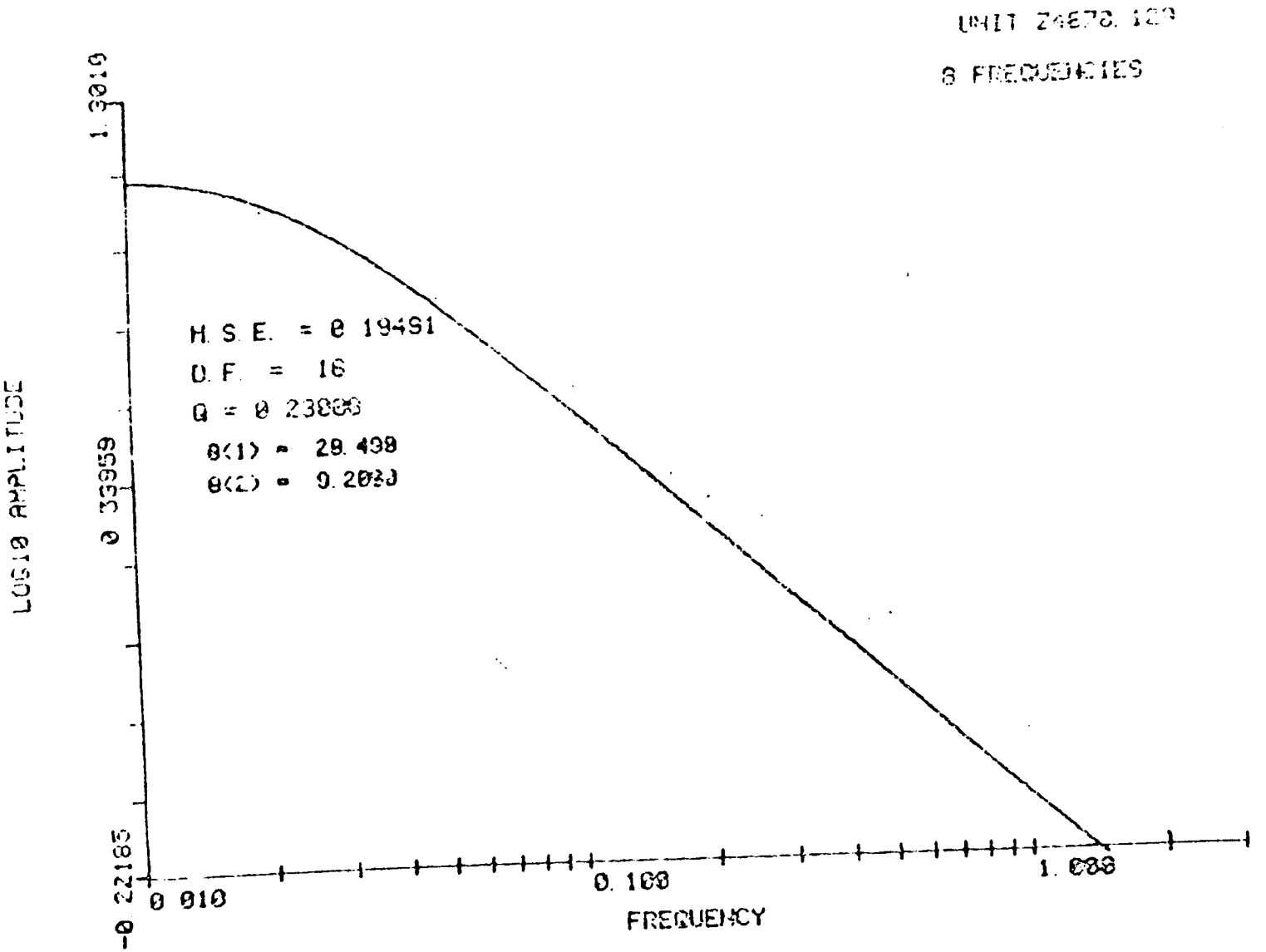

Figure 1a. Amplitude ratio of instantaneous frequency of primary afferent neural output relative to head acceleration of a representative unit. Best fit transfer function is indicated by the solid line.

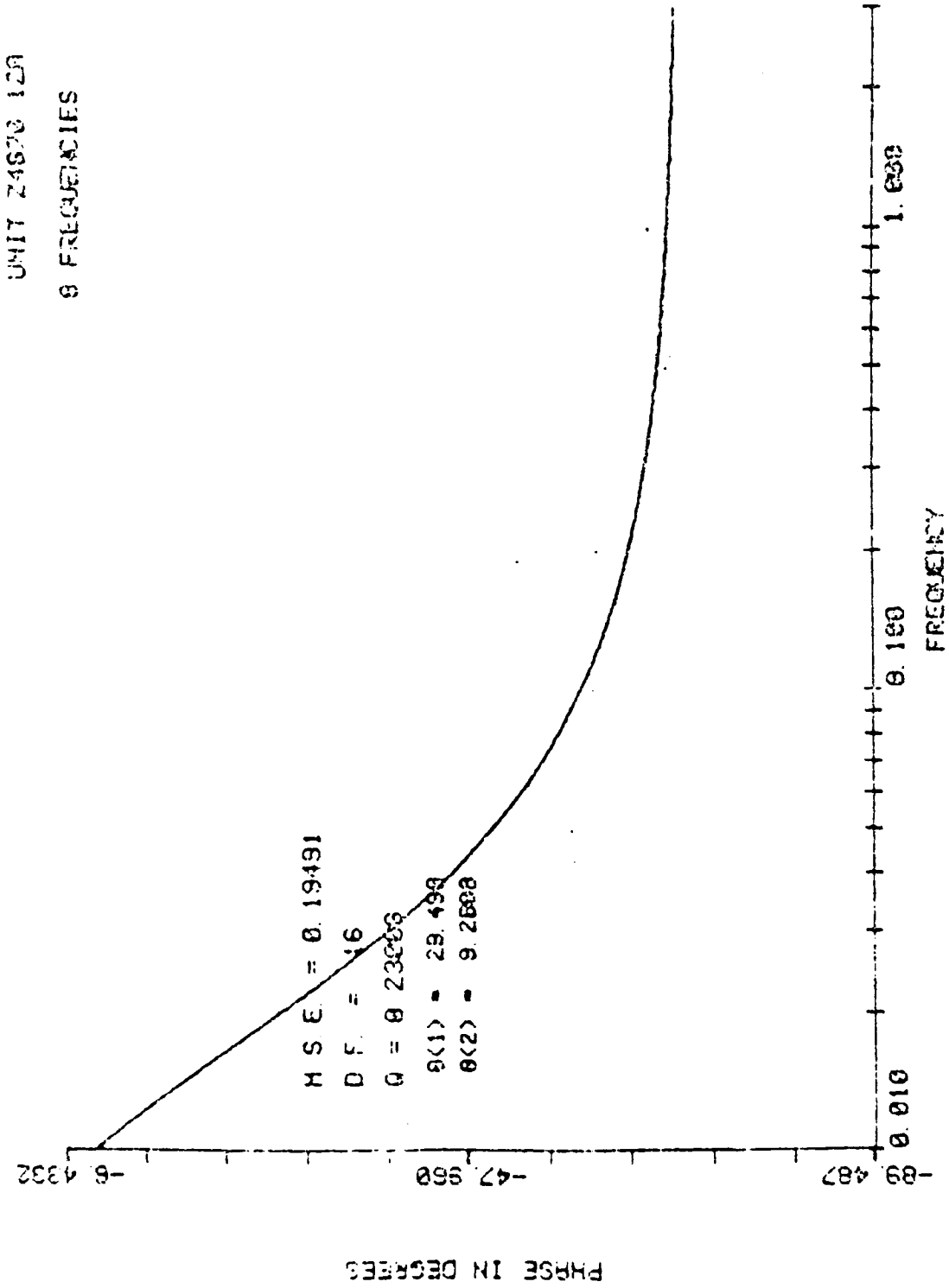

Figure 1b. Phase corresponding to amplitude ratio shown in (a).

Sine wave analysis - non-linear responses. Vestibular primary afferent responses to sine waves of varying intensities produce three types of non-linearities in some units. First, there is an amplitude dependent non-linearity in which the sine wave neural response becomes half-wave rectified during one-half of the rotational cycle. Second, there is an amplitude dependent non-linearity which exists for all sensory systems which can be termed a saturation non-linearity. Thus, as stimulus intensity is increased over many log units, the response follows as a power function. Third, the same non-linearity exists in the primary afferent system and has been described in the vestibular nuclei (Milsum and Melvill Jones, 1969). This dynamic asymmetry which is of a unidirectional rate sensitivity form, produces an asymmetry between the rising quarter-cycle of neural response and the falling quarter-cycle of the neural response. Examples of the three types of non-linearities described above are illustrated in Figs. 2, 3, and 4 respectively.

Wiener noise analysis of the driven response of fibers innervating the horizontal and anterior ampullary receptors has yielded the following information which essentially substantiates the results obtained with sine wave analysis.

Wiener noise analysis - linear responses. Using random noise input rotational stimuli, transfer functions have been calculated for 45 neural units innervating the horizontal and anterior ampullary receptors. Using this technique, the bandwidth of analysis has been extended from DC-2.0 Hz (sine wave analysis) to DC-15.0 Hz. However, using these techniques, the linear transfer function appears to be of the same form as that described above which was determined using sine wave analysis. A composite graph which illustrates the response of a representative neural unit to velocity input is shown in Fig. 5.

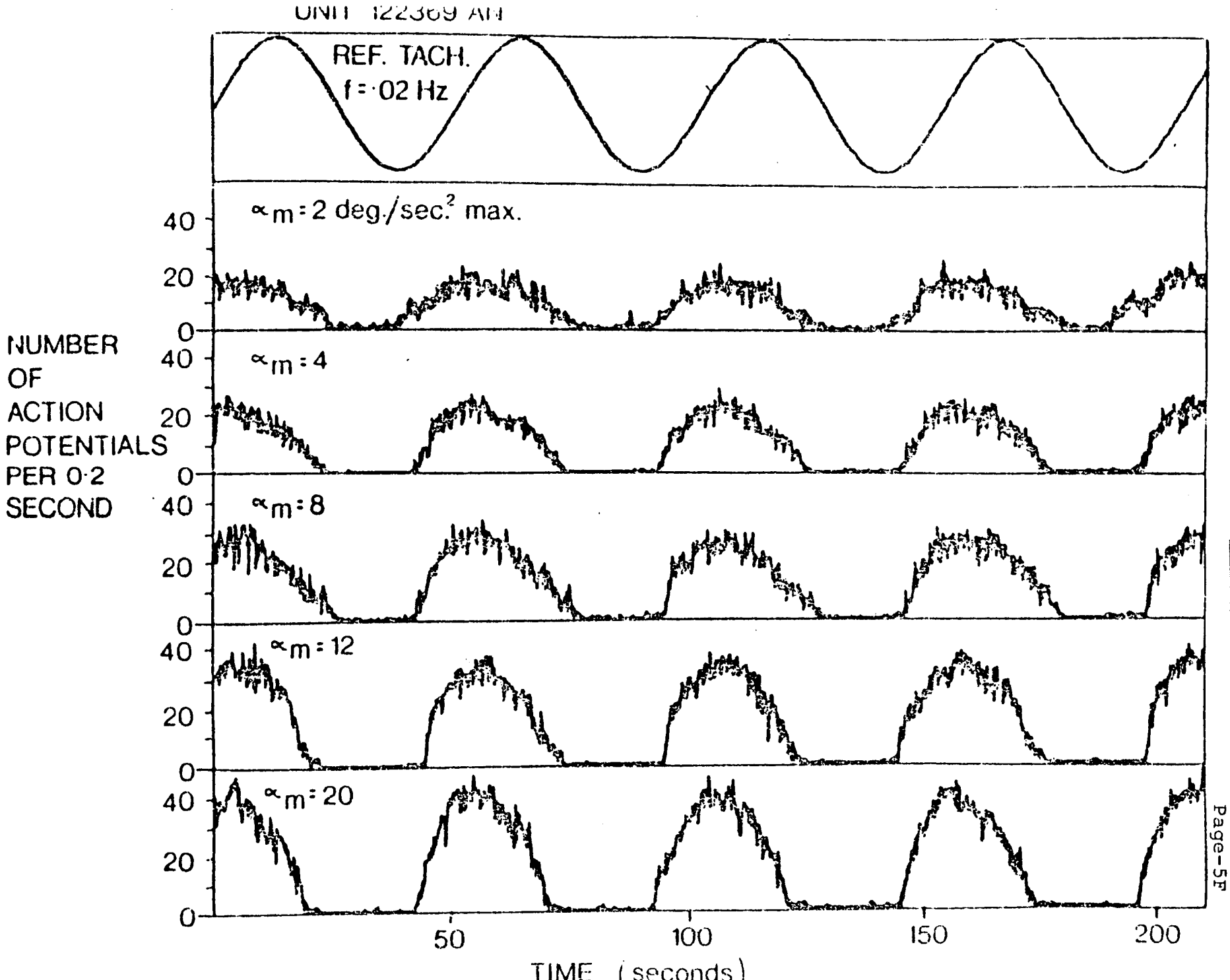

Figure 2. Plots of instantaneous frequency of firing of a vestibular neural unit exposed to increasing peak levels of angular acceleration. Note rectifying non-linearity at higher peak accelerations.

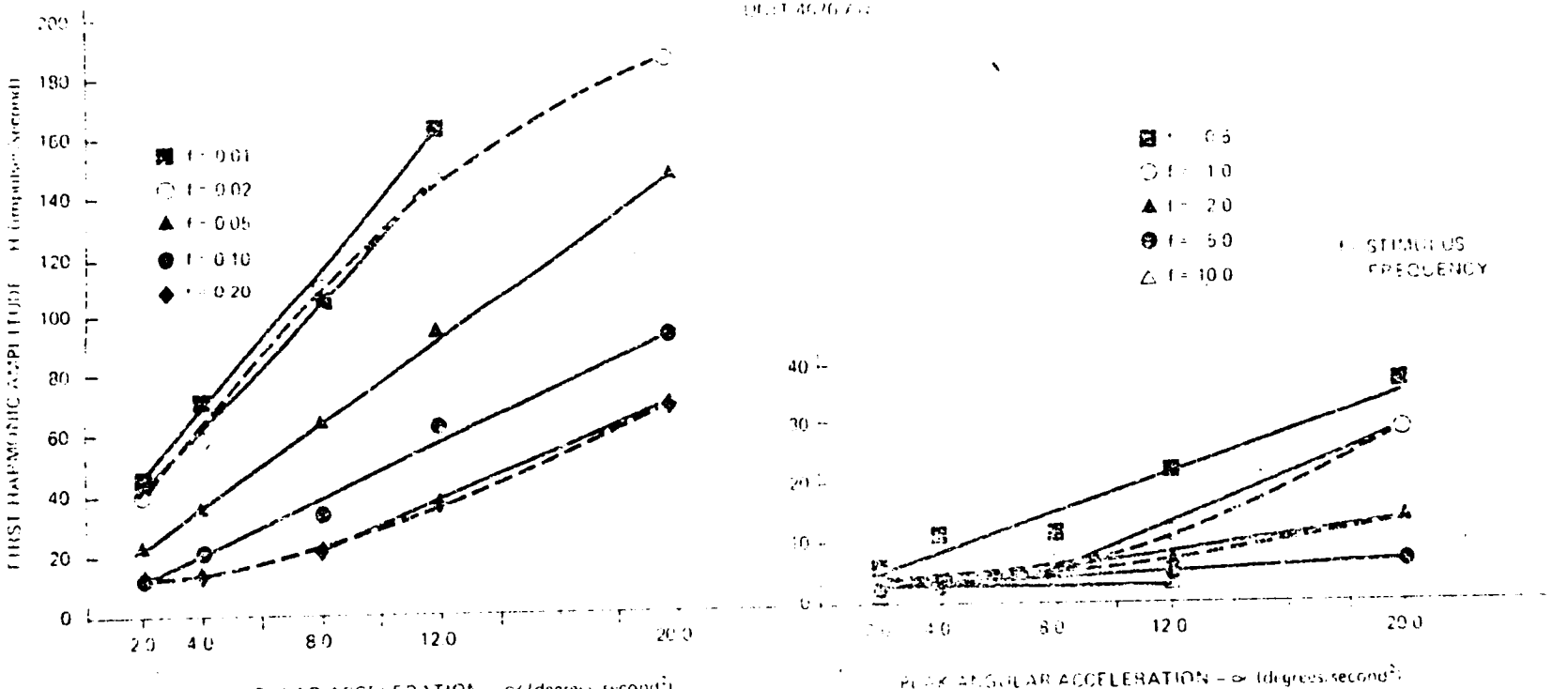

∝	f	REG EQ (1st harm)	SLOPE F	DEV FROM LINEARITY F	REG EQ (2 harmonics)
2, 4, 8, 12	0.01	H = 11.2∝ + 21.79	136.13**	0.48	
2, 4, 8, 12, 20	0.02	H = 8.1∝ + 31.64	93.82**	15.32*	H = 13.7∝ - 0.26∝² + 11.79
2, 4, 8, 12	0.02	H = 10.2∝ + 20.15	228.70**	0.24	
2, 4, 8, 12, 20	0.05	H = 6.9∝ + 7.88	1377.51**	6.85	
2, 4, 8, 12, 20	0.10	H = 4.6∝ + 1.86	335.82**	0.05	
2, 4, 8, 12, 20	0.20	H = 3.3∝ - 0.12	119.66**	27.54*	H = 1.2∝ + 0.09∝² + 7.28
8, 12, 20	0.20	H = 4.0∝ - 10.73	254.35**		
2, 4, 8, 12, 20	0.50	H = 1.6∝ + 2.24	128.54**	2.30	
2, 4, 8, 12, 20	1.00	H = 1.4∝ - 1.50	34.22**	71.01**	H = - 0.29∝ + 0.08∝² + 4.41
8, 12, 20	1.00	H = 1.9∝ - 0.10	254.35**		
2, 4, 8, 12, 20	2.00	H = 0.6∝ + 1.42	65.98**	11.44*	H = 0.11∝ + 0.02∝² + 3.17
8, 12, 20	2.00	H = 0.8∝ - 0.01	91.09**		
2, 4, 8, 12, 20	5.00	H = 0.3∝ + 1.94	15.42	0.03	* P < 0.05
2, 4, 8, 12, 20	10.00	H = 0.2∝ + 1.88	0.90	3.35	** P < 0.01

Figure 3. Plots of 1st harmonic neural response to increase in peak angular acceleration. At f = 0.02 Hz, a saturation non-linearity is apparent for higher levels of peak angular acceleration.

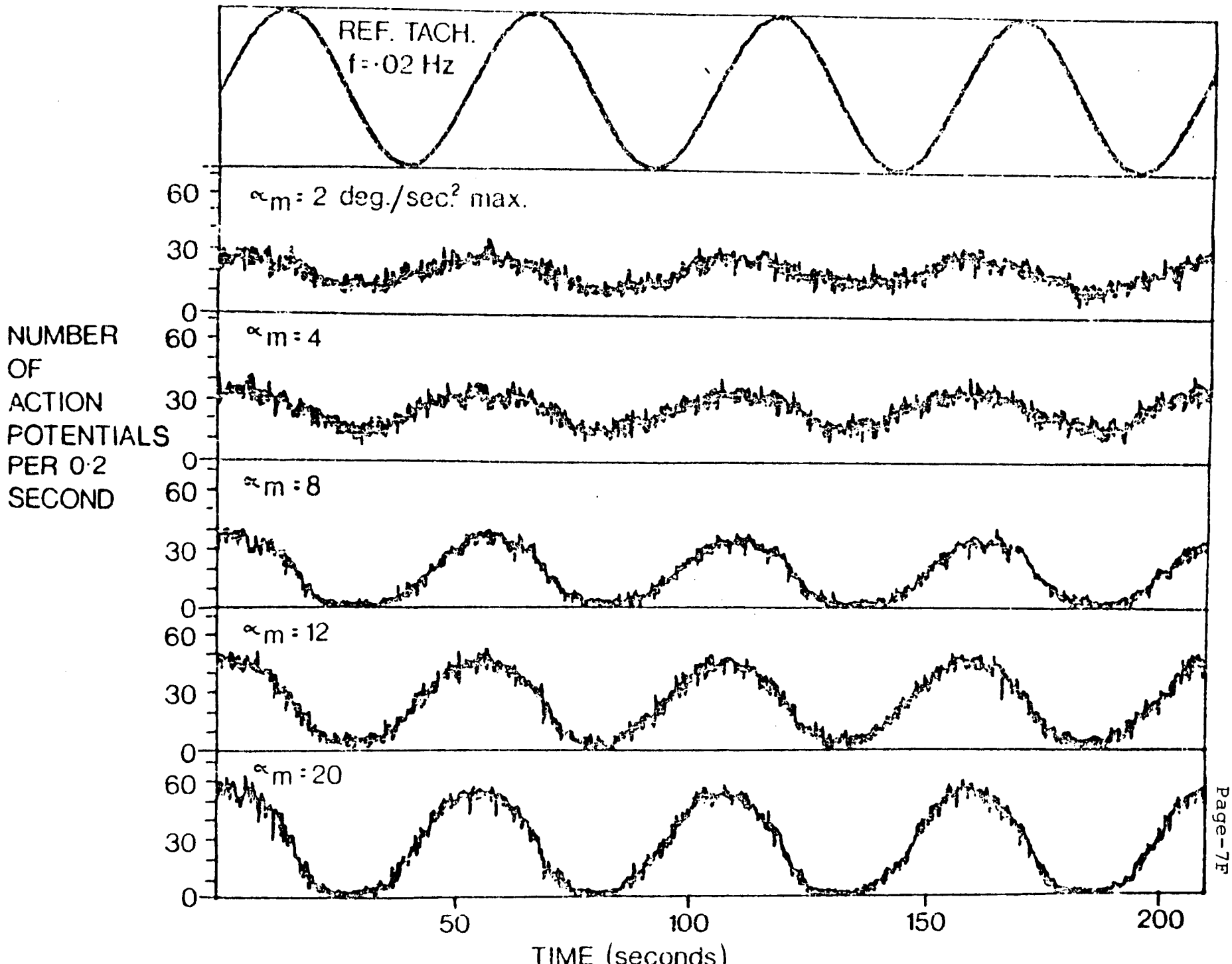

Figure 4. Plots of instantaneous frequency of firing of a vestibular neural unit exposed to increasing peak levels of angular acceleration. Note asymmetry non-linearity in the waveform.

Wiener noise analysis - non-linear responses. Wiener noise analysis of the second-order kernel produces a plot which is characteristic of a system which has a rectifying non-linearity. The characteristic which specifies this type of non-linearity is the positive peak which occurs along the main diagonal of the graph shown in Fig. 5 and which is concentrated near the coordinate points $\tau_1 = 0$, $\tau_2 = 0$. This type of non-linearity has been observed in other mechanoreceptors such as in the trochanternal hair plate sensilla in the cockroach (French and Wong, 1976). It should be stated that the graph shown in Fig. 5 is not representative for all of the neural units which we have examined, but represents a certain class which show the rectifying non-linearity which is illustrated in the sine wave analysis shown in Fig. 2.

2. A Biological Model of the Generating Mechanism for Spontaneous Discharge Observed on Primary Afferent Fibers Subserving the Ampullary Receptors

Using powerful statistical techniques, it has been determined that there are several models which can adequately describe the generating mechanism for spontaneous discharge on vestibular primary afferent fibers. A presentation and discussion of these models is presented in the accompanying reprint (Correia and Landolt, 1977). These analyses were based on data where interspike intervals (ISIs) were measured with a resolution of 1 ms. Subsequently, during the past year we have been measuring ISIs to greater resolution and several interesting findings have emerged. These findings can be illustrated by comparison of Figs. 6 and 7. Fig. 6 represents a plot of a group of units ploted using two coordinates, β_1, β_2-3. These coordinates, β_1 and β_2-3, are the coefficients of skewness and kurtosis respectively. It can be observed in Fig. 6 that for those units which were measured with the resolution of 1 ms, the units appeared to fall into two clusters, one which clustered along the Pearson type III line and the other which clustered along a line of minimal skewness

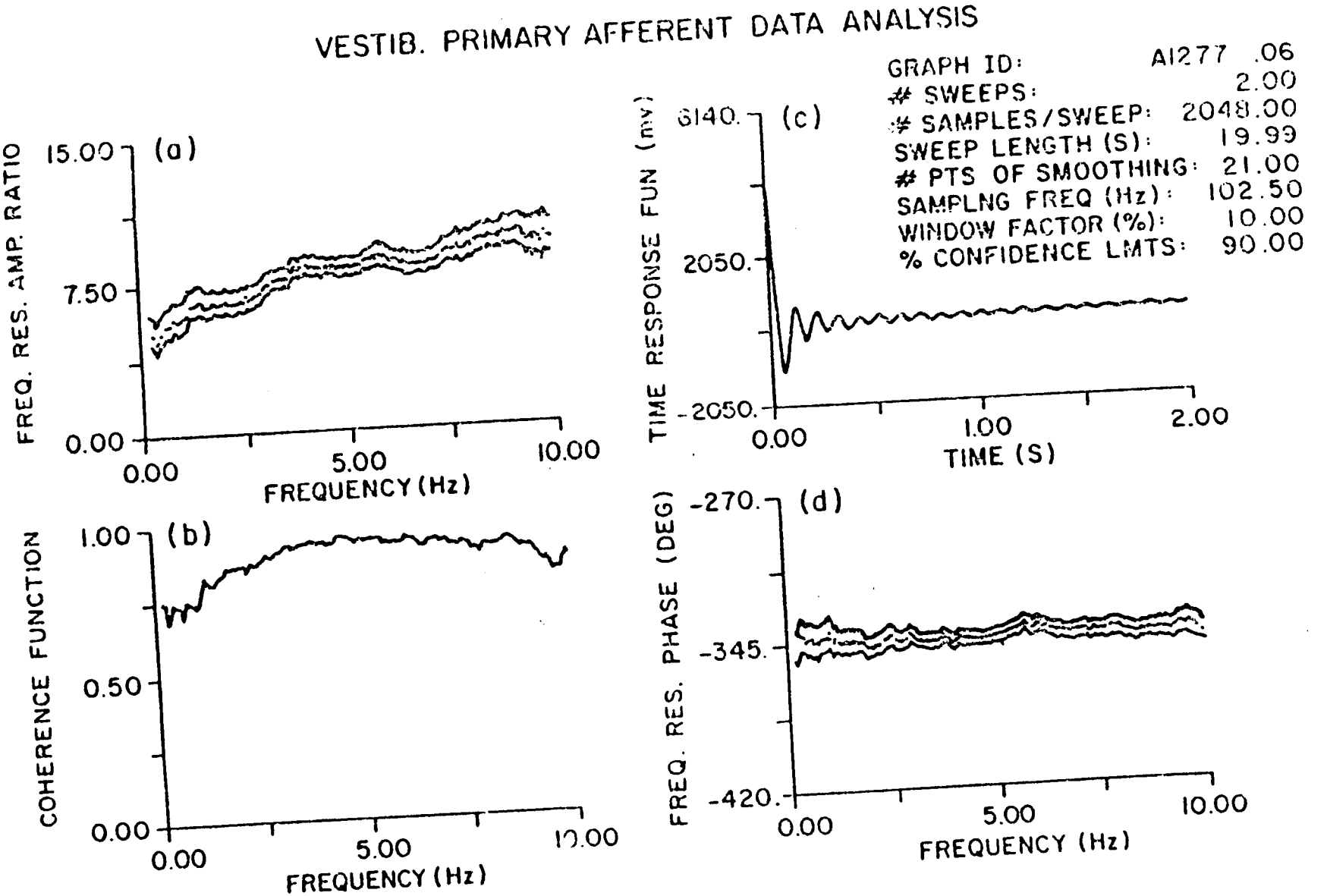

Figure 5. Composite graph showing functions which define the linear transfer characteristics of a vestibular primary afferent neural unit. Graphs were derived from data obtained during white noise rotational stimulation.

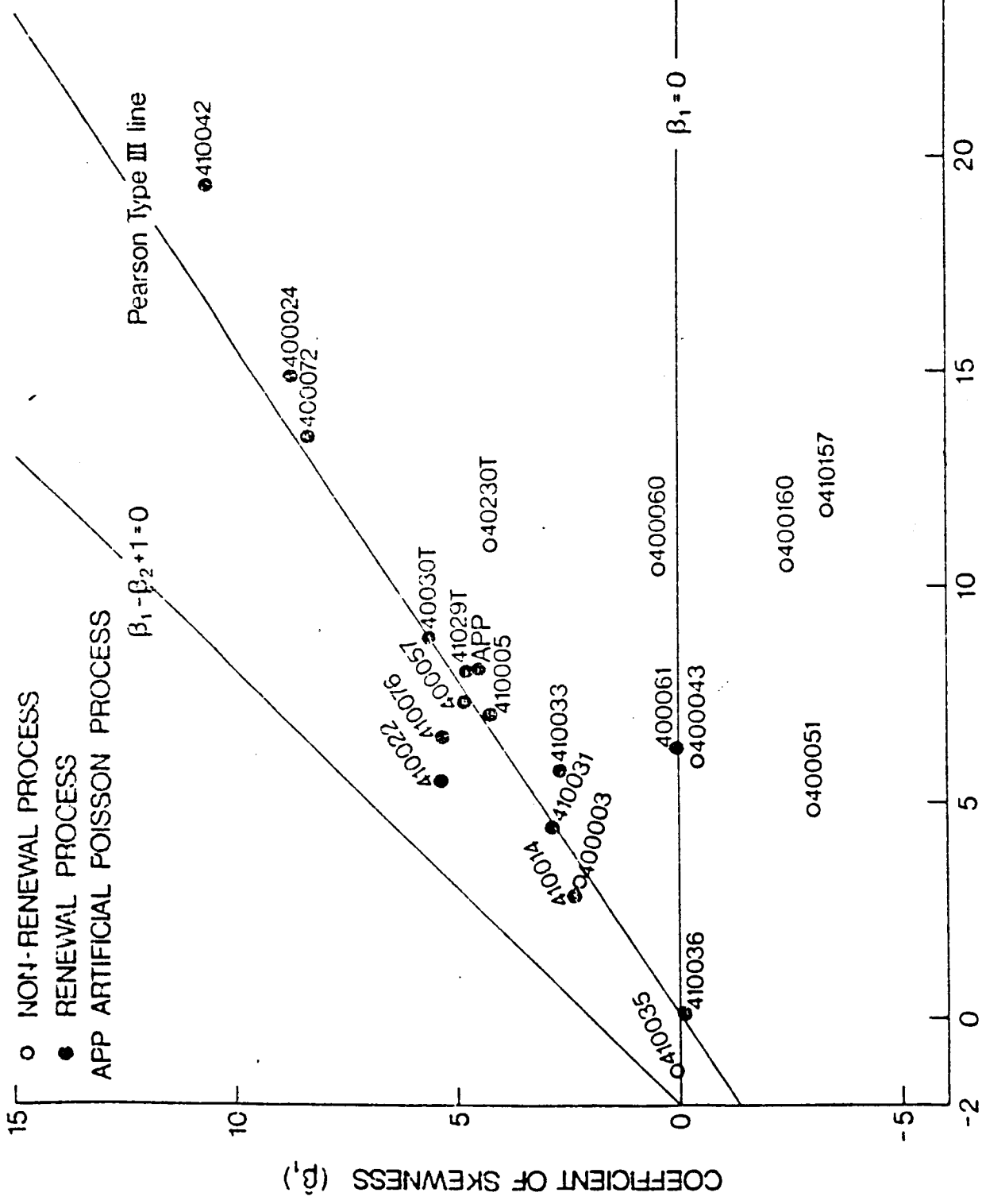

Figure 6. A plot of the coefs. of skewness (β_1) versus excess ($\beta_2 - 3$) for vestibular primary afferent neural units in an anesthetized pigeon. Note clustering of values along Pearson III line and the $\beta_1 = 0$ line.

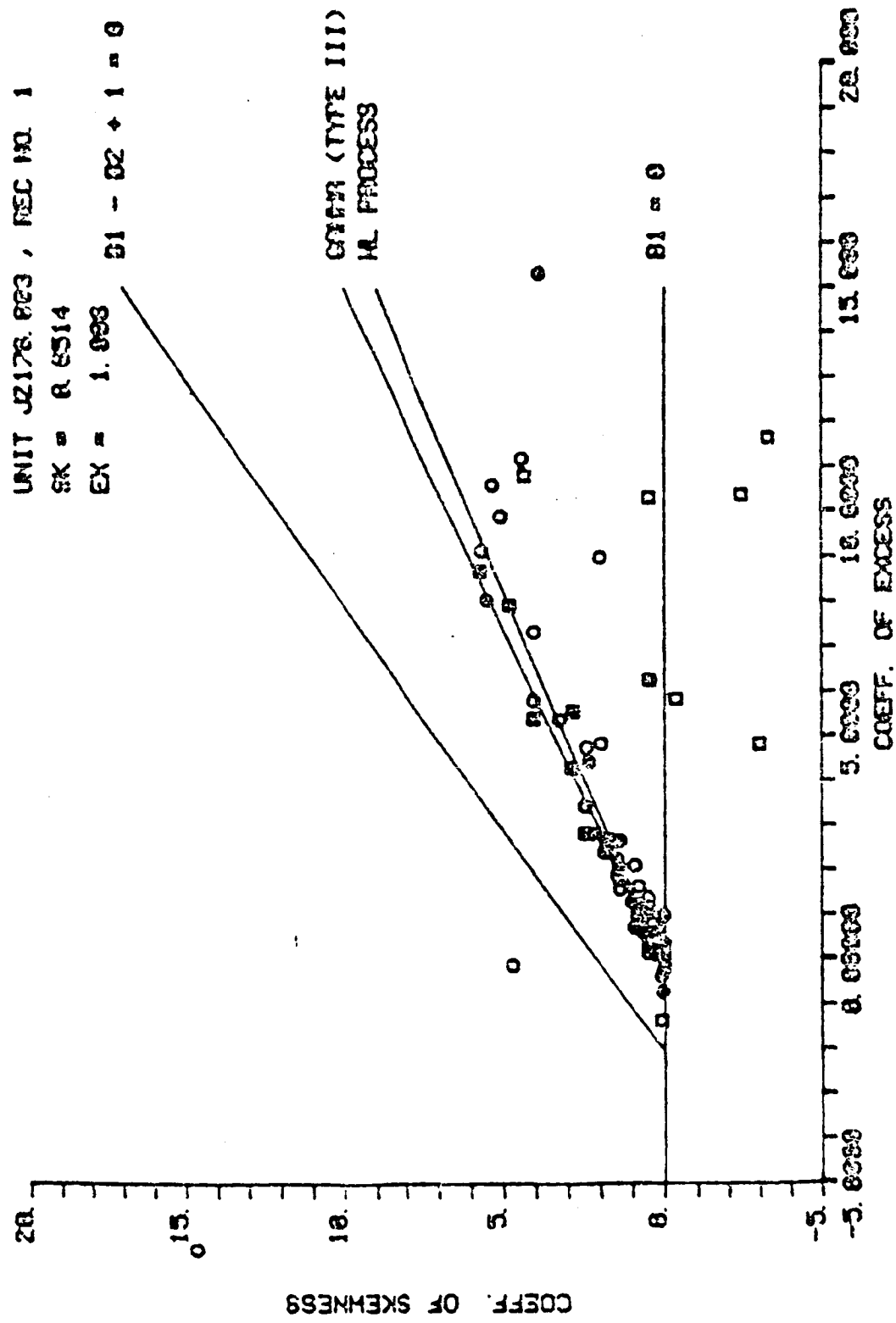

Figure 7 . A plot of the coefs. of skewness (β_1) versus excess (β_2-3) for vestibular primary afferent neural units in an encéphale isolé pigeon preparation. Note clustering of values around β_1=0, β_2-3=0 (the coordinates for a Gaussian distribution).

but measurable kurtosis. When spontaneous discharge from primary afferent fibers subserving the ampullary receptors were measured recently from an unanesthetized preparation, and using an ISI measurement resolution of 100 μs, it was determined that the majority of the fibers whose responses we analyzed, fell near coordinate points (0,0) on the β_1, β_2-3 plot as illustrated in Fig. 7. Thus, under these conditions, there is an apparent shift in distribution type from the distribution forms which we (Correia and Landolt, 1977) previously modeled by the Wiener-Levy or the Orstein-Erlenbeck process. It appears from analysis of the data presented in Fig. 7, that a normal or Gaussian distribution could possibly model the spontaneous discharge patterns which we are currently observing. We are in the process of conducting further studies to determine if it is the lack of anesthesia or the measurement resolution which has produced this apparent shift in distribution type for spontaneous discharge from primary afferent fibers subserving ampullary receptors.

3. Effects of Efferent Action from the Contralateral Ear on the Linear and Non-Linear Transfer Characteristics and Spontaneous Discharge Patterns Observed on Primary Afferent Fibers

During the past eight months, we have measured spontaneous and driven responses from a series of pigeons which were encéphale isolé preparations. These pigeons were divided into two groups. From one group, called the ear normal (EN) group, 96 units were obtained and an analysis was made of their spontaneous discharge patterns. Of these 96 units, 45 were exposed to sinusoidal and Gaussian noise rotation. In the other group, called the left ear ablated (LEA) group, 30 units have been analyzed as to their spontaneous discharge patterns and 23 have been analyzed with regard to their responses to a rotational driving functions which were either sinusoidal oscillations or random noise. In the LEA group, however, prior to the data acquisition, the left labyrinth was surgically exposed and all semicircular ducts were aspirated

The neural responses obtained from Scarpa's ganglion in the right ear were compared for the EN and LEA groups. The EN group data show linear and non-linear transfer characteristics which are comparable to those we have previously described (Correia and Landolt, 1973, 1977). However, the LEA group (where supposedly efferent feedback from the right ear was interrupted) the following observations were made.

Spontaneous discharge characteristics. Almost without exception, it has been observed that following ablation of the contralateral labyrinth, the spontaneous discharge from primary afferent fibers exhibit a cyclic trend in their ISI patterns. Figs. 8a and 8b illustrate this for a unit which is characterized as having a "regular" discharge pattern. Figs. 9a and 9b demonstrate the cyclic trend for a representative unit whose discharge pattern is characterized as being of an "irregular" pattern. For comparison, Figs. 10a and 10b illustrate spontaneous discharge characteristics of a representative unit from the EN group. Currently, statistical comparisons are being made between the first four moments of all of the units which comprise the LEA group and those which comprise the EN group.

Linear and non-linear transfer characteristics. The linear transfer characteristics obtained for the LEA group of units were also characteristicaly different from those obtained from units which comprised the EN group. The major characteristic change which appeared to occur in the LEA group is illustrated in Fig. 11, where it may be seen from a real-time plot of the frequency response amplitude ratio relating neural firing to table velocity that, over the frequency range from DC-3.0 Hz, there appears to be a deformation in the shape of the transfer characteristic. However, over the region from 3.0 Hz to 10.0 Hz, the linear transfer characteristic is quite similar to

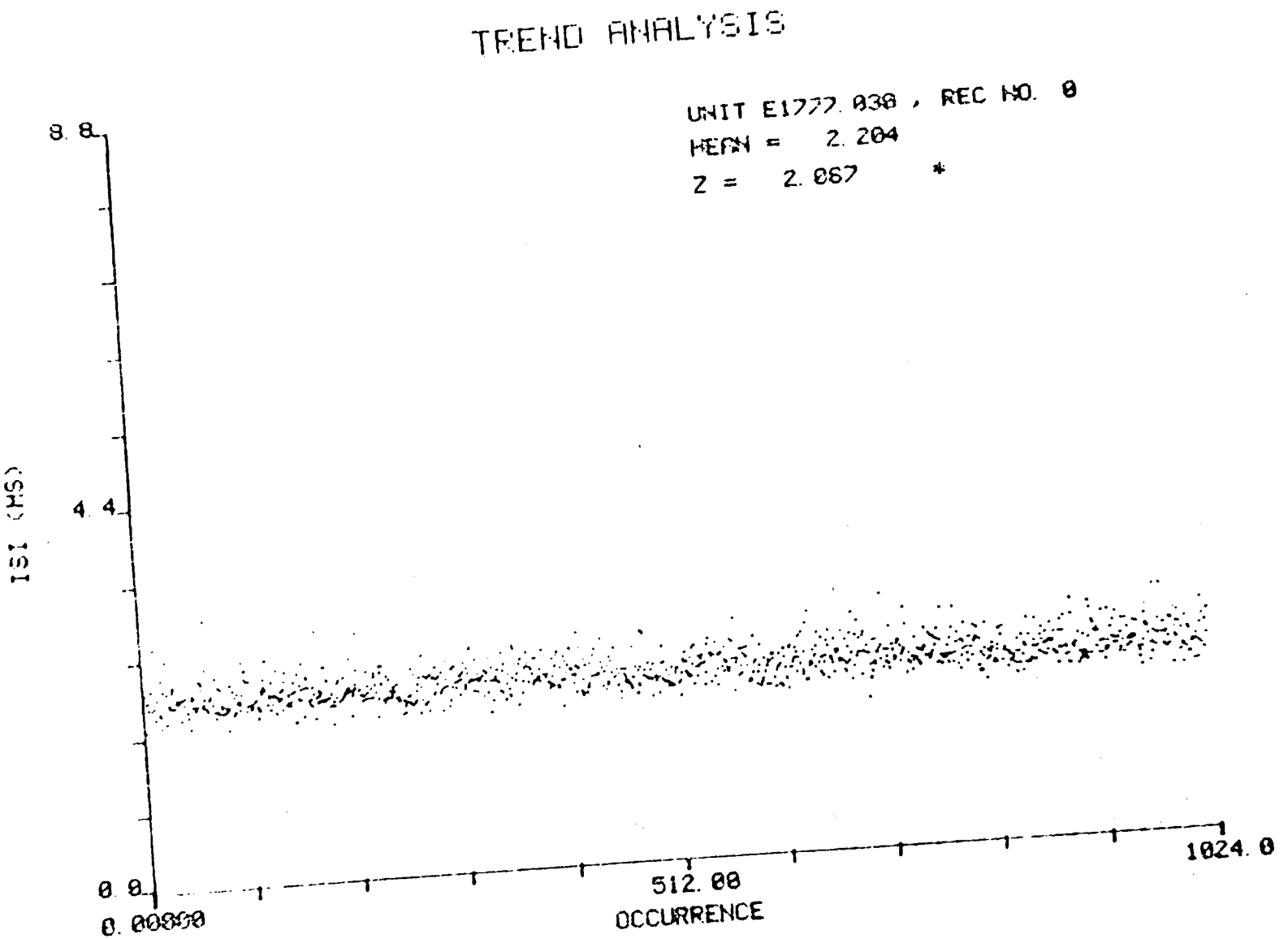

Figure 8a . Trend of ISI's ("regular" unit discharge) from encéphale isolé preparation following contralateral labyrinth ablation.

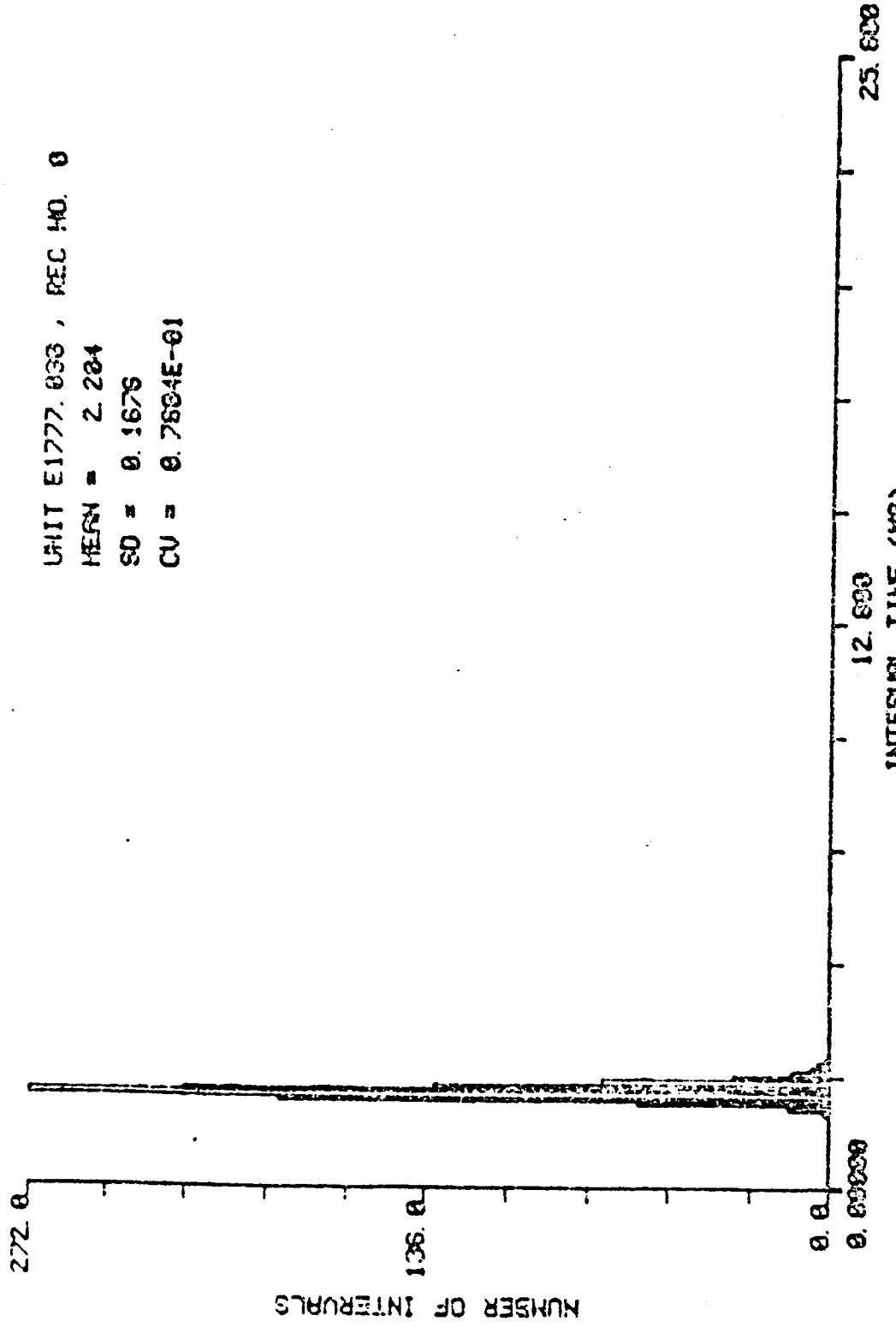

Figure 8b. ISI histogram formed from ISI's shown in (a). The Z statistic indicates positive trend ($P<0.05$).

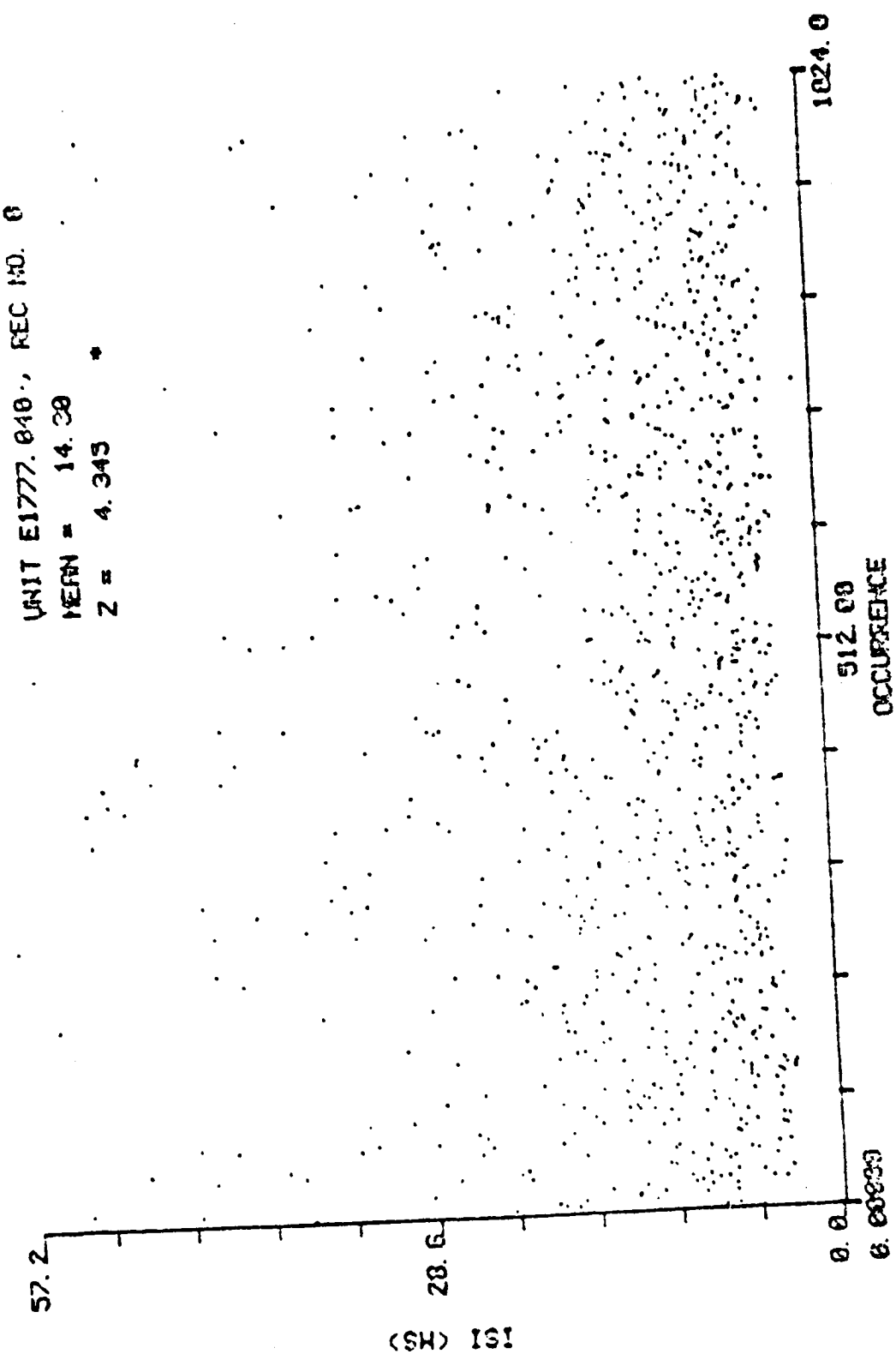

Figure 9a . Trend of ISI's ("irregular" unit discharge) from encéphale isolé preparation following contralateral labyrinth ablation.

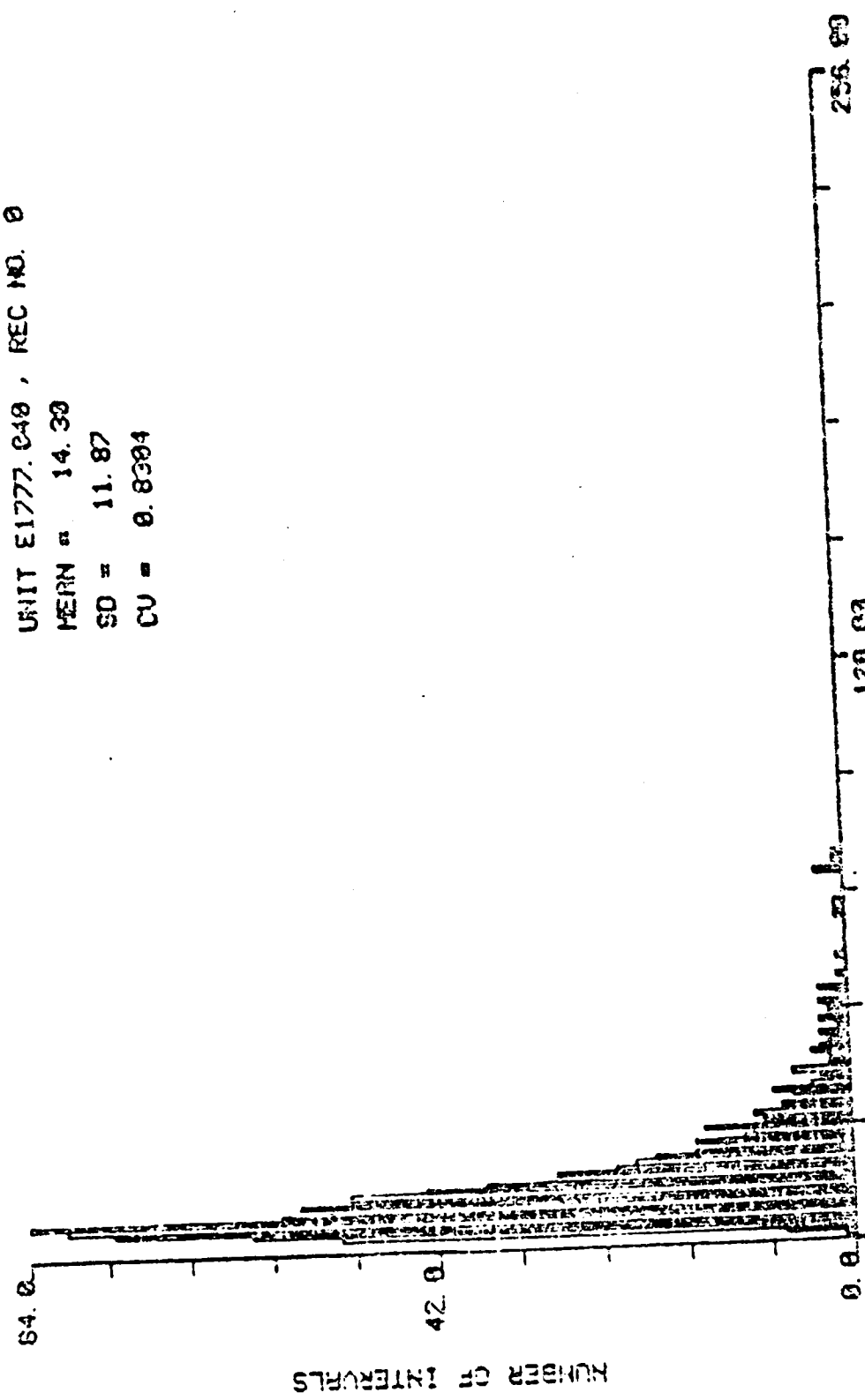

Figure 9b. ISI histogram formed from ISI's shown in (a). Note significant trend ($Z=4.35$, $P<0.05$).

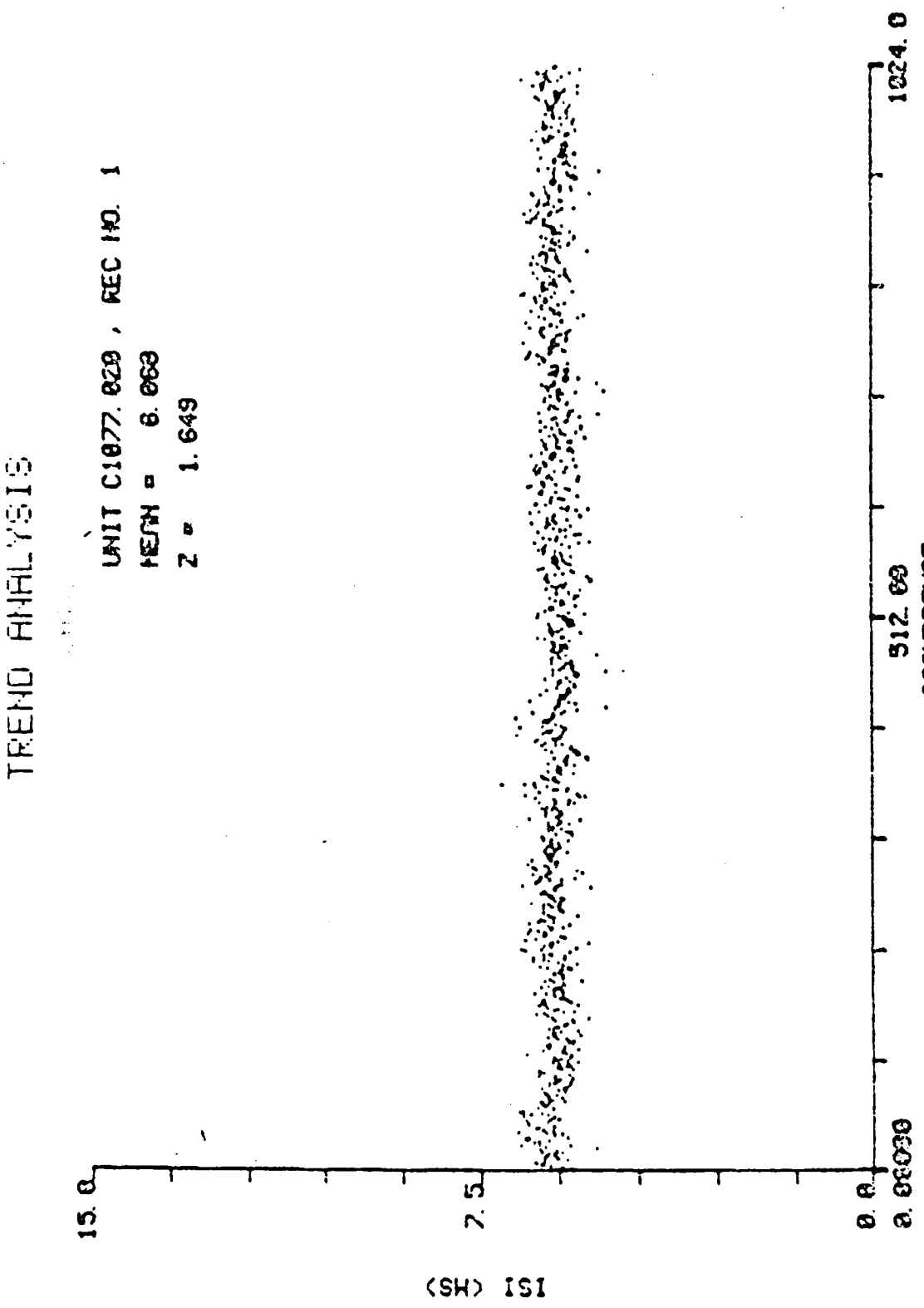

Figure 10a. Trend plot of ISI's from vestibular primary afferent neuron of encéphale isolé preparation with both ears "normal" (cf. Figures 8a and 8b.)

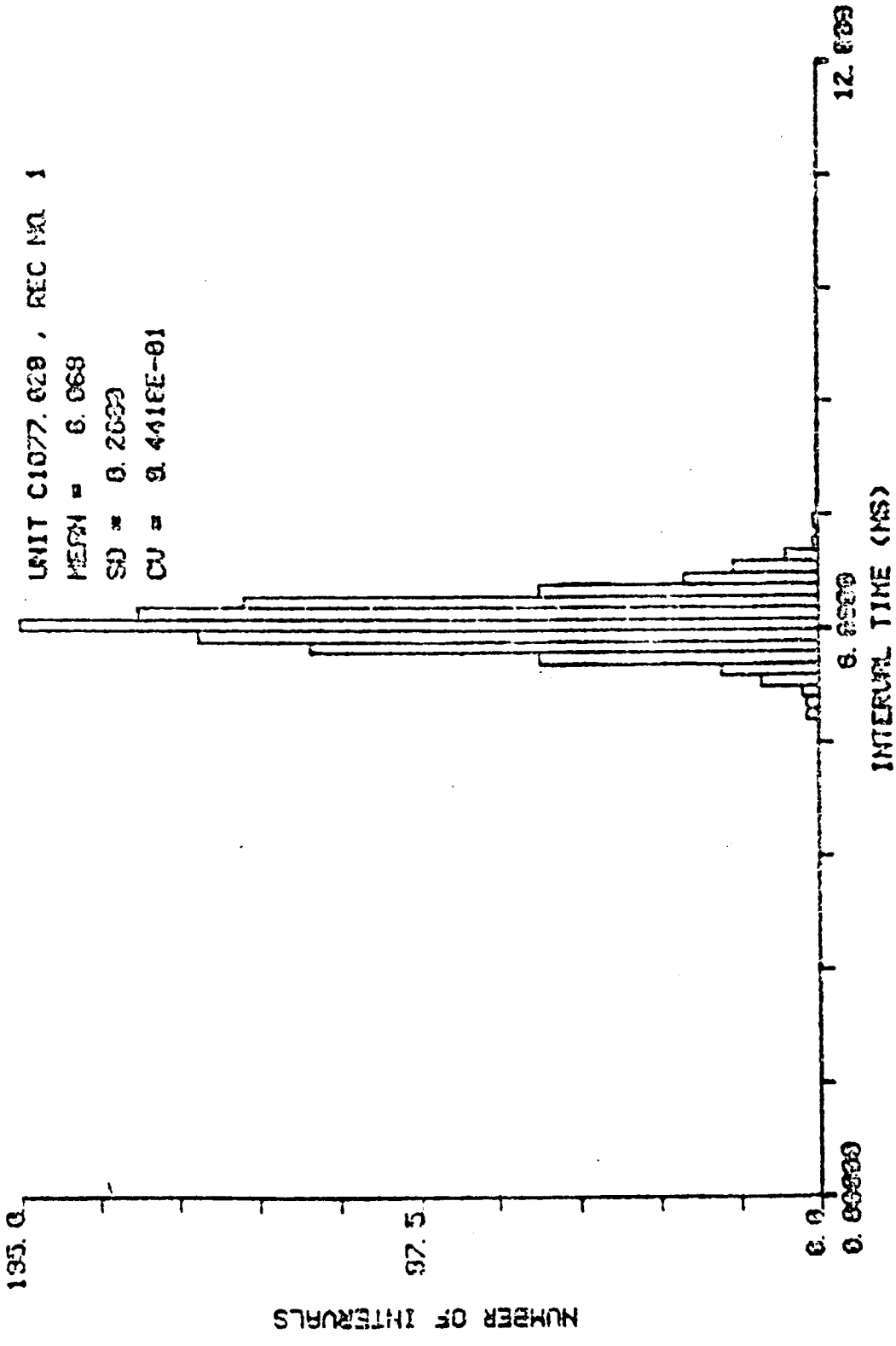

Figure 10b . ISI histogram of ISI's from vestibular primary afferent neuron of encéphale isolé preparation with both ears "normal" (cf. Figures 8a and 8b).

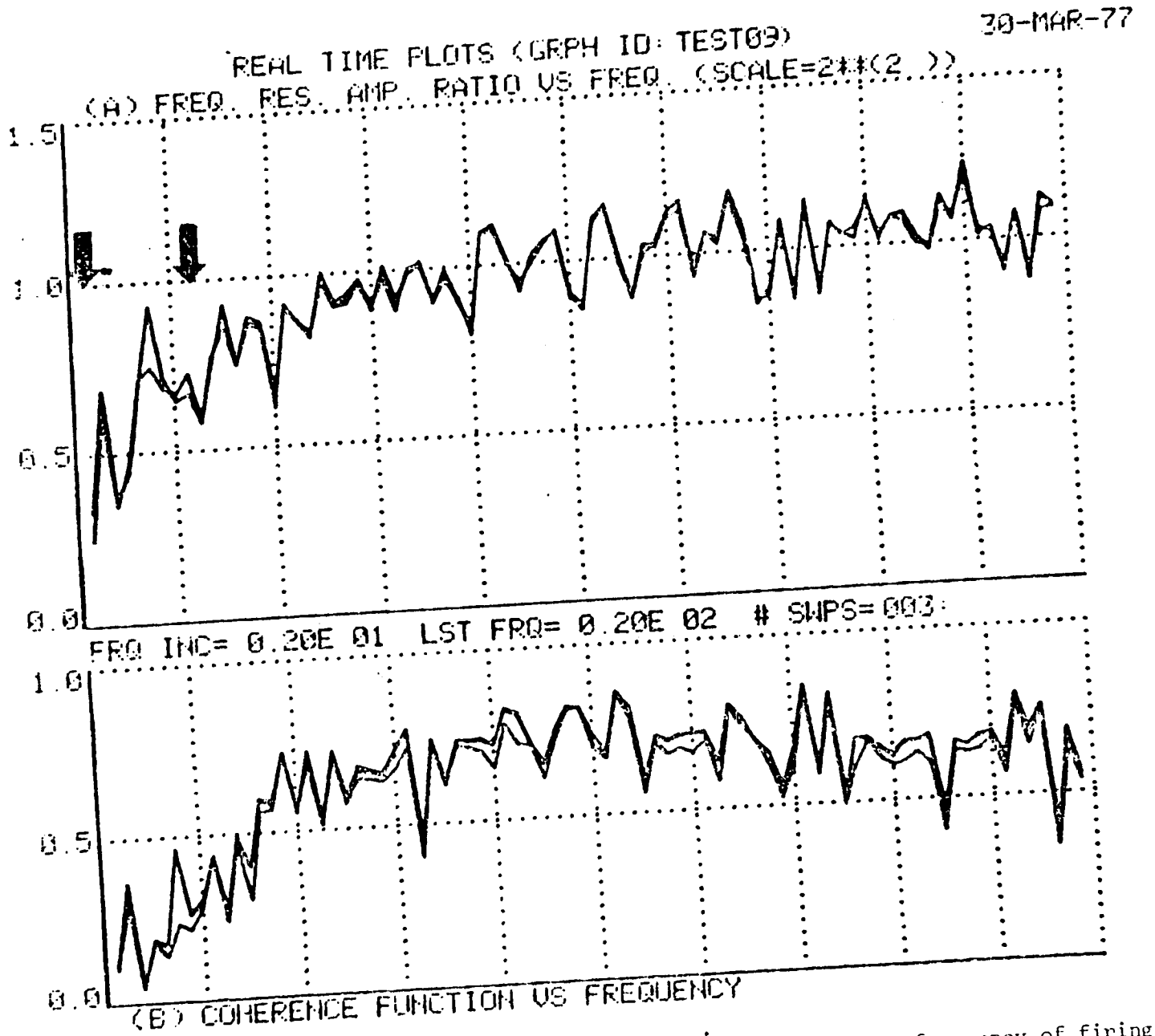

Figure 11. Plot of amplitude ratio and coherence function of instantaneous frequency of firing of a vestibular primary afferent neuron relative to head velocity. These data were obtained from [illegible] encéphale isolé preparation exposed to white noise rotational stimuli

that observed for units seen in the EN group (a representative transfer characteristic which is shown in Fig. 12). Currently, we hypothesize that over the bandpass from DC-3.0 Hz, the long time constant of the semicircular canal is modified and different transfer characteristics occur over this range, whereas the slight change noted for the bandpass 3.0 Hz to 10.0 Hz, reflects the lack of effect of efferent control on the dynamics of the system in a range which reflects the short-time constant, τ_2, and neural adaptation operators. We are currently trying to quantify these observations. The decrease in the coherence function in the range DC-3.0 Hz (cf. Figs. 11 and 12) for the LEA units suggest that non-linearities occur over this range. However, we have not been able to examine these effects systematically.

4. Examination of the Morphology of the Pigeon's Vestibular Neuroepithelium and Primary Afferent/Efferent System

Using scanning electron microscopy (SEM), we have been able to show that the surface topology of the pigeon's vestibular neuroepithelium has evolved so that a maximum packing density of hair cells can occur on the cristae ampullaris (Landolt et al., 1975). Moreover, we have conducted light microscopy pilot experiments which have provided provacative results which appear to demonstrate that the distribution of hair cells on the surface of the cristae ampullaris is in a prescribed pattern. That is, we have evidence which indicates that type II hair cells are concentrated mainly on the apex of the cristae ampullares, whereas, type I cells are concentrated mainly toward the periphery. In between these two regions there appears to be a mixture of the two types of hair cells. Using transmission electron microscopy (TEM), we have noticed that there is a very large ratio of gap junction synapses (electrical synapses) of primary afferent fibers on hair cells as compared to chemical synaptic junctions. These morphological results are consistent

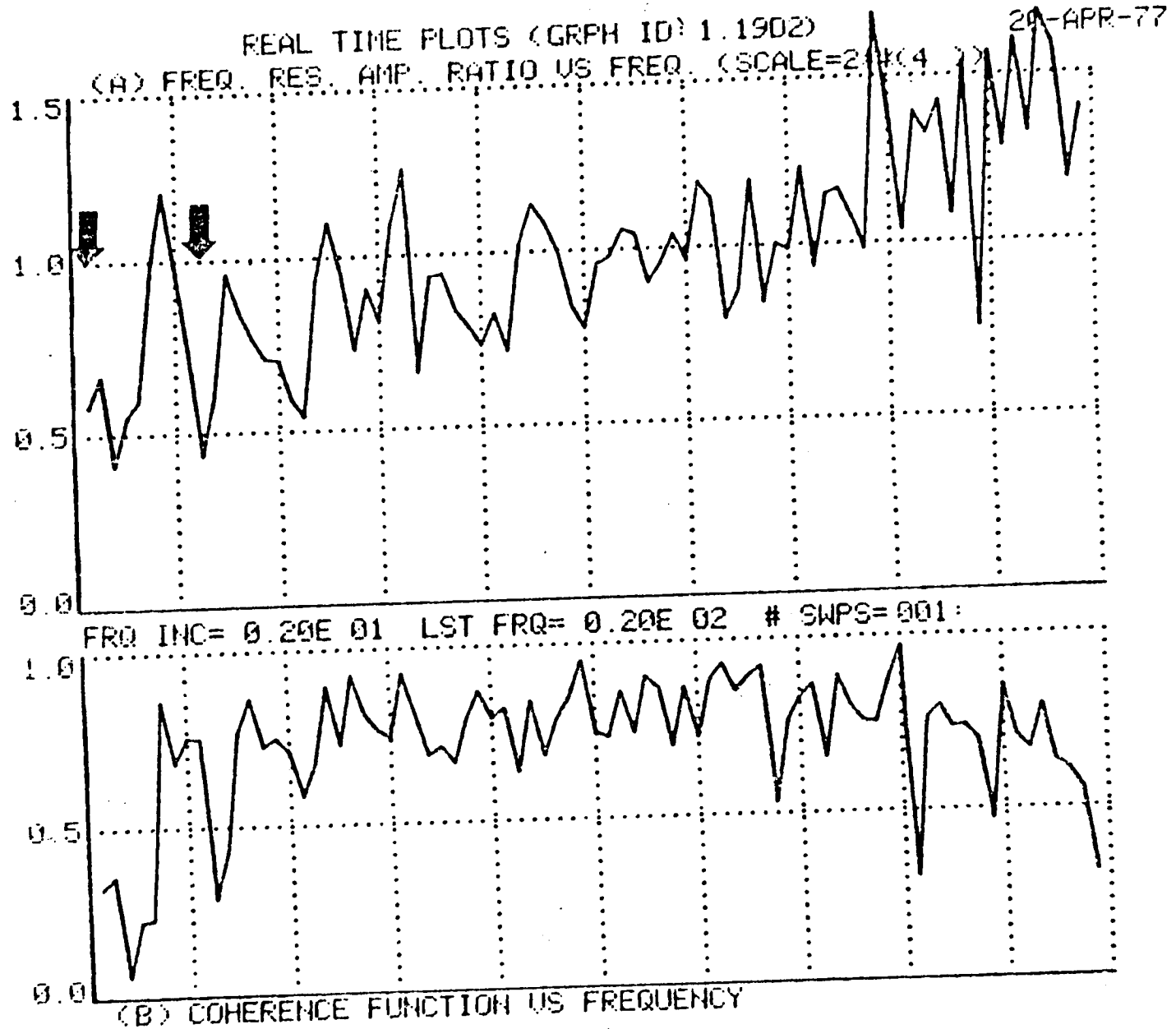

Figure 12. Plot of amplitude ratio and coherence function of instantaneous frequency of firing of a vestibular primary afferent nueron relative to head velocity. These data were obtained from a "left ear ablated" encéphale isolé preparation exposed to white noise rotational stimuli (bandpass-DC-20 Hz, segment length-20s, 1 segment). Note large value of AR (cf. with Figure 11) between black arrows. This may represent output without corresponding input caused by cyclic modulation of afferent discharge.

with the results of Wilson and Wylie (1970) (who demonstrated neurophysiological evidence for the existence of gap junctions in the pigeon's vestibular neuroepithelium). Finally, using TEM, we have noticed the presence of vesiculated boutons abutting hair cells in the cristae ampullares of the pigeon. These vesiculated boutons are usually taken as evidence of the efferent synapses. It is important to the model which we have presented (Correia and Landolt, 1977) that we determine the following conditions using morphological techniques. 1) What is the ratio of efferent synapses to afferent synapses within the neuroepithelium of the cristae ampullares. 2) What is the ratio of gap junction to chemical synaptic junctions for a given distribution of hair cells of both type I and type II within the neuroepithelium of the cristae ampullaris. 3) Where are the cells of origin of efferent fibers which project to the hair cells of the cristae ampullares. These questions will continue to be addressed during the succeeding years of the contract and the specific techniques that we will use to address these questions will be developed in the following sections of this proposal.

VII. PROGRESS - 1975

FIRST QUARTER PROGRESS - May 1, 1975/July 31, 1975

I Progress (Equipment Ordered)

Although this contract was awarded on 1 May 1975, the Principal Investigator did not receive an account number from the Office of Sponsored Research until June 6, 1975 at which time the following major equipment purchases were made:

A. A David Kopf microinjection unit

B. A Livingston Micropipette puller

C. A David Kopf intracellular stereotaxic frame assembly with pigeon adapter

D. An Ortec window discrimminator and instantaneous frequency/time meter

E. A storage oscilloscope

F. A Brown Type microelectrode beveler

F. Computer disk cartridges

II Progress (Surgical procedures)

The following surgical procedures were investigated during the reporting period:

A. Flow through-artificial respiration

Techniques were investigated to artificially ventilate birds so that they could be paralyzed with Flaxedil and maintained for long periods of time. It was observed that 95:5 O_2 - CO_2 unidirectional flow could

maintain animals if the posterior air sac was punctured with a needle and a tracheotomy performed.

No tests have been initiated with the use of Flaxedil because Vasoxyl has not been received. This drug lowers the heart rate elevated by Flaxedil. These techniques will be developed in the second quarter.

B. Encephale isole

Several pigeon cadavers were dissected and aspirated to develop a technique to produce an "isolated brain preparation". The skull overlying the forebrain was removed to the optic lobes. This technique is still under development. In the second quarter conscious pain sensitization will be tested. Once established, the procedure will be routinely used in data acquisition.

C. Receptor Isolation -

Rather than using procedures of receptor isolation using rotatory stimuli. Techniques are being developed to localize receptor origin of spontaneous action potential trains by use of the method of Wilson and Felpel. This technique (electrical isolation) will be useful when intracellular recordings will be obtained later in the project and where preparation vibration would introduce possible artifacts.

III Progress (Data Acquisition)

The computer program NIP (Neuronal Impulse Processor) has been written by Mr. Brassard. This program permits one to interactively proceed through spontaneous discharge analysis as follows:

A. Data is acquired in blocks of 1024 interspike intervals (ISIS). Ten such blocks can be accommodated (10KISIS). Following each block one

may

1. test for the trend (Wald Wolfowitz); display trend on 4010 graphics terminal (see attached copy) along with standard normal variate g and its level of significance (indicated by * for P<0.05).

2. perform auto-correlation of ISIS via the route of an inverse Discrete Fourier Transform (FFT technique) and display the resulting correlogram

3. form an interval histogram with its central movements (see attached copy)

4. present the relation of the current units coefficient of skweness and excess relative to a history of units thoroughly analyzed by the PI and Dr. Landolt (see attached copy). Once the unit meets the above criteria, it may be appended to a database which has been developed and which interfaces to data reduction programs.

IV. Data Reduction

We feel that we currently have statistical methods which enable us to detect subtle changes in firing pattern. Specifically, we can detect changes in a unit's firing trend and compare it statistically with itself. We can detect changes in higher order temporal patterns of spike train firing by the use of auto correlation. We can determine whether a unit is a renewal type, i.e., whether it can be completely categorized by its first order properties. If a unit is from a renewal process, we can fit it with eleven candidate probability density functions (see attached copy) and compare goodness of fit statistically by the coefficient of determination, Williams & Kloot test, rootmean square error and least square error.

SECOND QUARTER PLANS

In the second quarter we propose to continue to develop surgical techniques so that we may continue to obtain extra cellular control data on vestibular neurons in isolé encephalé preparations. This control data will be compared with drug influenced data which we shall obtain in the third and fourth quarters. In the second quarter when the equipment arrives, we shall initiate intracellular techniques to our preparation. However, the top priority will be to obtain a data base of spontaneous activity from anterior and horizontal canal neurons from an "awake preparation".

In the second quarter, the computer program NIP will be expanded to display on the computer terminal an ISI histogram with the best fit probability density function through it. Once this feature is incorporated into the program, we can proceed through data acquisition and data reduction "on line".

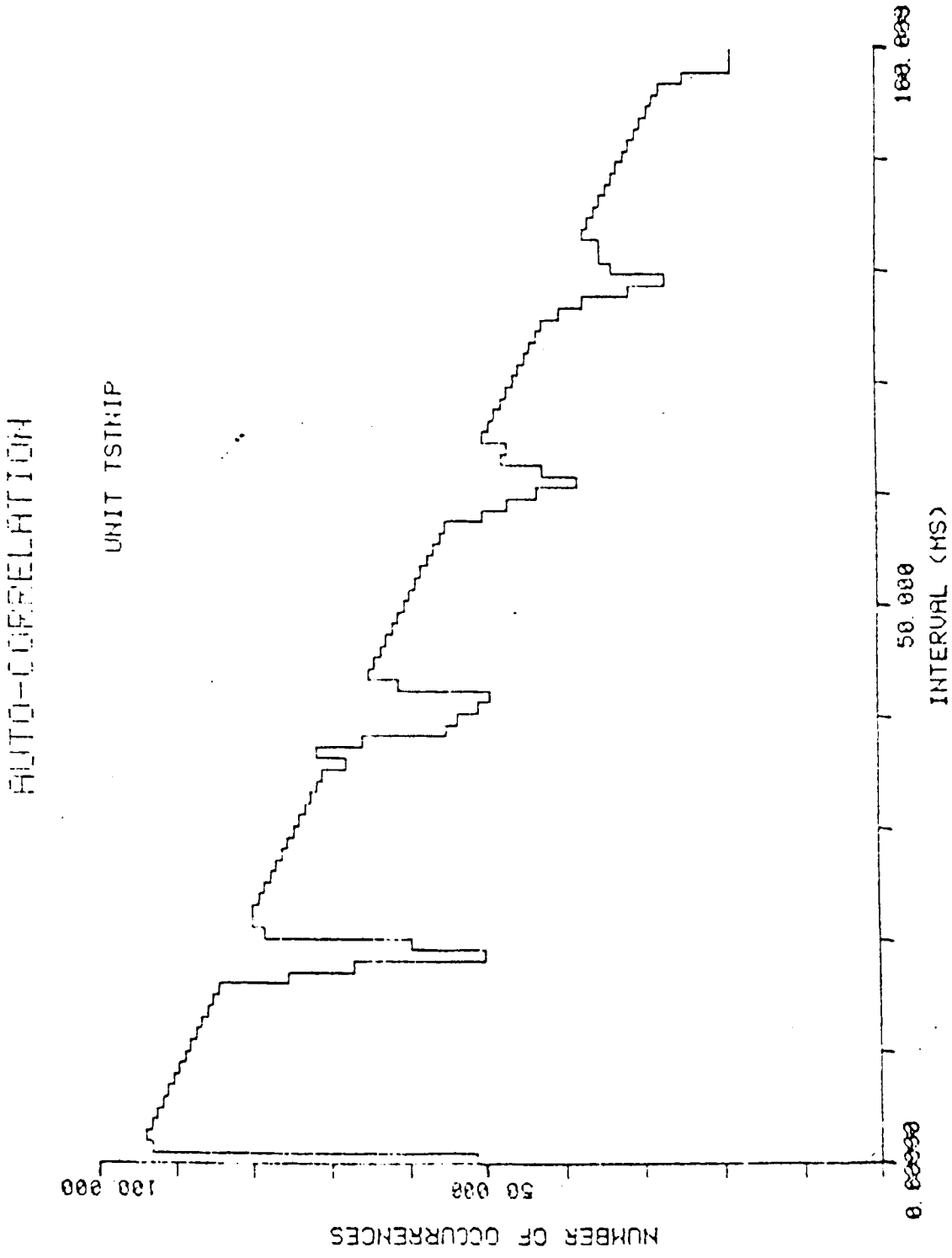
AUTO-CORRELATION
UNIT TSTNIP
NUMBER OF OCCURRENCES
0.000
50.000
100.000
INTERVAL (MS)

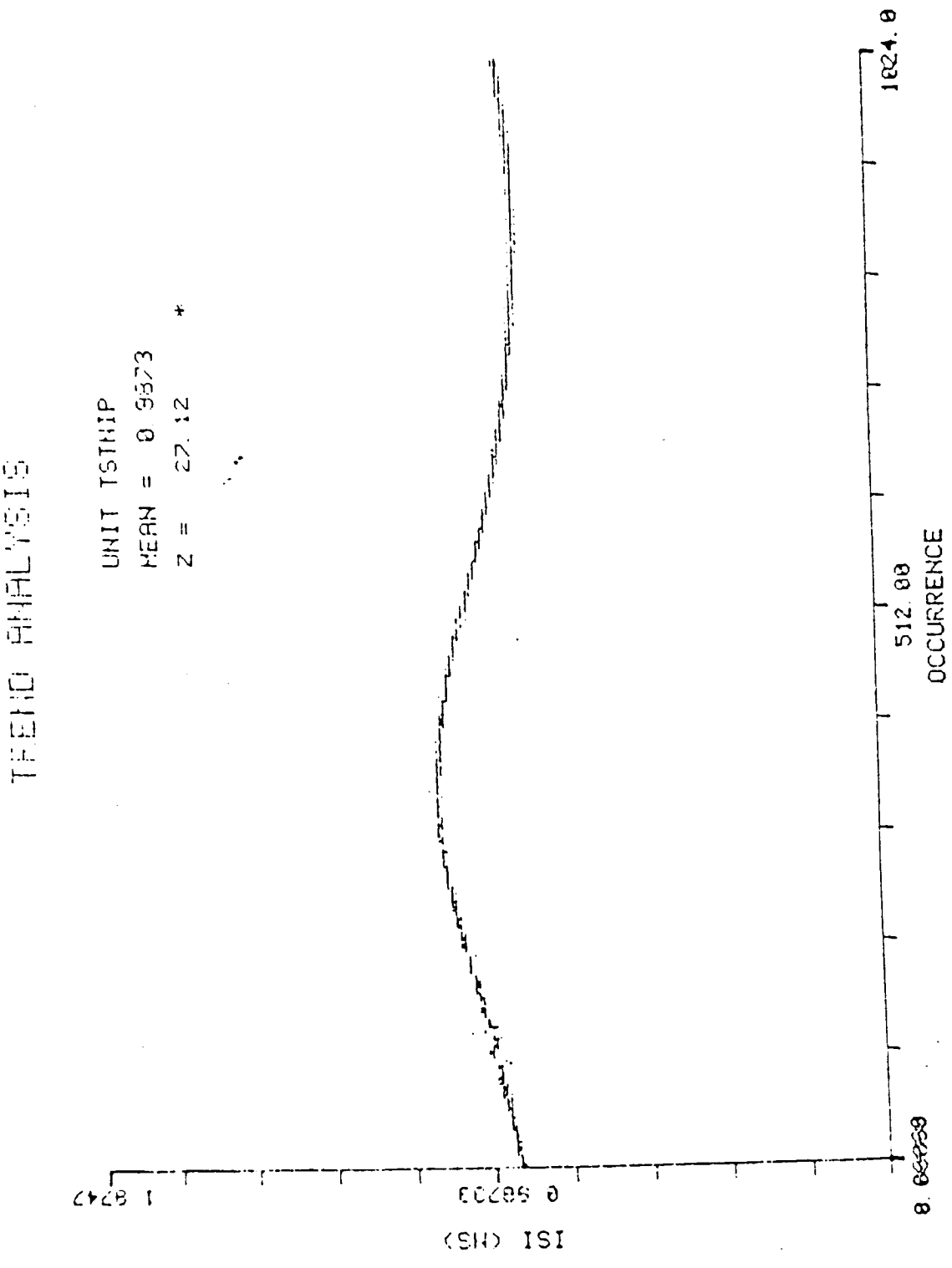
TREND ANALYSIS
UNIT TSTNIP
MEAN = 0.9573
Z = 27.12 *
1.0247
0.89233
ISI (MS)
0.00000
512.00
1024.0
OCCURRENCE

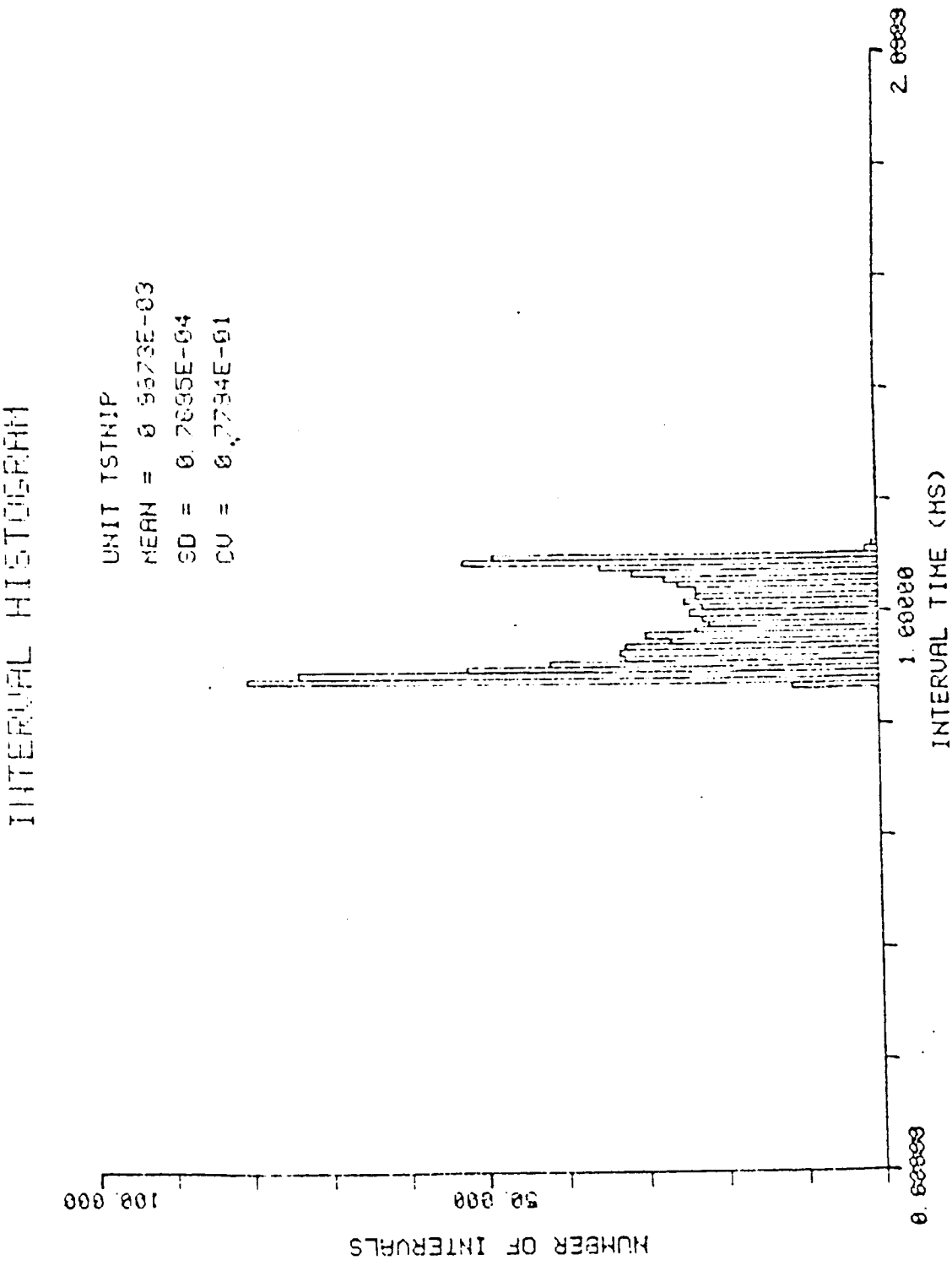
INTERVAL HISTOGRAM
UNIT TSTNIP
MEAN = 0.9973E-03
SD = 0.7695E-04
CV = 0.7734E-01
NUMBER OF INTERVALS
100.000
50.000
0.00000
1.00000
2.00000
INTERVAL TIME (MS)

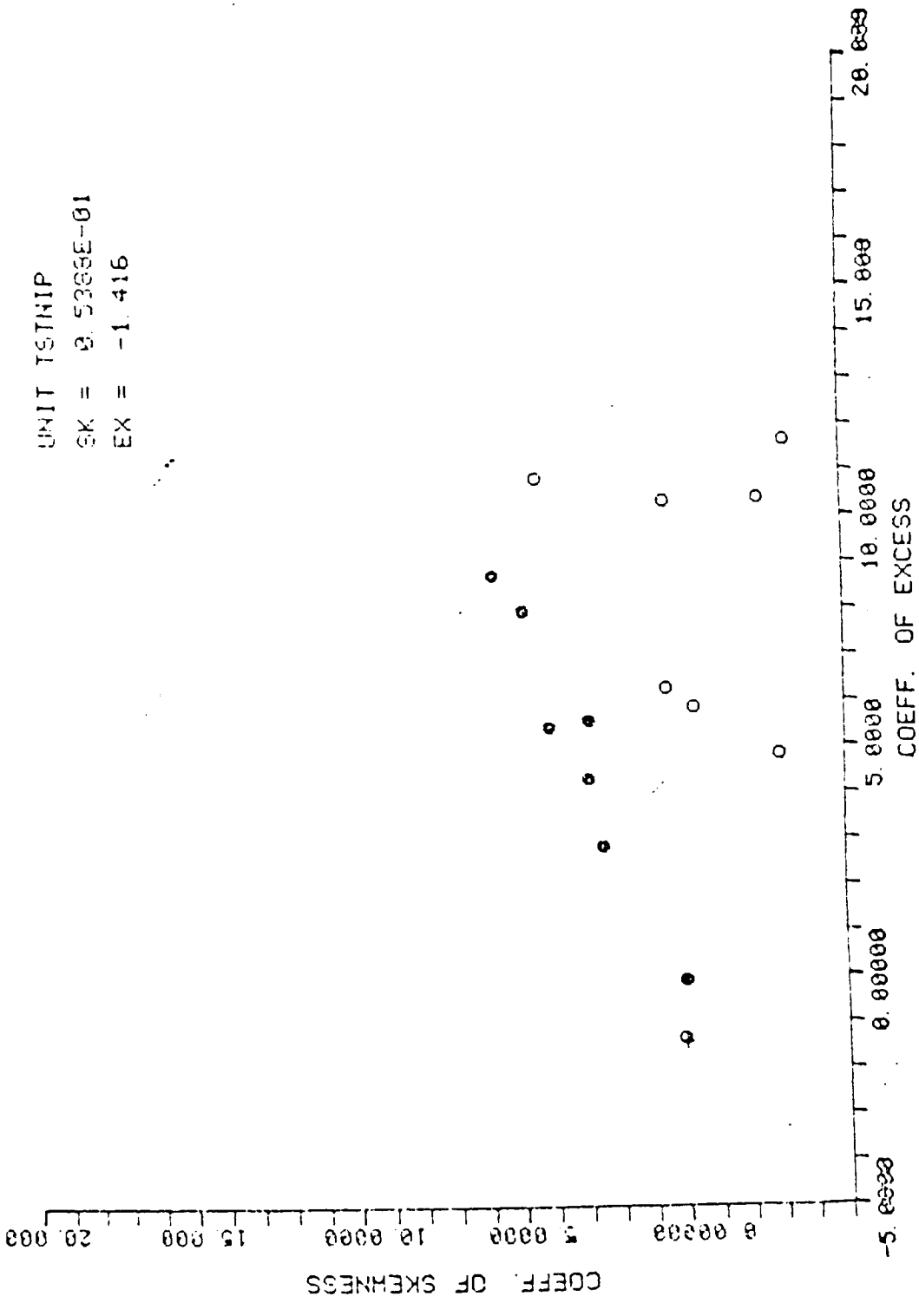
UNIT TSTNIP
SK = 2.5335E-01
EX = -1.416
COEFF. OF SKEWNESS
COEFF. OF EXCESS
-5.0000
0.00000
5.0000
10.0000
15.000
20.000

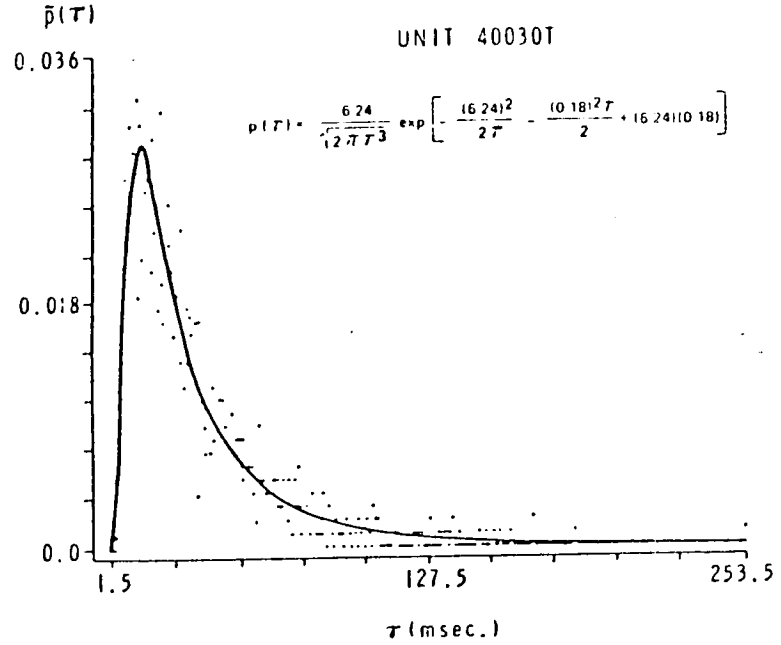
UNIT 400307
$\tilde{p}(\tau)$
$p(\tau) = \frac{6.24}{\sqrt{12\pi\tau^3}} \exp\left[-\frac{(6.24)^2}{2\tau} - \frac{(0.18)^2\tau}{2} + (6.24)(0.18)\right]$
0.036
0.018
0.0
1.5
127.5
253.5
τ (msec.)

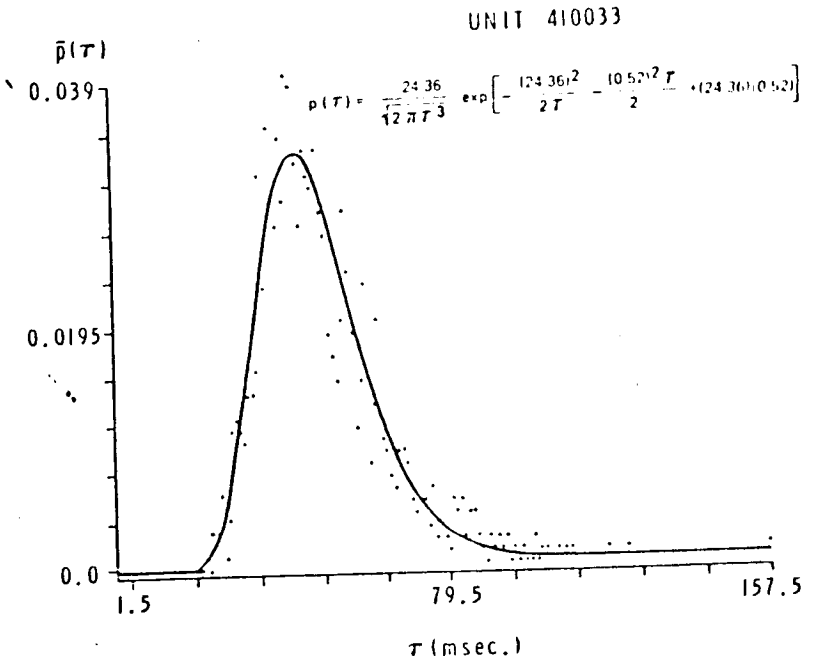
UNIT 410033
$\tilde{p}(\tau)$
$p(\tau) = \frac{24.36}{\sqrt{12\pi\tau^3}} \exp\left[-\frac{(24.36)^2}{2\tau} - \frac{(0.52)^2\tau}{2} + (24.36)(0.52)\right]$
0.039
0.0195
0.0
1.5
79.5
157.5
τ (msec.)

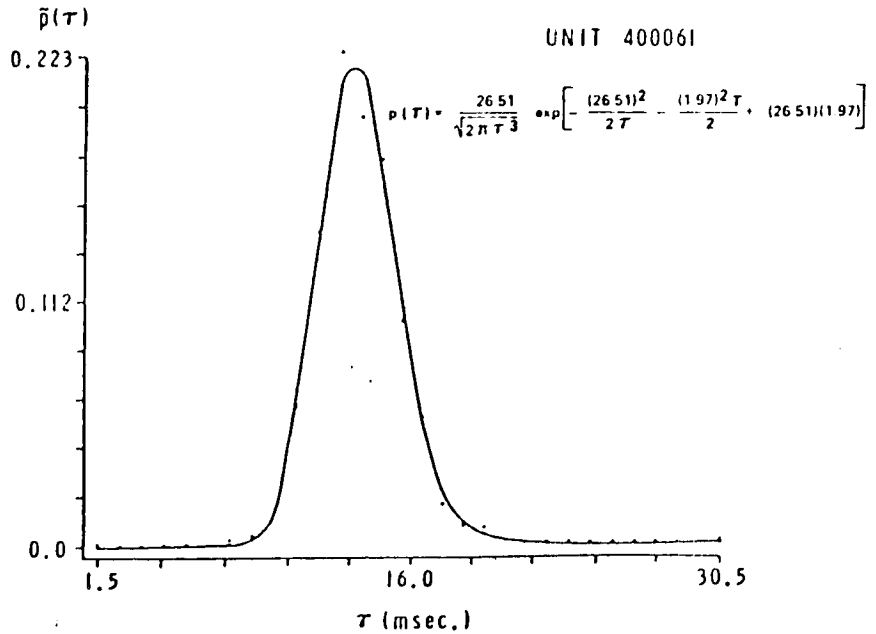
UNIT 400061
$\tilde{p}(\tau)$
$p(\tau) = \frac{26.51}{\sqrt{12\pi\tau^3}} \exp\left[-\frac{(26.51)^2}{2\tau} - \frac{(1.97)^2\tau}{2} + (26.51)(1.97)\right]$
0.223
0.112
0.0
1.5
16.0
30.5
τ (msec.)

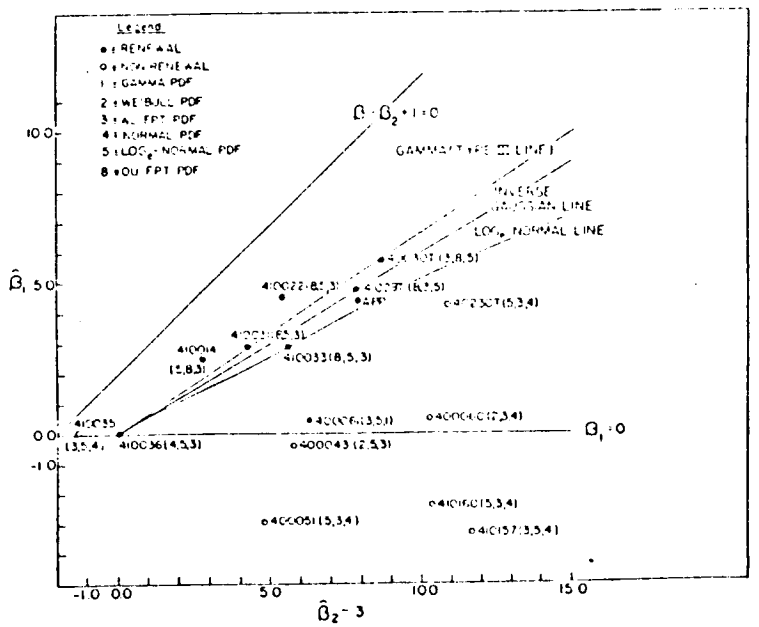
Legend
1 : GAMMA PDF
2 : WEIBULL PDF
3 : IG FPT PDF
4 : NORMAL PDF
5 : LOG$_e$-NORMAL PDF
8 : OU FPT PDF
$\beta_1 = \beta_2 + 1.0$
GAMMA (TYPE III) LINE
INVERSE GAUSSIAN LINE
LOG$_e$-NORMAL LINE
$\beta_1 = 0$
$\hat{\beta}_1$
$\hat{\beta}_2 - 3$
10.0
5.0
0.0
-1.0
-1.0 0.0
5.0
10.0
15.0

PROGRESS REPORT

NAS 9-14641

1 August 1975 - 31 September 1975

SECOND QUARTER PROGRESS

I. Progress (Equipment Received)

All equipment ordered in first quarter of contract was received with the exception of the Brown microelectrode beveler. David Kopf was notified of their late delivery. They promised delivery within 60 days.

II. Progress (Noise Isolation)

Three days were spent analyzing microelectrode system noise levels. By the use of a new amplifier and special noise and grounding procedures, system noise level was reduced to 100 μ volts with the amplifier band passing DC to 10 KHz. The following equipment is included in system: microelectrode, DC amplifier (X 1), Grass amplifier (X 1000), oscilloscope, window discriminator, analog magnetic tape unit. The above noise level also includes the following noisy signal sources proximal to the preparation: operating microscope, motor driven micromanipulator, cauterizing unit. This noise level will permit signal processing of extracellular and intracellular signals where DC recording is required (EPSP, membrane voltages) without special shielding procedures. Extracellular single unit recordings were made using this new system.

III. Progress (Surgical Procedures)

Experiments were made with seven pigeons. All were artificially respired using unidirectional-flow-through artificial respiration. This procedure greatly facilitates maintenance of the preparation in the face of considerable surgical trauma. In four animals the cortex was aspirated and a middle fossa approach was attempted to expose the vestibular nerve intracranially. All exposures resulted in failure due to excessive bleeding. Vestibular single units were obtained in one preparation,however, the bird died before prolonged recording could be achieved. A suboccipital approach was attempted on three pigeons. All surgery resulted in failure due to excessive blood loss. The above two procedures have the advantage that they allow the animal to be fixed in a stereotaxic apparatus and therefore permit rigid fixation of the head in the normal orientation relative to gravity. However, the surgical trauma associated with these procedures make their implementation undesirable. During the third quarter,data will be gathered using the Ewaldian approach which has been successful in the past for the principal investigator. The stereotaxic apparatus will be modified to permit rigid head fixation during this approach. This rigid fixation will be necessary for subsequent intracellular recording. Before the stereotaxic instrument is modified for the Ewaldian approach an attempt will be made to develop a dorsal approach to the vestibular nerve. This procedure has been used to gain access to the vestibular nuclei (Wilson, 1968). It should involve minimal bleeding and rigid fixation of the head for subsequent intracellular work.

IV. Progress (Data Acquisition and Data Reduction)

It was determined by the principal investigator that stationarity as well as drug induced changes in neural activity could be carefully examined on-line by a Fourier Analysis of frequency of firing of a neuron. This method is faster than the corresponding time domain auto correlation function and can present a history of firing patterns of a neuron over time. However, to prevent aliasing, neuronal pulses must be passed through an ideal low pass filter (sin x/x). To this end we acquired from Dr. French his program to achieve this filtering. Mr. Brassard has analyzed Dr. French's program (written in machine language), extracted the algorithm (see attached description), generalized the program to 1024 points and is currently encorporating the Fourier analysis module into the neuronal impulse processor. During this quarter the computer program which we shall use to analyze changes in the interspike interval histograms of vestibular primary afferents was published and a reprint is enclosed.

V. Progress (Publications)

The following publications which are related to this contract and their status are described below:

1. Brassard, J.R., Correia, M.J. and Landolt, J.P. A computer program for the graphical and iterative fitting of probability density functions to biological data. Computer Programs in Biomedicine 5: 11-38, 1975.

2. Landolt, J.P. and Correia, M.J. Neurophysiology of first-order vestibular units in the pigeon. I. The stochastic properties of the spontaneous activity in anterior semicircular canal units. (final draft completed, to be submitted to J. Neurophysiol.)

3. Correia, M.J. and Landolt, J.P. Neurophysiology of first-order vestibular units in the pigeon. II. A point prosess model of the impulse-generating mechanism in anterior semicircular canal units. (final draft completed, to be submitted to J. Neurophysiol - NASA support acknowledged)

THIRD QUARTER PLANS

During the third quarter data will be gathered from an "awake" preparation using the Ewald approach. Since the preparation will be awake, pain will be avoided by using local anesthetic infiltration of the neck muscles which must be partially severed. Also we will attempt to develop a dorsal approach to the intra cranial portion of the 8th nerve. During the third quarter the data reduction portion of the neuronal impulse processor should be completed. That is, the Fourier analysis module of Interspike Interval analysis should be completed, Tektronix 4010 graphical display of the probability density function program should be implemented. During the third quarter "normative" data will be gathered which will be compared to previous data gathered with barbituate anesthesia and 4th quarter data gathered under different drug conditions.

FAST FOURIER TRANSFORM OF INTEREVENT INTERVALS

Assume that during some sampling time period, T, a sample of consecutive, event occurrence times, $t_i (i = 0,1,2,\ldots,n_T)$, is obtained for each i by

$$t_i = \sum_{j=1}^{i} x_j \qquad (1)$$

where for each j, $x_j = t_j - t_{j-1}$ is an interevent interval.

A direct Fast Fourier Transform (FFT) of the interevent intervals, x_j, would not be meaningful since each interval time is dependent on the time, t_o, which is the initial time of the period T.

One could apply the FFT to the ordered set of event times $\{t_i\}$ computed in (1). However, because this is a set of discrete times, the problem of aliasing would arise.

A.S. French solved this problem by applying a "convolution" method to the set of values $\{t_i\}$ before using the FFT. This method consists in substituting the continuous function

$$g_i(t_i) = \sin(2\pi f_N t_i)/(2\pi f_N t_i) \qquad (2)$$

for each event t_i, $(i = 1,2,\ldots,n_T)$, where f_N is the Nyquist (folding) frequency,

$$f_N = \frac{1}{2\Delta\tau}, \qquad (3)$$

and where $\Delta\tau$ is the rate at which each g_i is to be sampled.

The functions $\{g_i(t_i)\}$ which are centered timewise at the respective events $\{t_i\}$, are then "sampled" (computed) at the selected rate, $\Delta\tau$.

For simplicity's sake, let $g(t)$ be a representative member of the set of functions $\{g_i(t_i)\}$ such that

$$g(t) = \sin(2\pi f_N t)/(2\pi f_N t) \tag{4}$$

which is centered at event t. By the Euclidean Algorithm, this event may be expanded in the form

$$t = n\Delta\tau + r \tag{5}$$

where n is an integer and $0 \leq r < \Delta\tau$.

Substituting (5) into (4) and expanding we have

$$g(t) = \frac{\sin\,[2\pi f_N(n\Delta\tau + r)]}{[2\pi f_N(n\Delta\tau + r)]}$$

$$g(t) = \frac{\sin\,(2\pi f_N n\Delta\tau)\,\cos\,2\pi f_N r}{[2\pi f_N(n\Delta\tau + r)]}$$

$$+ \frac{\cos(2\pi f_N n\Delta\tau)\sin\,2\pi f_N r}{[2\pi f_N(n\Delta\tau + r)]} \tag{6}$$

Then, substituting (3) into (6) we have

$$g(t) = \frac{\sin n\pi \cos\left(\frac{r\pi}{\Delta\tau}\right)}{\frac{\pi}{\Delta\tau}(n\,\Delta\tau + r)} + \frac{\cos n\pi \sin\left(\frac{r\pi}{\Delta\tau}\right)}{\frac{\pi}{\Delta\tau}(n\Delta\tau + r)} = \frac{(\pm 1)\cdot \sin\left(\frac{r\pi}{\Delta\tau}\right)}{\frac{\pi\,(n\Delta\tau + r)}{\Delta\tau}} = \frac{\sin\left(\pm\frac{r\pi}{\Delta\tau}\right)}{\frac{\pi(n\Delta\tau + r)}{\Delta\tau}} \qquad (7)$$

Since the remainder term, r, in (5) also represents the relative time location of the event t from the nth sample, by assuming that the occurrence time of the event is $t_o = 0$ and that the distance between samples is π radians, g(t) can be "sampled" (computed) as follows for every $k\pi$ radians, ($k = 0, \pm 1, \pm 2, \ldots, \pm m$), relative to the current location of the previous "nth" sample time [i.e., relative to $t = -\left(\frac{r}{\Delta\tau}\right)\pi - k\pi = \frac{-\pi(r+k\Delta\tau)}{\Delta\tau}$] until for the values $k = \pm m$ or for ε an arbitrary positive number, $|g^{*}(t)| < \varepsilon$:

$$g^{*}(t) = \frac{-\sin\frac{\pi(r+k\Delta\tau)}{\Delta\tau}}{\frac{-\pi(r+k\Delta\tau)}{\Delta\tau}} = \frac{\sin\left(\frac{r\pi}{\Delta\tau}\right)\cos k\pi}{\frac{\pi(r+k\Delta\tau)}{\Delta\tau}} = \pm\frac{\sin\left(\frac{r\pi}{\Delta\tau}\right)}{\frac{\pi(r+k\Delta\tau)}{\Delta\tau}} \qquad (8)$$

The sample functions $\{g_i^*(t_i)\}$, obtained from $\{g_i(t_i)\}$ for each i using (8), are added into a time array to form a sum, sample function

$$h(t) = \sum_{i=1}^{n_T} g_i^*(t_i) \qquad (9)$$

The FFT is then applied to the array containing (9), this array being the discrete replacement for the sequence of time events $\{t_i\}$. Note that because of (3) this array also removes the problem of aliasing.

PROGRESS REPORT

NAS 9-14641

1 October 1975 - 31 December 1975

THIRD QUARTER PROGRESS

I. Progress (Equipment Received)

All equipment ordered in the first quarter of the contract was received. Brown microelectrode beveler (David Kopf) was received, tested and accepted.

II. Progress (Experimental Results)

During this quarter's reporting period experiments were performed on 10 pigeons, single unit action potential neural activity from 30 neurons in the vestibular ganglion was monitored and stored on analog magnetic tape. All experiments were performed on the pigeons in an "awake preparation" anesthetic condition. The sequencing of anesthesia to produce this condition was as follows: At 8:30 A.M., 50 milligrams of Ketajec, "Ketamine Hydrochloride" was injected intramuscularly into the breast muscle of the pigeon. In approximately 10 minutes the bird was in a state of general anesthesia. During this level of anesthesia, a tracheotomy was performed after the area surrounding the incision had been infiltrated with xylocaine (lidocaine). Following infiltration of the surrounding area with xylocaine, a midline incision was made from the bird's vent to the breast bone, the posterior air sac was punctured, and a 95% to 5% O_2 - CO_2 mixture was blown through the animal at a rate of 500 ml/min. After infiltrating the neck muscles which overlie the parietal bone, with xylocaine, Scarpa's ganglion

was exposed by the Ewald approach. Recordings were made from a region which had been previously confirmed as the location of cell bodies of the anterior semicircular canals. Recording sessions usually began at 3:00 P.M. with no subsequent injections of Ketamine following the initial injection at 8:30. Prior to the recording session the animal was paralyzed with 10 milligrams of Flaxadil (Gallamine triethiodide). Recordings were obtained with 3M NaCl glass microelectrodes whose resistance was 1 Meg. ohm.

Data reduction plots of single unit action potential trains, which were obtained under the above anesthetic conditions, are displayed in Figures 1 - 11. Two units are presented which are representative of those which have previously been described as "regular" (Figures 1-5) and "irregular" (Figures 6-11). The first order statistics presented in Figure 1 illustrate that a "regular" firing unit obtained from an "awake" preparation has a mean and standard deviation which falls within the range of those obtained from a preparation under barbiturate anesthesia. Specifically, the mean interspike interval for the "regular" firing unit displayed in Figure 1 was 7.4 milliseconds. The range of interspike intervals obtained for vestibular units with barbiturate anesthesia was from 4.0 milliseconds to 51.2 milliseconds. Similarly the standard deviation of 0.57 for the unit illustrated in Figure 1 falls within the range of standard deviations for barbiturate units which is between 0.18 milliseconds and 32.07 milliseconds. Figure 2 indicates that a periodicity exists in the "regular" firing interspike interval train. This is further supported by the autocorrelation plot presented in Figure 3. The trend analysis in Figure 2 indicates that the periodicity, which produces a highly

significant Wald-Wolfowitz Z value, is produced primarily by the inherent periodicity in a very regularly repeating interspike intervals which is inherent in "regular" firing units. It is interesting, however, to note that the trend analysis plot indicates that the unit's statistical characteristics do not change over time. That is, the firing pattern observed from the first to the 512th interspike interval is very similar of that observed for the 513th through the 1,024th interspike interval. This paradox points out that one must be careful in using the Wald-Wolfowitz and auto-correlation functions as indicators of stationarity. While the first and second moments are comparable for a "regular" unit observed from an "awake preparation and a preparation under barbiturate anesthesia, the third and fourth moments are not. The coefficient of skewness obtained for this unit was 15.13 and the coefficient of excess was 41.73. In our previous work we have never obtained a coefficient of excess with such a large value (see Figure 9). Another difference is illustrated in Figures 4 and 5. The Kolmogorov Smirnov statistic of probability of good fit for the p.d.f. whose distribution function is the normal distribution and the Wiener-Levy first passage time distribution functions are 0.0869 and 0.375 respectively. When the same models were fit to interspike interval histograms obtained from discharge patterns in barbiturate anesthetized animals, the "best fit" Kolmogorov Smirnov statistics for comparable discharge patterns was 1.0 for the normal and 0.998 for the Wiener-Levy. A Kolmogorov Smirnov probability of 1.0 indicates a perfect fit.

Therefore, in summary, these preliminary data, based on a very small sample, indicate that a "regular" firing vestibular unit

obtained from an "awake" preparation produces a discharge pattern whose mean, standard deviation and coefficient of variation are similar to that obtained from a comparable unit in a barbiturate anesthetized preparation. However, the coefficient of excess and the coefficient of skewness, which are based on the fourth and third moments respectively, are grossly different for an "awake" preparation vis-à-vis a barbiturate anesthetized preparation. Also probability density function models which produced good fits to "regular" unit interspike interval histograms obtained with barbiturate anesthesia do not appear to fit those obtained from an "awake" preparation. It should be reemphasized that the above conclusions are very preliminary and can only be stated with certainity when a much larger sample has been obtained and when a range of probability density functions have been fit to these data and compared to those obtained from barbiturate anesthetized preparations.

The "irregular" units obtained from an "awake" preparation displays statistical properties which correspond more closely to those obtained under barbiturate anesthesia. The unit presented in Figures 6, 7, and 9 has first, second, third and fourth moment statistics which are comparable to those which were obtained for "irregular" units under barbiturate anesthetic conditions. Specifically, the Z statistic in Figure 6, indicates that no significant trend was observed in the action potential train of 1024 impulses. This lack of periodicity is supported by the auto-correlation function presented in Figure 7. The mean and standard deviation of the interspike intervals, which comprise the interval histogram in Figure 8, fall within the range of values obtained from preparations under barbiturate anesthesia (vide supra). In Figure

9, the "irregular" unit obtained in the present study is indicated by + and its relation to units obtained in a previous study under barbiturate anesthesia can be noted. The black circle values indicate units whose properties allowed us to classify them as renewal units and the closed circle values indicate nonrenewal units. When we compare the Kolmogorov Smirnov probability values (Pks) for the "goodness of fit" of the probability density functions for the Wiener-Levy process and the Ornstein-Uhlenbeck process illustrated in Figures 10 and 11 respectively, we obtain Pks values of 0.057 and 0.376. These "goodness of fit" indicators are higher than those obtained for a unit which falls in a comparable region on the B1, B2-3 plot (Figure 9) and which was gathered under the conditions of barbiturate anesthesia. It appears therefore that barbiturate anesthesia does not significantly influence the statistical properties of an "irregular" type vestibular unit, at least in comparison to "regular" units and as far as we can presently determine from the very small sample of units which we have obtained. The biological implications of this finding will require careful analysis.

III. Fourth Quarter Plans

During the fourth quarter our efforts will be devoted to two areas. First, we will continue to increase our sample of vestibular units obtained from an "awake" preparation. If differences continue to appear between these units and those which we have previously obtained under barbiturate anesthesia we shall perform the following experiment. We shall locate a "regular" vestibular unit, obtain its statistical properties "on line", and then administer intravenously 1 cc of Equithesin anesthesia. We then will record the statistical

properties of the same unit at various time intervals following administration of the barbiturate anesthesia. We will repeat the experiment with an "irregular" unit. These experiments will allow us to monitor the dynamic time course of the effect of anesthesia on spontaneous discharge pattern from the same neuron. In the second area, we will compare the statistical properties of the discharge patterns we have obtained from the "awake" preparations with those which we shall obtain from preparations who have received injections into the otic capsule of the following drugs: 1) 10^{-5} molar strychnine, 2) 10^{-4} molar atropine. These acelylcholinesterase blockers has been shown to be effective in eliminating efferent spontaneous activity within the vestibular neuroepithelium. We suspect the efferent activity within the vestibular neuroepithelium plays a role in the origin of the spontaneous afferent activity. Therefore these drugs should significantly modify the statistical characteristics of the spontaneous discharges which we observe from vestibular primary afferents following their application. Drugs which have been associated with the prevention or diminution of motion sickness, such as diazepam and dimenhydrate will also be injected into the perilymphatic space and the spontaneous afferent discharge from the vestibular neuroepithelia will be monitored at variable interval lengths following their application.

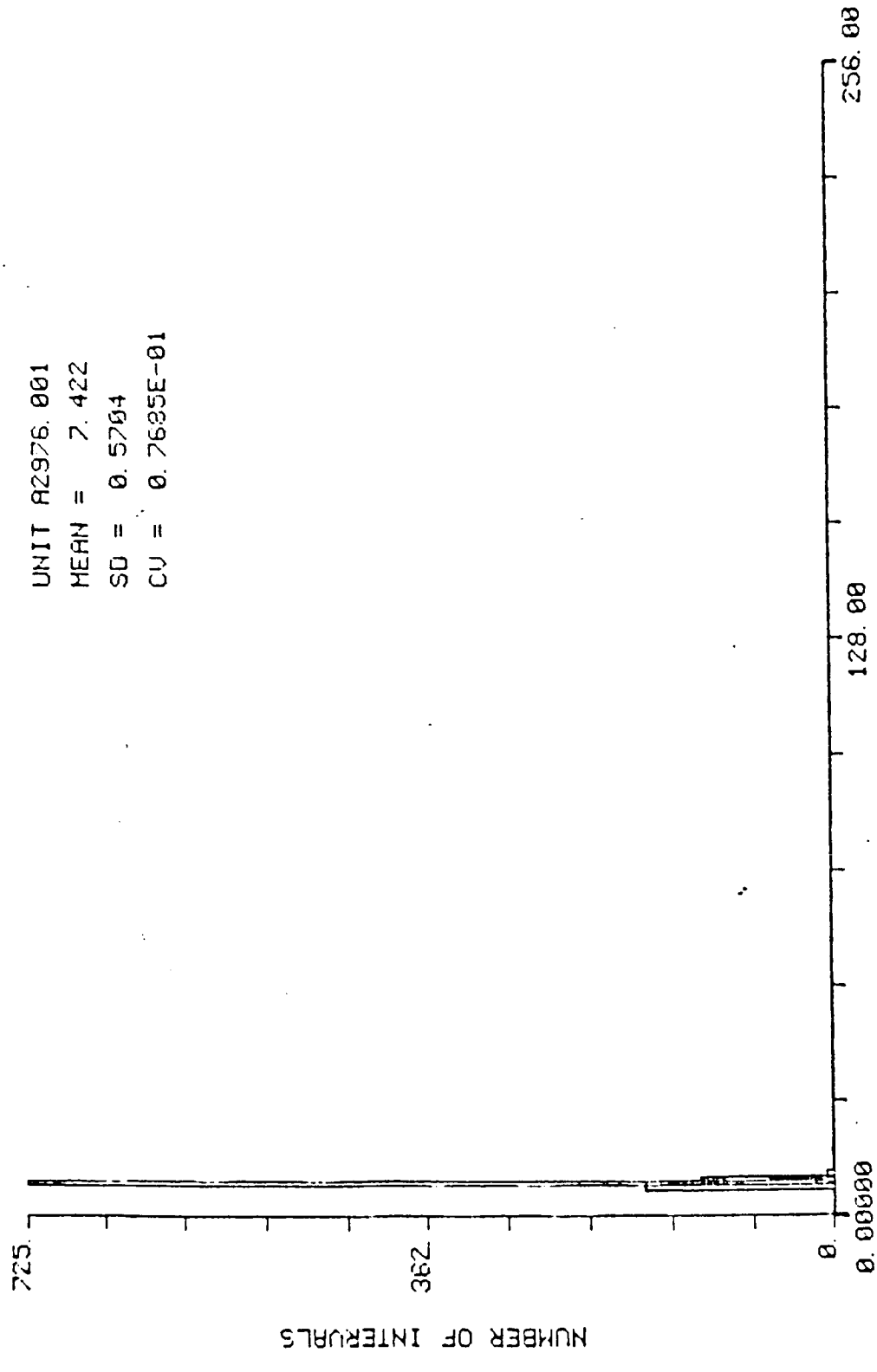
INTERVAL HISTOGRAM
UNIT A2976.001
MEAN = 7.422
SD = 0.5704
CV = 0.7685E-01
NUMBER OF INTERVALS
725.
362.
0.
0.00000
128.00
256.00
INTERVAL TIME (MS)

FIGURE 1

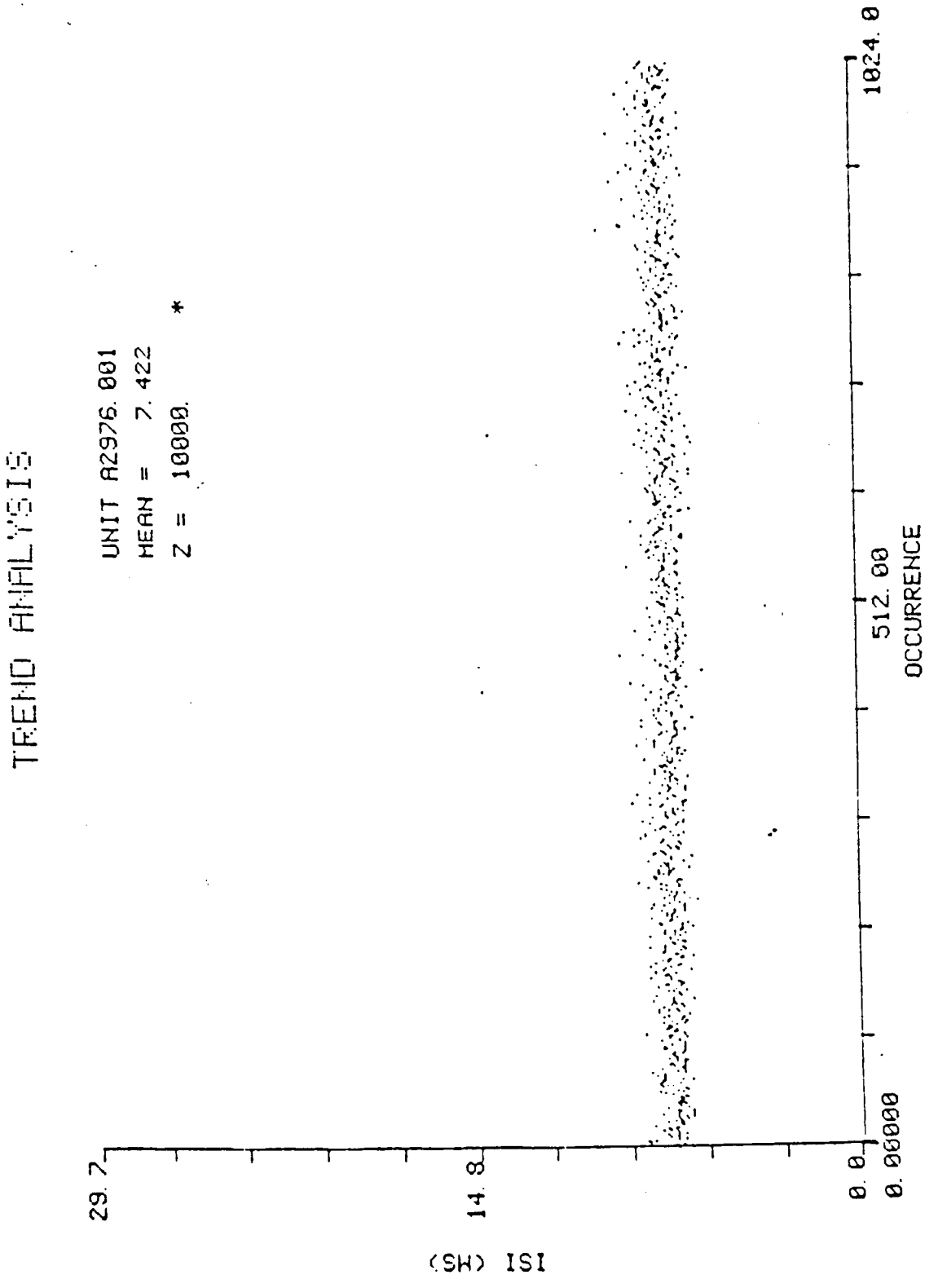
TREND ANALYSIS
UNIT A2976.001
MEAN = 7.422
Z = 10000.
*
29.7
14.8
0.0
ISI (MS)
0.00000
512.00
1024.0
OCCURRENCE

FIGURE 2

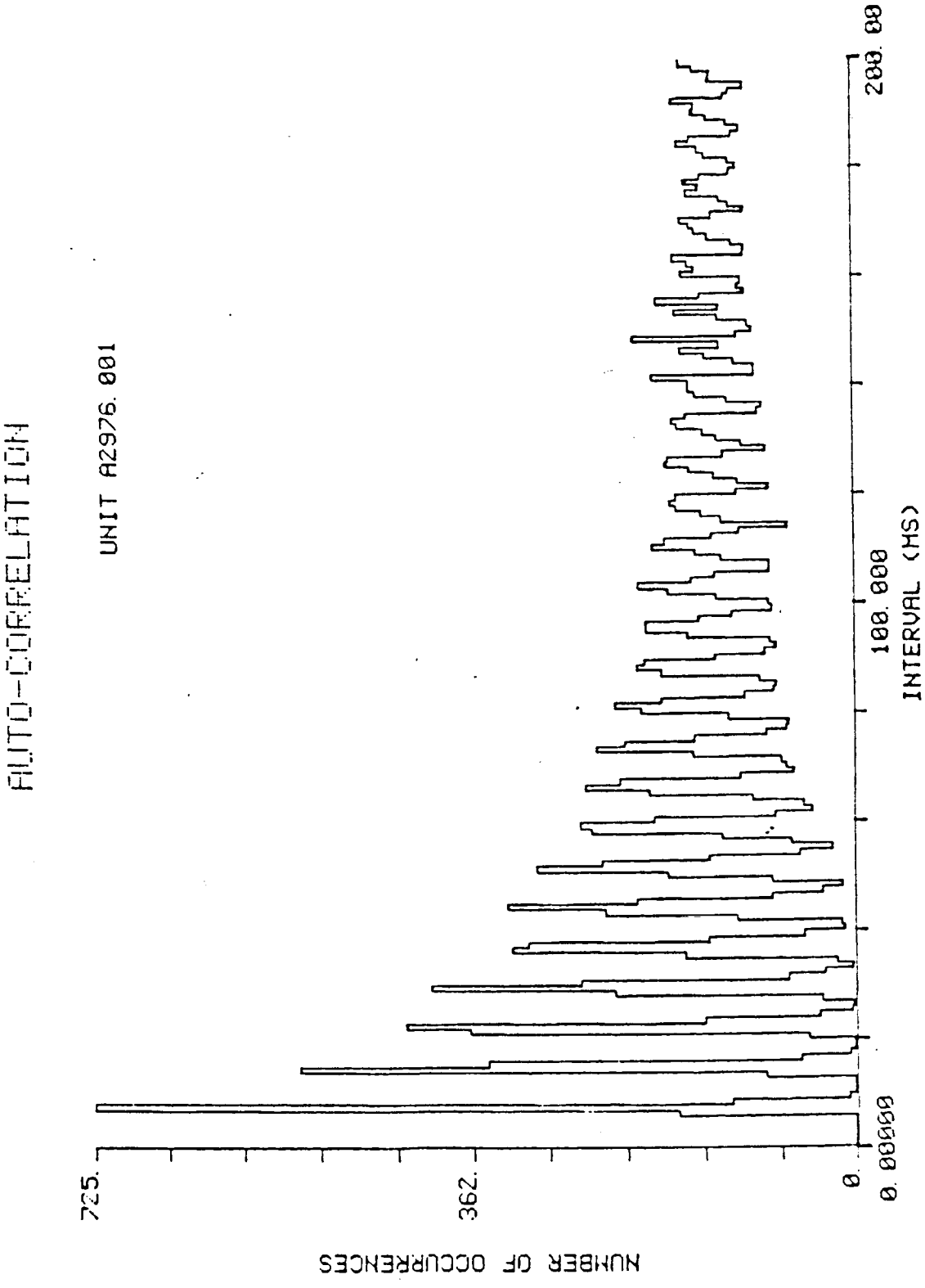
AUTO-CORRELATION
UNIT A2976.001
NUMBER OF OCCURRENCES
725.
362.
0.
0.00000
100.000
200.00
INTERVAL (MS)

FIGURE 3

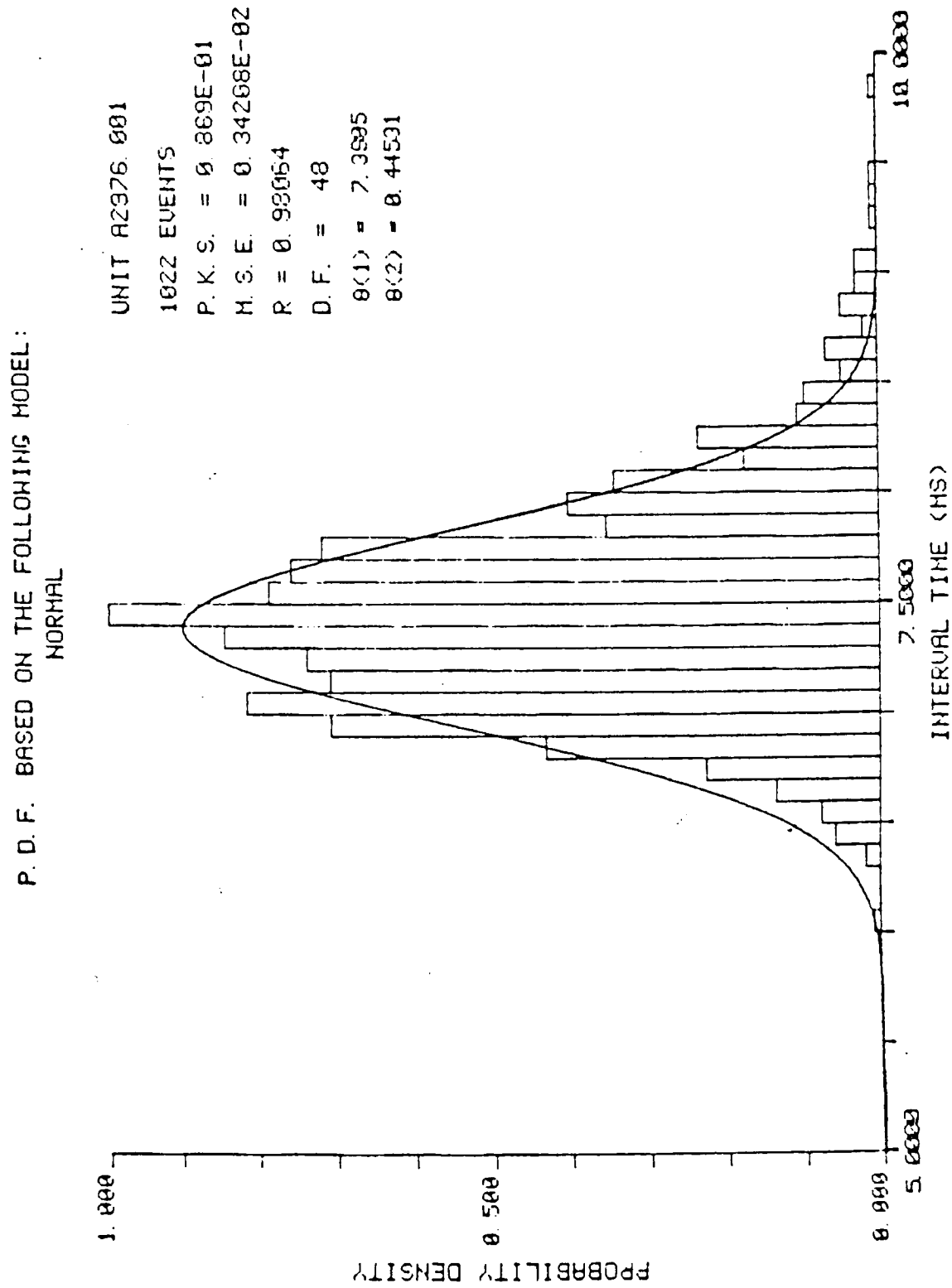
P. D. F. BASED ON THE FOLLOWING MODEL:
NORMAL
UNIT A2376 001
1022 EVENTS
P. K. S. = 0.869E-01
M. S. E. = 0.34268E-02
R = 0.99064
D. F. = 48
θ(1) = 7.3995
θ(2) = 0.44531
PROBABILITY DENSITY
1.000
0.500
0.000
5.0000
7.5000
10.0000
INTERVAL TIME (HS)

FIGURE 4

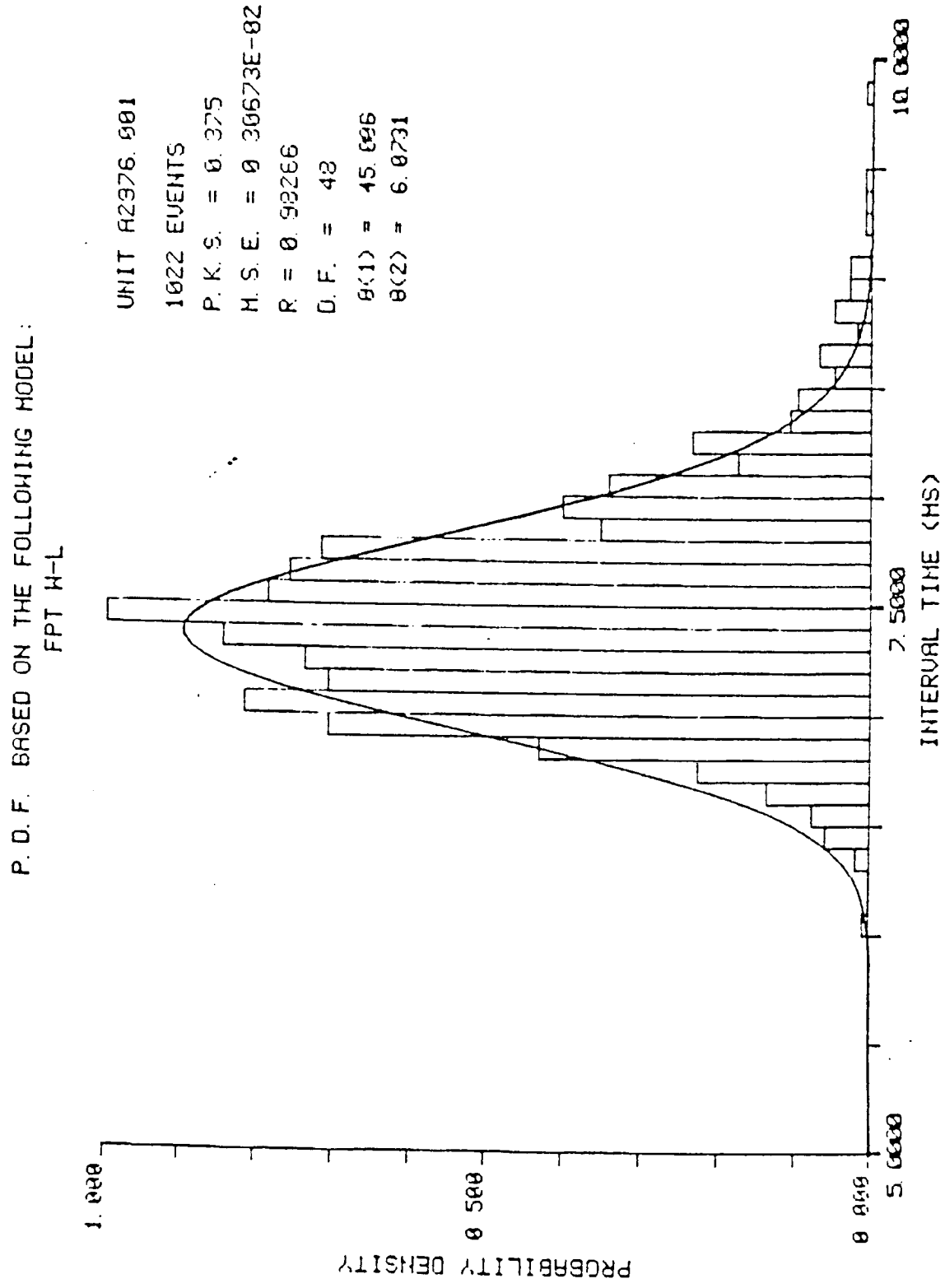
P. D. F. BASED ON THE FOLLOWING MODEL:
FPT H-L
UNIT A2376.001
1022 EVENTS
P. K. S. = 0.375
H. S. E. = 0.30673E-02
R = 0.99266
D. F. = 48
θ(1) = 45.696
θ(2) = 6.0731
PROBABILITY DENSITY
1.000
0.500
0.000
5.0000
7.5000
10.0000
INTERVAL TIME (HS)

FIGURE 5

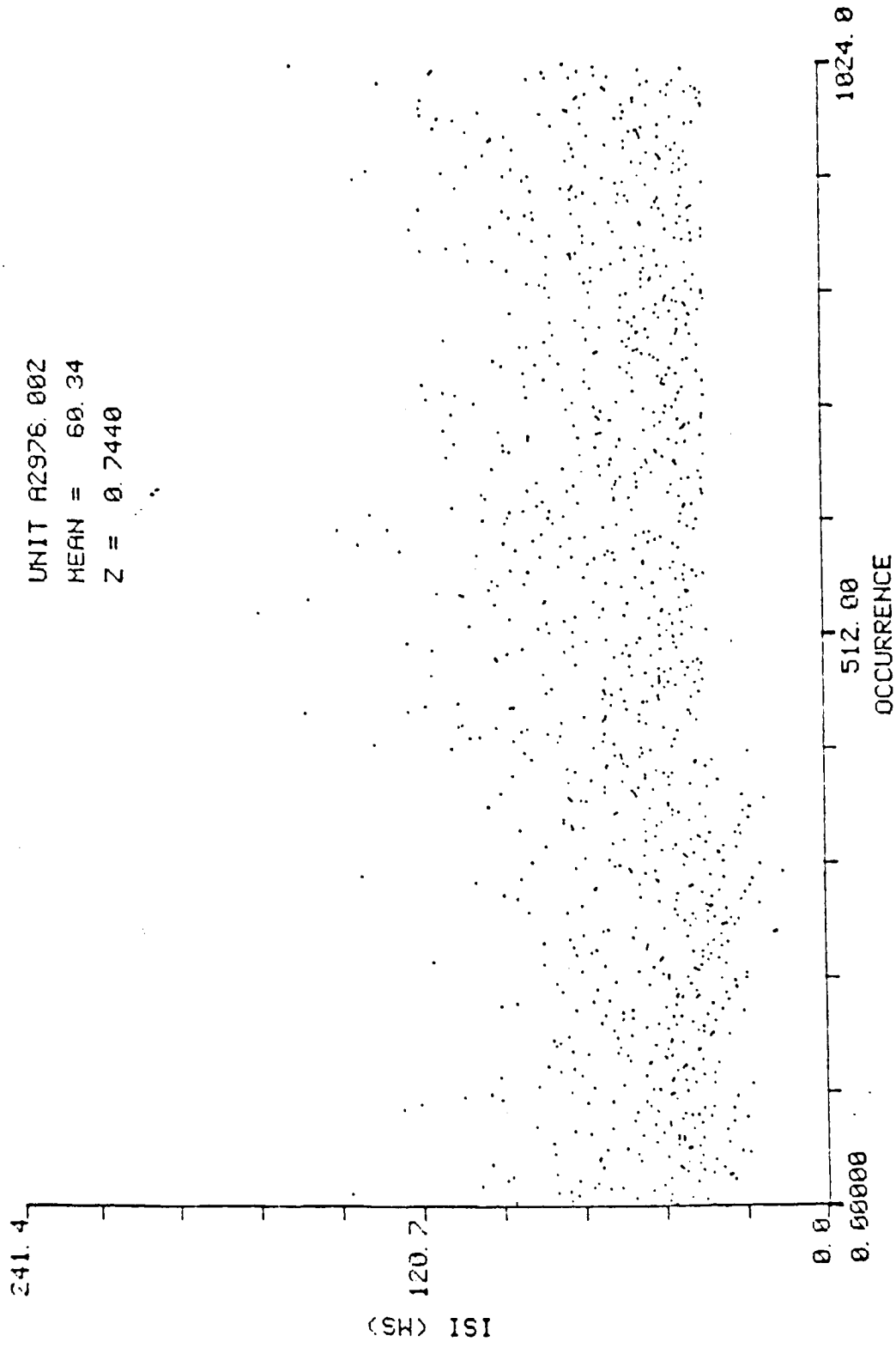
TREND ANALYSIS
UNIT A2976.002
MEAN = 60.34
Z = 0.7440
241.4
120.7
0.0
ISI (MS)
0.00000
512.00
1024.0
OCCURRENCE

FIGURE 6

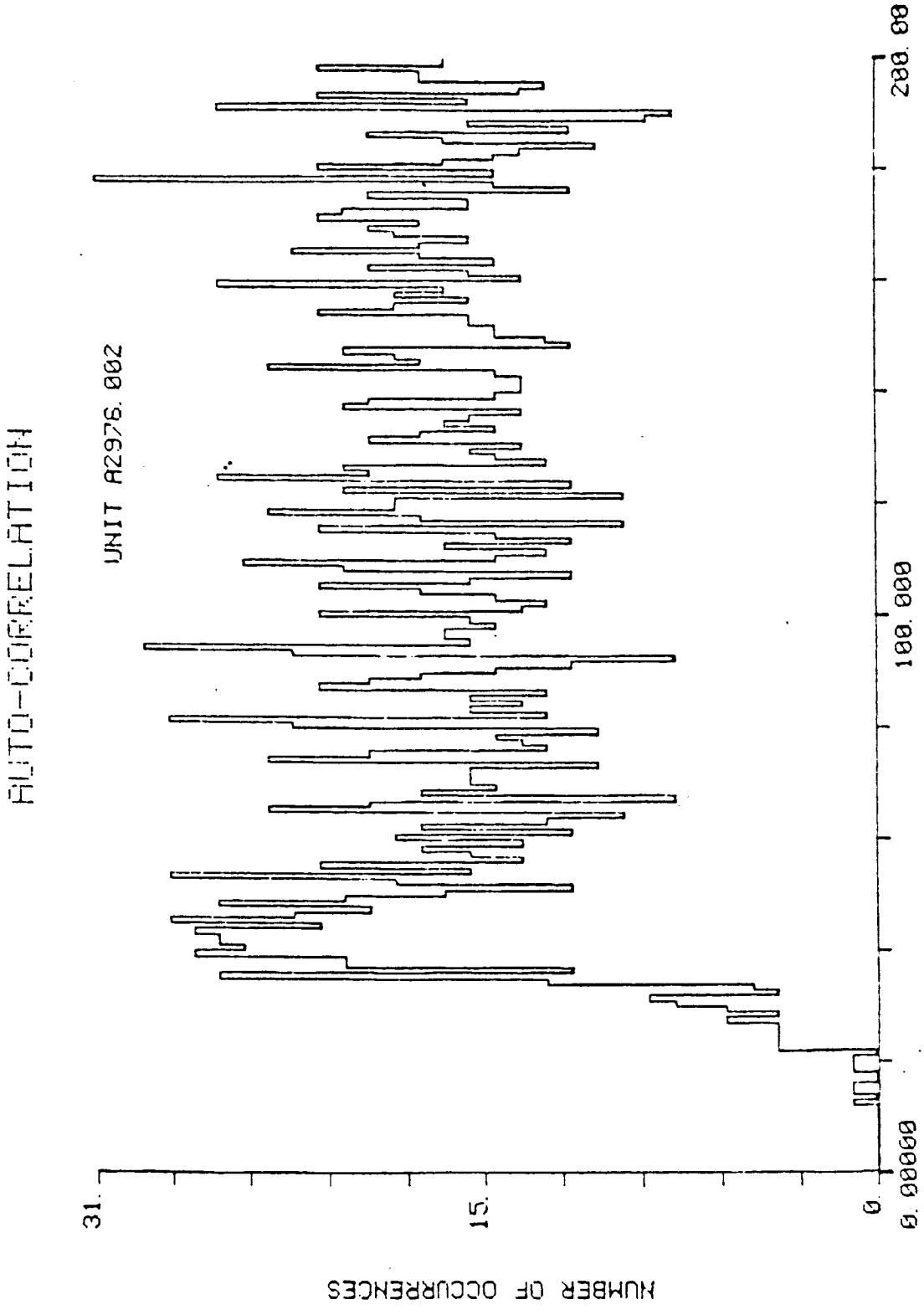
AUTO-CORRELATION
UNIT A2978.002
NUMBER OF OCCURRENCES
31.
15.
0
0.00000
100.000
200.00
INTERVAL (MS)

FIGURE 7

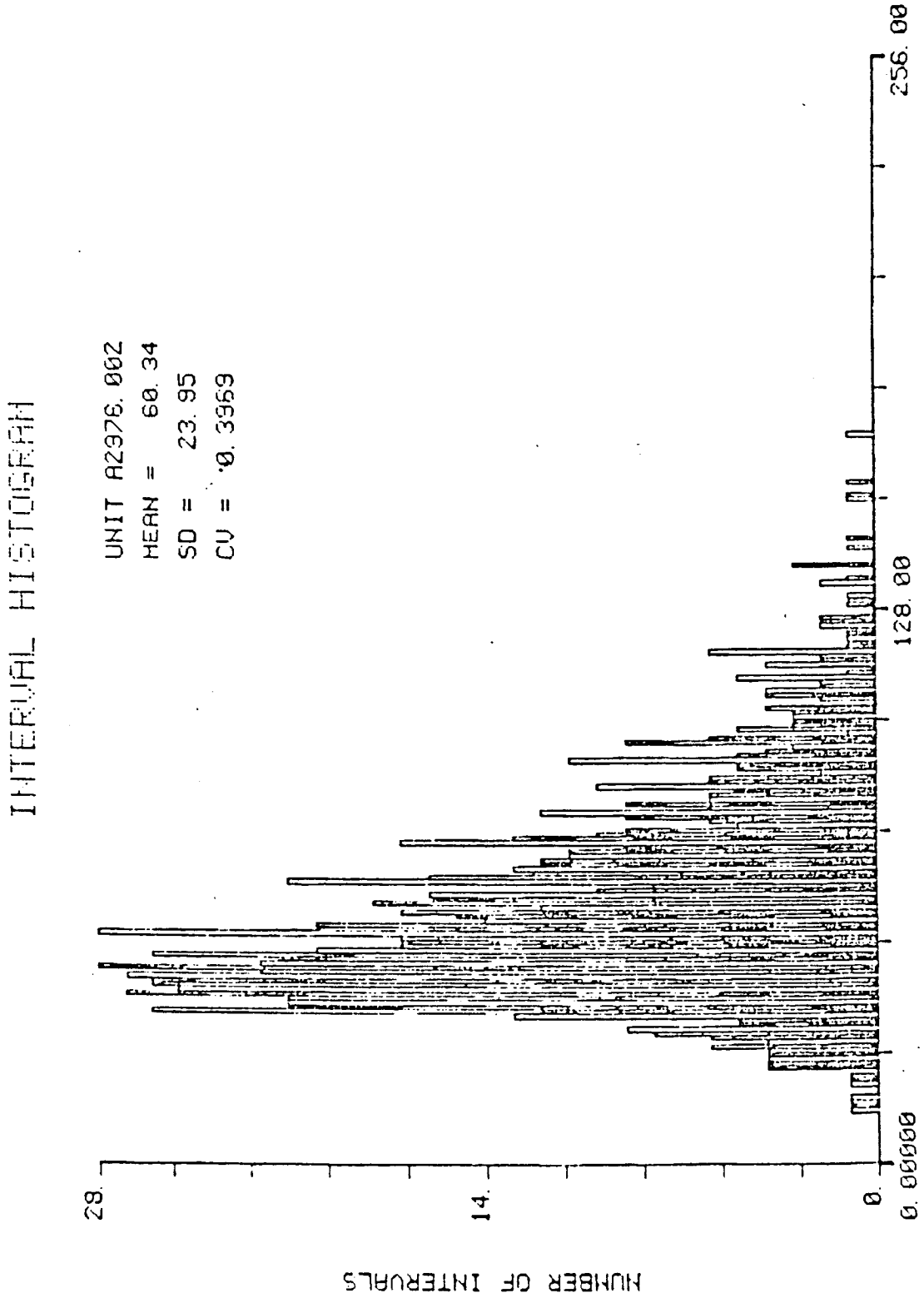
INTERVAL HISTOGRAM
UNIT A2976.002
MEAN = 60.34
SD = 23.95
CV = 0.3969
NUMBER OF INTERVALS
28.
14.
0.
0.00000
128.00
256.00
INTERVAL TIME (MS)

FIGURE 8

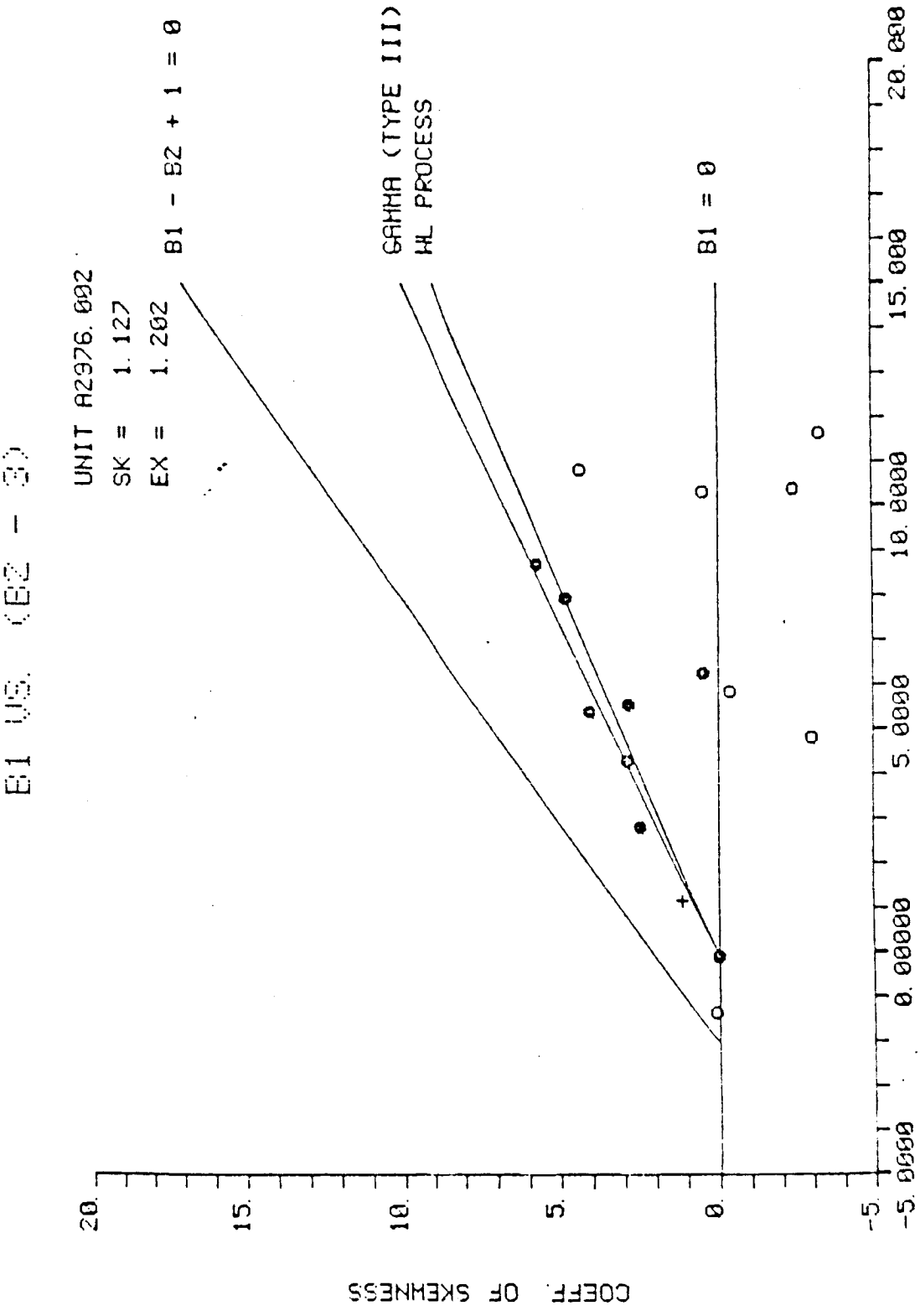
B1 VS. (B2 - 3)
UNIT A2376.002
SK = 1.127
EX = 1.202
B1 - B2 + 1 = 0
GAMMA (TYPE III)
ML PROCESS
B1 = 0
COEFF. OF SKEWNESS
COEFF. OF EXCESS
20.
15.
10.
5.
0.
-5.
-5.0000
0.00000
5.0000
10.0000
15.000
20.000

FIGURE 9

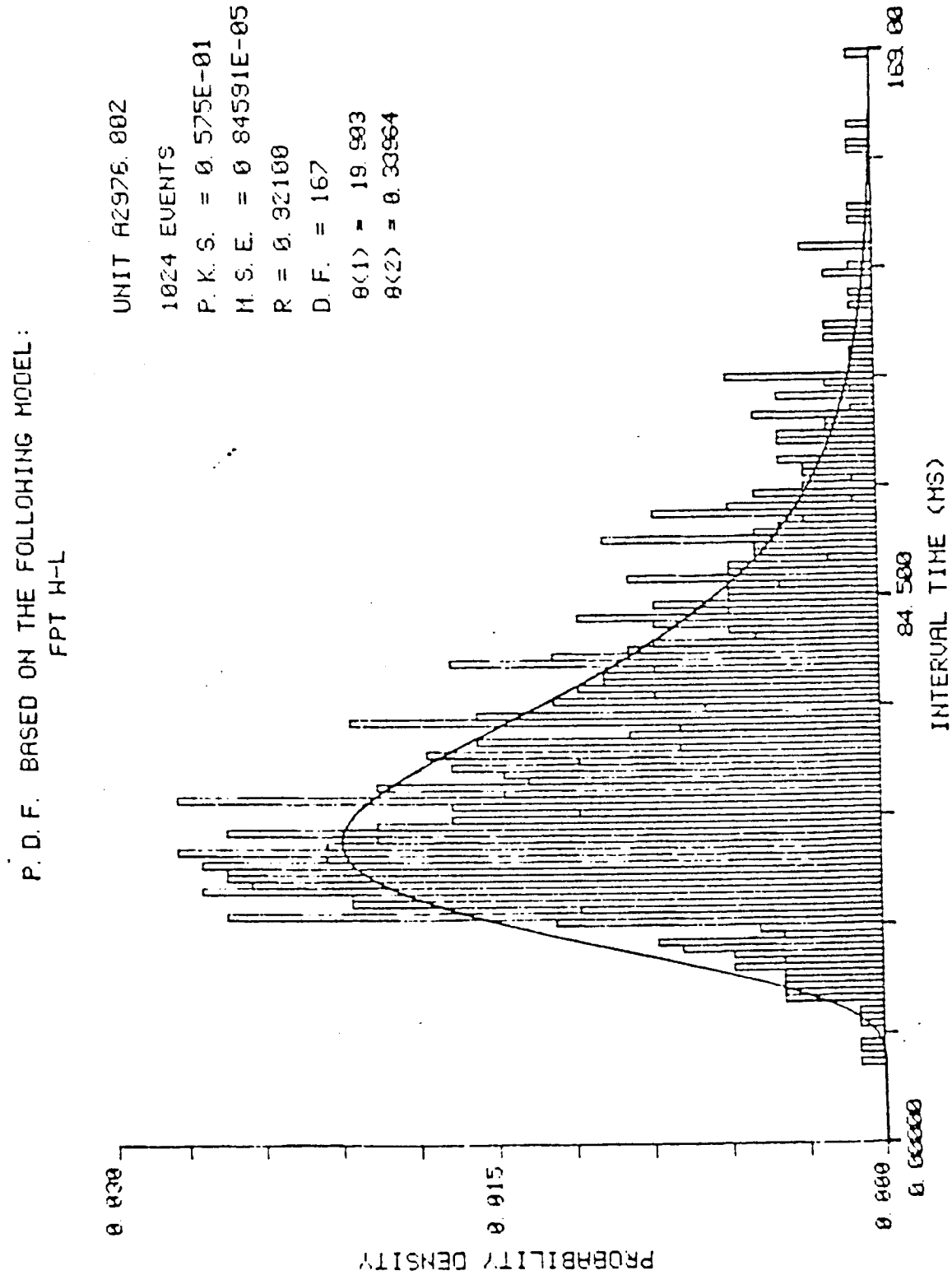
P. D. F. BASED ON THE FOLLOWING MODEL:
FPT H-L
UNIT A2976.002
1024 EVENTS
P. K. S. = 0.575E-01
M. S. E. = 0 84591E-05
R = 0.32100
D. F. = 167
θ(1) = 19.993
θ(2) = 0.33964
0.030
0.015
0.000
PROBABILITY DENSITY
84.500
169.00
INTERVAL TIME (MS)

FIGURE 10

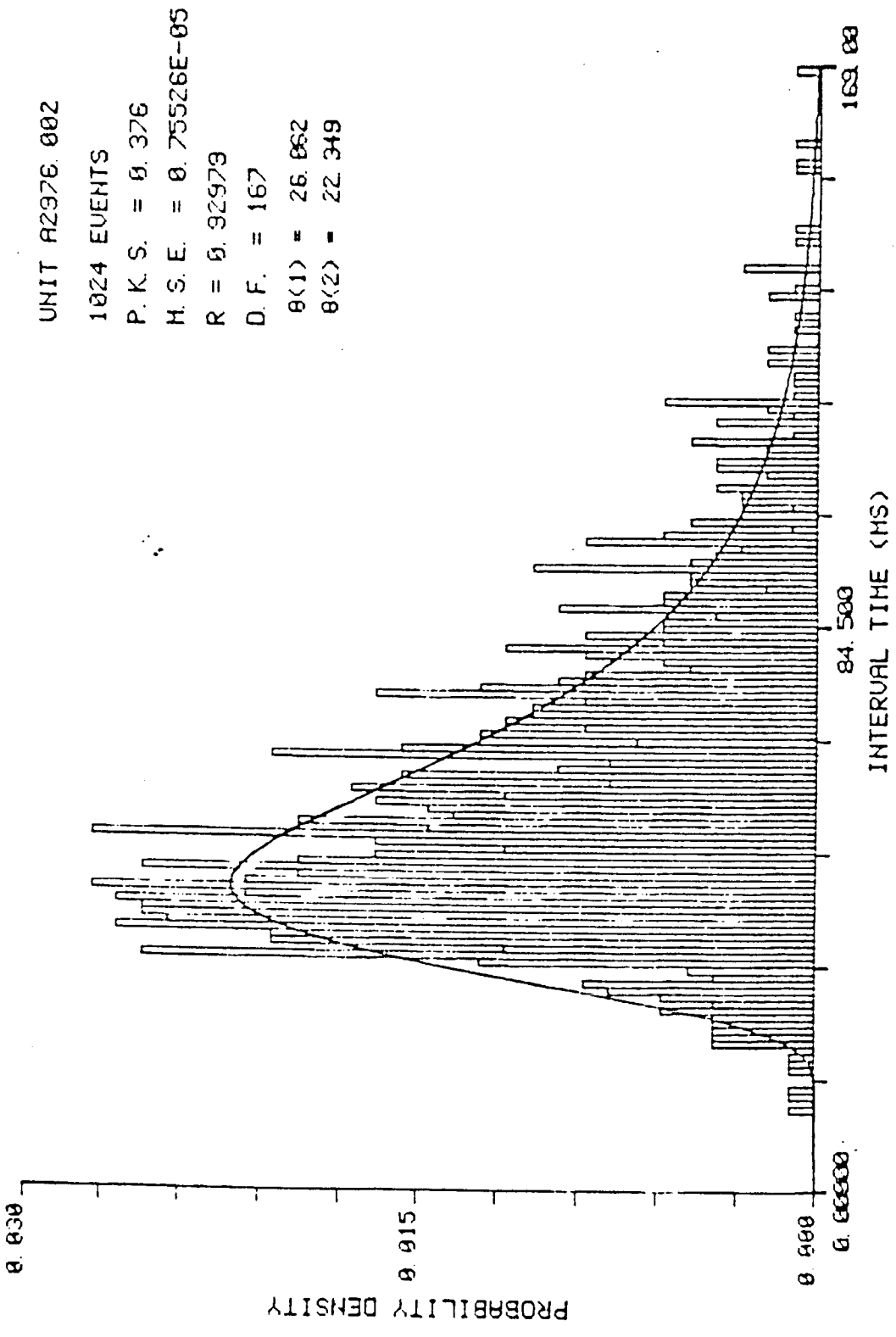
P. D. F. BASED ON THE FOLLOWING MODEL:
FPT 0-U
UNIT A2976.002
1024 EVENTS
P. K. S. = 0.376
M. S. E. = 0.75526E-05
R = 0.32979
D. F. = 167
θ(1) = 26.862
θ(2) = 22.349
0.030
0.015
0.000
PROBABILITY DENSITY
84.500
169.00
INTERVAL TIME (MS)

FIGURE 11

VIII. PROPOSED DIRECTION OF FUTURE WORK

PROPOSAL - April 1, 1984/September 30, 1985 (1 1/2 years)

A. Specific Aims

1. Examine Scarpa's ganglion in three pigeons and three gerbils using light (interference) microscopy and TEM.

a) Determine the ratio of myelinated cell bodies to unmyelinated cell bodies, b) determine the ratio of multipolar cell bodies to bipolar cell bodies, and c) determine if synaptic processes exist in Scarpa's ganglion.

2. Record intracellularly from Scarpa's ganglion cell bodies in the pigeon.

a) Determine if postsynaptic potentials exist, b) determine whether the postsynaptic potentials are excitatory or inhibitory, c) form interevent histograms for the postsynaptic potentials, and d) inject Lucifer yellow dye into the cells and determine if cells are bipolar or multipolar.

3. Use light (interference) microscopy and TEM to examine serial sections of the cristae ampullaris in three pigeons and three gerbils.

a) Determine the distribution (produce a histogram) of number of type I hair cells in a single nerve calyx, b) determine the distribution of multiple type I hair cells, single type I hair cells and II hair cells over the surface of the crista ampullaris, particularly with reference to the apex and the base.

4. Record intracelluarly from hair cells and afferent/efferent processes in the crista ampullaris of the pigeon.

a) Determine if both excitatory and inhibitory postsynaptic potentials exist in the sensory neuroepithelium. b) Determine the distribution of interevent intervals of the postsynaptic potentials, and c) inject Lucifer yellow dye into the processes and determine if a given process innervates a calyx with one or multiple type I hair cells, a type II hair cell or combinations of multiple hair cells.

B. Rationale

Anatomical and electrophysiological evidence is accumulating to indicate that a greater amount of neural processing occures in the vestibular sensory neuroepithelium and its peripheral processes than was previously thought. Caston and his colleagues (Caston, 1972; Caston and Gribenski, 1975, 1977, 1982) have recorded the spontaneous activity on single fibers from one (usually the anterior) of the ampullary nerves, in the isolated frog head preparation, while applying electrical stimulation to one of the remaining ampullary nerve branches or a nerve branch subserving one of the otolith organs. They have found that electrical

stimulation of each of these nerve branches has a strong inhibitory influence on the spontaneous activity of afferent vestibular fibers subserving either the horizontal or vertical SC's. These results led them to suggest that a small percentage (6-8%) of the total number of fibers in the ampullary nerves are receptor-receptor fibers from the other labyrinthine sense organs. They further suggested that excitation of these receptor-receptor fibers has a strong inhibitory influence on the spontaneous activity of ampullary afferent fibers. In their most recent study (Caston and Gribenski, 1982), these investigators chronically sectioned the whole vestibular nerve either lateral and medial to SG, recorded the activity on single ampullary afferent fibers from the anterior SC during electrical stimulation of either the saccular nerve, horizontal canal nerve, or posterior canal nerve. When the whole vestibular nerve was sectioned medial to SG, electrical stimulation of the saccular nerve resulted in inhibition of spontaneous activity in 21% (12/57) of vertical ampullary afferent fibers tested. Inhibition of spontaneous activity was noted in a similar percentage of anterior ampullary afferent fibers during discrete stimulation of either the horizontal or posterior SC nerve branches. When these investigators (Caston and Gribenski, 1982) sectioned the nerve lateral to SG, inhibition was noted in only 2 of 160 anterior ampullary afferent fibers during electrical stimulation of the horizontal canal nerve. These results led Caston and Gribenski (1982) to suggest the existence of an inhibitory feedback loop outside the brain but including SG and mediated by receptor-receptor fibers. Schwartz et al. (1978) using HRP histochemistry and autoradiography have demonstrated receptor-to-receptor connections by collateralizing efferent axons in the pigeon. They injected small alloquats of HRP or tritiated adenosine into the sensory neuroepithelium of one of the ampullae and the second marker in one of the other ampullae and noted double labeling in efferent neurons in the reticular formation. These investigators did not examine SG to determine if injections into separate ampullae double labeled SG cells. The possibility of collateralizing dendrites from SG cells has been enhanced by the documentation (using light and TEM microscopy) of multipolar neurons in the vestibular ganglion of several species. Chat and Sans (1979) have identified multipolar neurons in the cat's vestibular ganglion. Ballentine and Engstrom (1969) have reported multipolar cells in the guinea pig's vestibular ganglion. Perachio et al. (1983) have reported multipolar cells in the gerbil vestibular ganglion. Ylikoski and Belal (1981) and Kitamura and Kimura (1983) have reported multipolar cells in the human vestibular ganglion. Surprisingly, Kitamura and Kimura (1983) also observed that the majority of vestibular ganglion cells (in one human) were unmyelinated. Kitamura and Kimura (1983) described two types of vestibular ganglion cells; the majority of which were bipolar but some of which were multipolar. They also noted that there were two classes of multipolar cells. One of them was large and like bipolar cells, did not make synaptic contact with any neural processes. However, a second class of small multipolar cells synapsed with nerve fibers.

Also, there appears to be a complicated network of innervation in the neuroepithelium of the cristae and maculae. This innervation is illustrated, for example, in Fig. 9.

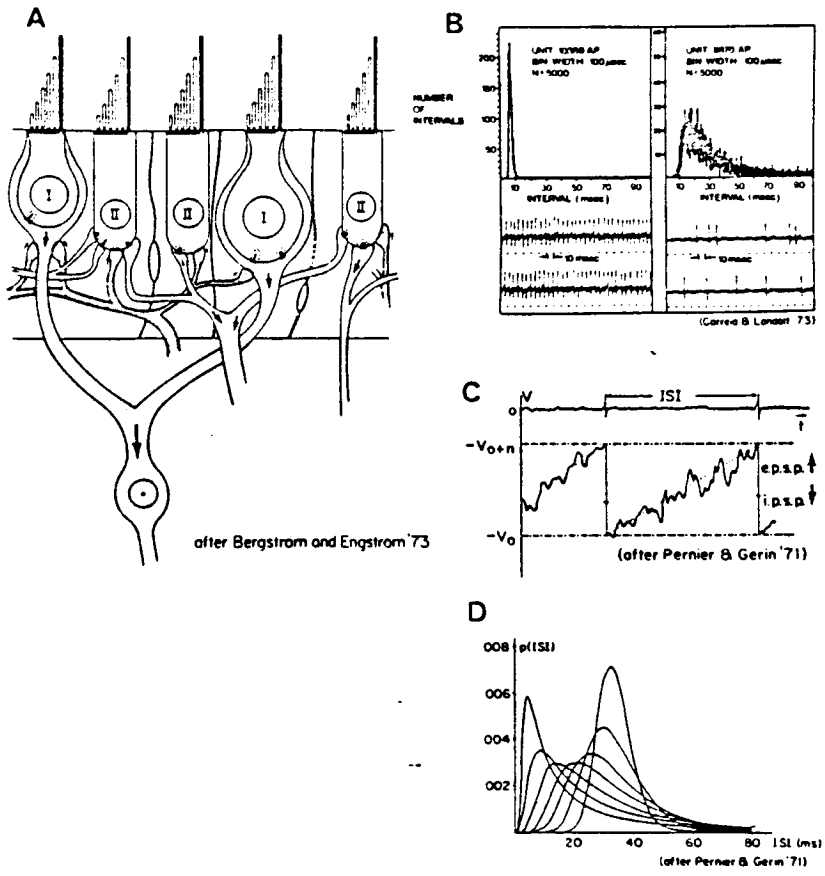

Figure 9

A collage of figures indicating the neuroanatomical and neurophysiological correlates which we (Correia and Landolt, 1978) have suggested are associated with the origin of spontaneous activity recorded on vestibular primary afferents. (A) A schematic conceptualization of the complex unmyelinated processes within the vestibular sensory neuroepithelium of mammals. Note the similarity between the synaptic structures associated with the type I hair cell on the right side of the figure and those presented in Fig. 8C for the pigeon. (B) Two action potential trains with their resulting interspike interval histograms. These data were obtained from single anterior afferents in the barbiturate anesthetized pigeon. The action potential train and ISI histogram on the left side represents a regularly firing afferent; whereas the action potential train and ISI histogram on the right side of the figure illustrates an irregularly firing afferent. Note that these two ISI histograms are incorporated in the family of probability density functions

(see Fig. 9D) which describe the first passage time of a Wiener-Levy process with absorbent barrier. (C) A conceptualization of the relationship between a single unit action potential train and the membrane voltage of the neural unit which produces the train. Depolarizing EPSP's drive the membrane toward threshold and the production of an action potential while hyperpolarizing IPSP's work to drive the membrane away from threshold. Based on this conceptualization the ISI histogram is determined by the absolute number of EPSP's, or when present, the ratio of IPSP's to EPSP's as these graded potentials contribute to the generator potential which is believed to produce the action potential on a vestibular primary afferent at the spike originating locus (SOL). The SOL is thought to be located at the point of myelinization of vestibular primary afferents as they exit the basement membrane of the sensory neuroepithelium. (D) A family of probability density functions for the Wiener-Levy process. This process, has a rigorous mathematical foundation, and has been used to describe the Brownian motion of a particle before it passes through an absorbent barrier.

In Fig. 9A shaded neural processes represent efferent axons. Unshaded neural processes represents afferent dendrites. In birds, mammals, and some reptiles there are two types of hair cells (Wersall et al., 1965) and they are innervated in fundamentaly different ways (Ades and Engstrom, 1965; Engstrom, 1968; Engstrom et al., 1972; Engstrom et al., 1965). Usually the unmyelinated dendrite, which innervates the type I hair cell, forms a nerve calyx around most of the subsurface portion of the sensory cell. In some cases, the unmyelinated dendrite may branch and form individual nerve calyxes with up to 10 other separate type I hair cells. In the the neuroepithelia of the vestibular apparatus of some species, for example, in the bird, a single nerve calyx may surround up to 12 type I hair cells (Friedmann and Bird, 1967; Jorgenson, 1970, 1972, 1973). The type II hair cell on the other hand, is innervated by a bouton-like terminal from the unmyelinated dendrite of the primary afferent bouton. As in the case of the type I hair cell, several type II hair cells may be innervated by branches from a single dendrite. A dendrite may even branch, differentiate into a calyx or bouton and then form a synaptic junction with another type I and/or type II hair cell. Other even more complex synaptic arrangements are also possible (Bergstrom and Engstrom, 1973). For example, a nerve calyx may form a synapse with a type I hair cell on its innermost side and at the same time form a synapse with a soma of an adjacent type II cell on its outer most surface (Engstrom et al., 1972). Even reciprocal synapses between hair cells have been noted (Dunn, 1980) in the bulfrog.

The fibers which innervate the hair cells form a complicated neural plexus. It has been known for some time that thick, medium, and thin fibers innervate the sensory epithelium of the crista ampullaris (Raymon-y-Cajal, 1908). Thick fibers have been shown to branch into 4 or 5 thinner fibers each of which forms a nerve calyx with a type I cell. Medium size fibers form calyxes with type I hair cells in a similar manner. There are also fibers which branch and form afferent terminal endings (boutons) on the somas of one or more type II hair cells. Thin fibers branch and form <u>en passant</u> and terminal endings (boutons) on the

somas on type II hair cells (an axo-somatic synapse) and on the unmyelinated axon calyx surrounding the type I hair cell. Efferent (centrifugal) fibers are known to synapse on hair cells in the vestibular neuroepithelia (see for example, Klinke and Galley, 1974). Bouton terminals for these fibers synapse on type II hair cells and the calyxes of type I hair cells. The efferent bouton terminals on type II hair cells are presynaptic with regard to the afferent synapse in the same cell. This means that an efferent synapse could control (increase or decrease) the amount of transmitter substance released at an afferent synaptic site. It it controversial as to whether the vestibular efferent system is inhibitory or excitatory (Fex, 1962; Flock and Russell, 1973; Gleisner and Henriksson, 1963; Salla, 1965; Schmit, 1963; vis-a-vis Goldberg and Fernandez, 1980).

There is good anatomical (e.g. Engstrom et al., 1972) but limited electrophysiological (Schessel and Highstein, 1981; Rossi et al., 1980) evidence to suggest that it is primarily neurochemical synaptic transmission that occurs within the vestibular neuroepithelium. For example, presynaptic structures are found in the hair cells. These structures, which may be elongated, spherical, or omega shaped, are always surrounded by synaptic vesicles; the latter of which have been associated with synapses that release the neural transmitter substance. Similarly, the bouton endings of efferent fibers are characterized by having small vesicles inside the nerve ending and a synaptic cisterna in close opposition to the postsynaptic membrane.

Electrophysiological support has been given for the existence of excitatory postsynaptic potentials (EPSP's) in the vestibular neuroepithelia. Ishi et al. (1971) and Furukawa and Ishi (1967) have recorded intracellular spontaneous and sound-driven graded potentials in the sensory axons of the VIIIth nerve of the goldfish. These potentials, which were recorded near the basement membrane in the macula sacculi, were regarded to be postsynaptic EPSP's. Schessel and Highstein (1981) recorded intracellularly from irregular vestibular afferents in the lizard near the basement membrane of one of the cristae. They observed spontaneous EPSP's (5-15 mv) with a rapid decay of the falling phase. These potentials did not reverse polarity (become IPSP's) with hyperpolarizing current injection. Rossi et al. (1980) made intra-axonal recordings from frog primary afferents innervating the posterior canal. They recorded EPSP's and action potentials. Following electrical stimulation of the distal cut end of the posterior nerve at 50 pulses/sec, orthodromic spikes were eliminated and the frequency and amplitude of the EPSP's were slightly reduced. Flock and Russell (1973) have recorded nerve potentials from lateral line organs in the fish (Burbot) and they have identified EPSP's as belonging to the afferent system and IPSP's as belonging to the efferent system. These investigators' electrophysiological results were obtained during stimulation of the end organ. However, spontaneous EPSP's and IPSP's may occur as a result of a spontaneous random release of quantal portions of transmitter substance in a way similar to that occurring with minature end plate potentials at neuromuscular junctions. Highstein and Baker (1983) recorded from antidromically identified efferent neurons in the toadfish. They observed that the efferent neurons were spontaneously active. Thus, in summary, it appears that at least in some species (primarily cold-blooded species which are the only ones to have been tested so far) spontaneous EPSP's

have been recorded at or near the sensory neuroepithelium. Efferent neurons are spontaneously active. IPSP's have been recorded from the lateral line organ during stimulation of efferent fibers. To date, we are unaware of studies directed at studying spontaneous EPSP's and/or IPSP's in an unanesthetized warm-blooded animal's vestibular neuroepithelium. To conduct these studies in the unanesthetized but destriate pigeon is one of the specific aims of the present proposal. Our interest in this problem stems from our previous work in which we studied spontaneous activity on vestibular primary afferents. In 1978, we (Correia and Landolt, 1978) examined the spontaneous activity on postganglionic ampullary afferents in the anesthetized pigeon using point process theory. We determined that 60% of the ampullary afferent spontaneous discharge spike trains could be modeled as a renewal process. That is, it was determined by a rigorous set of tests that the spike trains contained interevent intervals which were stationary, independent, and identically distributed. It is known from renewal theory, that the realization of a renewal point porcess can be completely described by its first order statistical properties, that is, its pdf. Six candidate pdf's were fit to ISI histograms of the spike trains (shown, for example, in Fig. 9B) The pdf which provided the best-fit to all ISI histograms was a pdf associated with a model which has been used to describe the motion of a particle undergoing Brownian motion before it passes through an absorbent barrier for the first time. This particular model-the Wiener-Levy model and a family of probability density functions (for various parameters) for this model are shown in Fig. 9D. The model was adopted to the description of neuronal activity by Pernier and Gerin (1971) and assumes that an action potential is produced at the spike originating locus whenever the resting membrane potential ($-V_0$) of a neural unit is depolarized by n units to its threshold potential ($-V_0 + n$) (see simplified operation in Fig. 9C) Fig. 9C also illustrates that the net effect of summated EPSP's is to drive the membrane potential to the threshold value. The net effect of the IPSP's would be to force this potential in an opposite direction (demonstrated by the erratic curve in Fig. 9C). Following the generation of an action potential (or absorption of a particle by a barrier), the membrane potential is presumed to be reset to the resting membrane potential and the process is repeated. It should be emphasized that the model does not necessarily require the existence of IPSP's for its operation. It does, however, work best when the membrane's potential is considered to take account of the net effect of EPSP's to the net effect of IPSP's or alternatively, the net effect of the total number of EPSP's (in the absence of and IPSP) that contribute to action potential generation. We (Correia and Landolt, 1978) adapted the model to the vestibular neuroepithelium by suggesting that anatomical studies and sparce electrophysiological studies suggest that afferent and efferent processes in the vestibular neuroepithelium contribute graded potentials which when summated (spatially or temporarily) produce a generator potential which in turn fires an action potential at the spike originiating locus. Among other things, this model predicts that high firing-regular afferents should innervate more hair cells than irregularly firing afferents. Assuming no IPSP's, this prediction is based on the assumption of shorter ISI's due to spatial and temporal summation of more EPSP's from multiple hair cell postsynaptic potentials as they drive the generator potential to threshold. Schessel and Highstein (1981) marked with HRP one afferent whose discharge pattern was irregular (no statement was made about relative MFR). The afferent innervated five

type I hair cells in a single calyx. The model also predicts that if IPSP's exist as postsynaptic potentials on the unmyelinated afferent dendrites in the vestibular neuroepithelium, the ratio of IPSP's to EPSP's prior to spike initiation will be greatest for irregularly firing afferents. Finally, if as in squirrel monkey (Goldberg and Fernandez, 1980) efferents are excitatory (produce EPSP's) and if general anesthesia blocks efferent activity in pigeon as in frog (Schmidt, 1963), then the model predicts that in alert pigeon the firing rate should be higher than in the barbiturate anesthetized pigeon. In our studies summarized in section II.C.1 we found that the MFR on ampullary afferents was increased 83% in the alert pigeon.

C. Methods

1. Anatomical studies

Three pigeons, deeply anesthetized with intramuscular ketamine hydrochloride (10-15 mg/kg) and intramuscular sodium pentobarbital (15-20 mg/kg), will be perfused with fixative by an in vivo transcardiac bilateral carotid catheterization method (Eden and Correia, 1981). Three gerbils, also deeply anesthetized will receive intracardiac pump perfusion of fixative. In both cases the fixative will be 5% glutaraldehyde in 0.1 molar phosphate buffer. Following perfusion, the labyrinths and vestibular ganglia will be removed. Each ampulla will be separated and the ampullae and ganglia will be placed in a 1% phosphate buffered osmium tetroxide solution for 1 hour. Following two water rinses the vestibular ganglia and labyrinthine structures will be placed in a uranyl acetate solution (1%) for 1-2 hours. The tissue will then be exposed to a graded series of ethanols for the purpose of dehydration. Following dehydration, the tissue will be placed in a graded series of 100% alcohol-propoline oxide in a ratio of two to one, followed by a ratio of one to one, followed by a ratio of one to two, followed by immersion in propoline oxide. Following this procedure, tissue will be exposed to a graded series of propoline oxide/plastic. Epon has been the plastic used in the past (e.g. in Figs. 8A, 8C, and 6). The ratio of propoline oxide to plastic will be two to one, one to one, one to two, followed by vacuum embedding in plastic for 1 hour. Tissue will then be set in a 60 degree oven overnight. The contents of three of the six pigeon and gerbil labyrinths and three vestibular ganglia will be blocked and cut with an LKBIII ultramicrotome at a section thickness of 1 micron. The tissue will be oriented so that sections will be orthogonal to the long axis of the crista (Landolt et al., 1975; Fig. 8B in this proposal). These sections will be observed using high power light but primarily interference microscopy. The remaining three labyrinths and three vestibular ganglion will be thin sectioned and subsequently examined using a JOEL 100-CX transmission electron microscope. Thick serial sections through the labyrinths in the pigeon and gerbil will be examined to determine the number of type I hair cells in a single nerve calyx. Counts of number of type I cells in a calyx will be overlayed on a 3-D representation of the surface of the crista. Moreover, a count will be made of the number of type I (including single cell in calyx) and type II hair cells on the surface of the crista. This will be accomplished by focusing through serial sections using interference microscopy identifying type I and II hair cells and noting their topographical distribution over the surface of the crista. Thick sections of the vestibular ganglia

of the pigeon and gerbil will be examined using interference and light microscopy. Orientation of the ganglia will be maintained by leaving part of the vestibular nerve trunk attached to the ganglia. The tissue will be sectioned in the plane of the soma and both axons of bipolar cells (Fig. 9). The serial sections will be scanned to determine the ratio of myelinated cell bodies to unmyelinated cell bodies as well as the ratio of multipolar cell bodies to bipolar cell bodies within the ganglion. Moreover, size and location of unmyelinated bipolar and multipolar cells will be noted. These results will be confirmed using TEM of thin (silver) sections of the vestibular ganglion. These sections will be scanned and sampled with low power TEM to determine the ratio of myelinated cell bodies to unmyelinated cell bodies, the ratio of multipolar cell bodies to bipolar cell bodies and if chemical or electronic synaptic processes exist in SG on to the perikaryon and dendrites. If synaptic processes are found in the vestibular ganglion, a qualitative description will be provided of the synaptic clefts, presynaptic and postsynaptic bodies and synaptic vesicles.

2. Neurophysiological studies

A series of pigeons will be prepared for intracellular penetration of hair cells and sensory processes in the vestibular neuroepithelium or cells in SG. The animals will be prepared by methods already developed and whose description follows. On the recording day, each pigeon will be anesthetized using ketamine hydrochloride. The cranium will be removed and a bilateral destriation will be performed. Following destriation, no supplementary doses of ketamine will be provided. The thorax will be opened, the air sacks ruptured, and a tracheotomy performed. A mixture of oxygen and carbon dioxide (95:5) will be passed through the respiratory system of the bird at a rate of 200 ml/min. The animal will then be given a dosage of Flaxedil (see Pitfalls section). Finally, using a lateral approach to the otic capsule, the anterior semicircular duct will be transected near the ampulla (Correia et al., 1973; Eden and Correia, 1982) and microelectrodes will be advanced into the vestibular neuroepithelium from above using a Burleigh microdrive. Initially the microelectrodes will be micropipettes filled with a 3-5% solution of Lucifer yellow dissolved in 1 molar lithium chloride (Stewart, 1978). Subsequent experiments will use micropipettes filled with 5% HRP and reacted with DAB (Perachio et al., 1983). We will use Lucifer yellow initially to: a) lower electrode resistance; b) bypass the DAB reaction process and evaluate the sensitivity of Lucifer yellow as a marker of fine processes. The micropitettes will be pulled so that they have extremely fine tips but as low DC resistances as possible (< 100 Mohms). Voltage fluctuations will be monitored using the WPI 700A amplifier and stored on FM tape. Intracellular penetration of afferent or efferent terminals will be differentiated from intracellular penetration of hair cells by the presence of action potentials interspersed between graded postsynaptic potentials (for example, see Fig. 1 in Schessel and Highstein, 1981). Following a period of recording spontaneous activity from within an afferent/efferent terminal or hair cell, the membrane potential will be hyperpolarized by injecting current through the microelectrode. The resulting graded potentials will be examined to determine if they reverse their polarity (Eccles, 1969). This latter test will be performed to determine if IPSP's not originally seen are masked by EPSP's. Following hyperpolarization of the membrane and capturing the

graded potentials on FM analog tape, Lucifer yellow will be injected into the terminal/hair cell using iontophoresis. Processes will be injected by continuing to pass constant-current hyperpolarizing pulses of 1 sec duration at a rate of one every 2 sec. Dye will be iontophoresed from the microelectrode by applying a negative potential through a 1,000 Mohm limiting resistor to the back of the micropipette (Stewart, 1978). Dye injection time (nA-min) will be determined empirically. Start values will be 5-10nA for 20 min. or until action potentials fall to 1/3 of their initial height. Following injection, the ampulla will be removed. During initial experiments, the tissue will be fixed by inversion of the ampulla into a 4% formaldehyde fixative in a 0.1M phosphate buffer (pH 7.4) for 4 hrs. The tissue will then be blocked (ampulla bisected), dehydrated, and infiltrated with monomer (glycal methacrylate or Spurrs medium) on a coverslipped slide. The monomer will be polymerized with heat or light. The whole mount will subsequently be viewed with a Leitz Dialux 20 microscope with appropriate barrier and excitor filters. The paradigm described above for the sensory neuroepithelium will be applied to a second series of animals in which an attempt will be made to intracellularly penetrate SG cells or their proximal axons. These experiments presume that in the pigeon, synaptic processes and multipolar cells were identified by the anatomical studies. The ganglion will be exposed using a lateral approach (Correia and Landolt, 1973; Correia et al. 1973). Prior to attempted intracellular recordings a cotton pledget saturated with collagenase will be laid on top of the ganglion. An attempt will be made to penetrate ganglion cells and deposit Lucifer yellow dye inside them. Graded potentials and action potentials will be recorded from these cells. Following penetration, iontophoretic injection of Lucifer dye will be carried out. The tissue will be prepared (as described above) for subsequent observation using fluorescent microscopy. Note will be made of whether labeled cells are multipolar or bipolar and their location within the ganglion. A correlation will be made between types of postsynaptic potentials and cell morphology in both the vestibular neuroepithelium and SG.

D. Time Table

During the first 6 months, the PI, Dr. Kevetter, and the research tech. will process 24 pieces of tissue; 6 labyrinths and 6 ganglia from 3 gerbils and 6 labyrinths and 6 ganglia from 3 pigeons. Initially, 3 labyrinths and 3 ganglia from a pigeon and a gerbil will be plastic embedded, sectioned at 1 micron thickness and viewed using light and interference microscopy. The remaining tissue will be processed and viewed on a JOEL 100-CX electron microscope. We anticipate that we can process one piece of tissue per week. This includes preparation of tissue, viewing the tissue using the light or electron microscope and producing topographical maps with counts to meet the specific aims listed above. By the end of the first six months, it should be clear whether there are multipolar neurons in the pigeon vestibular ganglion, how many exist, where they are located, and whether these multipolar neurons and some of the bipolar neurons are unmyelinated. It should be clear whether our preliminary findings of multipolar neurons (labeled with HRP) in the gerbil (a small mammal) vestibular ganglion (Perachio et al., 1983) are confirmed. Also during this time period we should be able to determine whether synaptic processes exist within the vestibular ganglion of the pigeon and gerbil. Finally, during this time period we should be able to

produce a map of the distribution of multiple and single type I and type II hair cells on the cristae of the pigeon. These results will determine the direction of the electrophysiological experiments which will be conducted during the remaining 12 months of the first half of this proposal. If snyapses are found in SG, then in the electrophysiological studies we will attempt to penetrate and mark neural processes in both SG and the vestibular neuroepithelium. Twelve months will be devoted to these electrophysiological studies. If few multipolar cells or bipolar cells with synaptic processes are found in SG, efforts will be concentrated on recording from hair cells and processes within the sensory neuroepithelium.

The majority of the procedures have already been developed which will be used in the electrophysiological studies. For example, we have experience with the bilateral destriate-flaxedil-artificially respired pigeon preparation. Dr. Perachio and the PI (Perachio et al., 1983) have experience with intracellular recordings from postganglionic vestibular primary afferents in the gerbil. We have experience with iontophoretic deposition of HRP inside these axons. We have experience with obtaining access to SG and the individual ampullae in the pigeon preparation (Correia et al., 1973). We (Eden and Correia, 1982; Correia, et al., 1983) have used this access to deposit various substances (for example, HRP and tritiated proline and fucose) within the endolymphatic space.

However, we will have to develop procedures for recording from unmyelinated afferent and efferent processes within the sensory neuroepithelium. Moreover, we will have to develop procedures for iontophoretic injection of Lucifer yellow into these structures and preparation of whole mount specimens for subsequent viewing using fluorescent light microscopy. The PI and Dr. Kevetter both have experience in using fluorescent microscopy to visualize cells in the central nervous system which have been labeled by fluorescent dyes (for example, nuclear yellow, true blue, and DAPI - for example, Eden and Correia, 1982). We anticipate that it will take a full 12 months to penetrate a sufficient number of afferent terminals and cell bodies to make a statement about the type of postsynaptic potentials which we record from within these structures and their anatomical correlates. This projection is based on our past 1 1/2 years experience with trying to penetrate and recover HRP labeled postganglionic tilt sensitive primary afferent fibers in the gerbil.

E. Pitfalls

Opening the ampulla to approach the cristae from above with a microelectrode will disturb the homoestasis of the endolymphatic space and possibly the cupula. These factors may reduce, distort, or eliminate the generator potentials within the neuroepithelium. As an alternate, early on, a series of animals will be studied in which a microelectrode will be advanced into the crista from below the basement membrane (a la Schessel and Highstein, 1981). The PI has used this approach to record extra cellular potentials from ampullary afferents in the pigeon (Correia and Dohlman, unpublished observations). The approach which produces the highest yield of postsynaptic potentials and healthy action potentials will be adopted.

In the Methods, we propose to use Flaxedil. This drug is a cholinergic blocker. Therefore, its use during the proposed studies may abolish IPSP's or EPSP's produced by efferent (cholinergic) neurons. We will develop (in parallel with the early studies described above, a spinalized pigeon preparation. If we are successful in developing this preparation, we will abandon the Flaxedil. We have no a priori reason to believe that we can't develop such a preparation. However, Flaxedil will be used in the first studies to enhance chances of successful penetration of neural processes.

PROPOSAL - October 1, 1985/March 31, 1987 (1 1/2 years)

A. Specific Aims

1. To determine the effects of systemically acting scopolamine on SC and otolith afferent single unit responses to rotation, tilt, and electrical stimulation in the unanesthetized pigeon preparation.

2. To determine the effects of systemically acting scopolamine on graded potentials within the vestibular sensory neuroepithelium in the bilateral destriate pigeon preparation.

B. Rationale

In recent years, scopolamine plus amphetamine has been the drug mixture of choice for prophylactic therapy for space motion sickness (Kohl and Homick, 1983). The astronaut packs contain oral scop-dex in a standard mixture of 0.4 mg scopolamine-5 mg dexadrine to be taken every four hours (Homick, personal communication). The scopolamine is the presumed antimotion sickness agent (muscarenic cholinergic blocker) and the dexadrine negates the drowsiness related to the scopolamine. Neurophysiological studies of the effects of scopolamine on unitary discharge in the vestibular nuclei have been limited in number and scope (Jaju et al., 1970); Kirsten and Schoener, 1973; Matsuoka et al., 1975; Kirsten and Shauma, 1976). These studies have been primarily concerned with the effects of scopolamine on the spontaneous MFR, and change in frequency of firing during electrical and rotatory stimulation. For example, Matsuoka et al. (1975), studied single cells in the lateral vestibular nucleus, in cat, following administration of scopolamine in a dose of 0.5 mg/kg i.v., the MFR was reduced to 14.2 $\pm$ 0.6 imp/sec from a control group MFR of 19.8 $\pm$ 1.6 imp/sec. Jaju et al. (1970), studied effects of scopolamine on vestibular nuclei neurons in encephale isole cats. They found that when they recorded from a cell in the medial vestibular nucleus 2 hrs. after administration of 5 ug/kg of scopolamine both the peak of the ISI histogram and the peak of the cycle histogram (response to $\pm$ 50 degrees at a frequency of 10 cycles/min) was reduced.

Since we were unable to find any literature which addressed the effects of scopolamine on the dynamic response characteristics of vestibular nuclei neurons, we developed methods and studied, in the alert pigeon, responses of several lateral vestibular nuclei neurons to polarizing current applied to the labyrinth (Lifschitz, 1973). We applied step currencts of various magnitudes and durations and formed frequency

of firing histograms. A response, typical of those we obtained, is presented in Fig. 4A. The same stimulus was delivered at 10 min following intracardiac injection of 0.173 mg/kg of scopolamine. The resulting frequency of firing histogram is presented in Fig. 4B. A comparison of the results presented in these figures shows that we extended the half-amplitude decay time to the depolarizing step by 19 times following scopolamine injection. We also noted in the same neuron a decreased spontaneous MFR from 48 imp/sec pre-injection to 24 imp/sec post-injection (50% decrease). Since we used electrical stimulation, we presumed that we by passed the mechanical component of the cupula-endolymph system and prolonged the decay of the processes associated with neuroelectric transmission. However, we realized that the effects we observed could be the result of the systemic action of scopolamine on several neural systems which project to the vestibular nuclei including fibers from the periphery, cerebellum, and other vestibular nuclei (see, for example, Correia et al., 1983 - appended galley proofs). In this proposal, we wish to retreat to the periphery and first study the effects of scopolamine on single primary afferent discharge in the alert pigeon.

In our literature review, we were unable to find studies of the effects of scopolamine on primary afferent discharge. However, there is reason to suspect that scopolamine, classically regarded as an anticholinergic drug, might act on the vestibular sensory neuroepithelium by blockage of cholinergic efferent fiber synapses within the vestibular neuroepithelium. Efferent vestibular neurons are thought to be cholinergic. The high content of acetylcholinesterase (AChE) in efferent fibers has been used to demonstrate the course and distribution of efferent fibers in the vestibular neuroepithelium (Dohlman et al., 1958; Hilding and Wersall, 1962; Ireland and Frakashidy, 1961) and in the brainstem (Gacek et al, 1965; Goldberg and Fernandez, 1980). Moreover, Precht (1981) cites an unpublished observation by Hartman who noted in goldfish, a slight increase in afferent discharge (possibly resulting from disinhibition) following application of Flaxedil. We propose to study spontaneous and driven responses of primary afferents during continuous injection of scopolamine via an intracardiac catheter. Using scopolamine dosed animals we will repeat the spontaneous discharge and rotatory studies we reported in section II.C.1 and we will study ampullary afferent discharge to polarizing currents applied to the labyrinth. We will compare the results gathered during rotation vis-a-vis electrical stimulation to differential the possibility that scopolamine directly affects the cupula-endolymph system like alcohol, heavy water etc. (Money and Myles, 1974).

Finally, we will study the effects of scopolamine on the graded potentials within the vestibular neuroepithelium by using the animal preparation we developed during the first half of the grant to see if we can alter postsynaptic potentials by systemic action of scopolamine. The results of these studies will be compared to those which we conducted in the first half of the grant period.

C. Methods

1. Animal preparation

It is estimated that 20 pigeons will be used to conduct the studies proposed during the last 1 1/2 years of this proposal. All 20 animals will be prepared for recording from vestibular primary afferents while the animal is unanesthetized (see section II.C.1; Fig. 1). In 10 of the animals, an indwelling venus catheter will be installed several days prior to the aniticipated recording session. These animals will subsequently be tested using a rotatory and tilt paradigm which is described below. In 10 other animals, guide tubes to support a bipolar electrical stimulating electrode will be implanted in the pigeons' skulls (see section II.C.2) prior to the recording sessions and indwelling venus catheters will be implanted into the animals' hearts. These animals will receive electrical stimulation using the same voltage waveforms as the other group of animals who received rotatory and tilt stimulation.

2. Drug infusion

On a given test day, once vestibular primary afferents are located, an initial bolus of scopolamine will be infused into the animal using an infusion pump. Thereafter, the drug will be administered at a rate to provide a constant blood level of 0.10 mg/kg of scopolamine. In four control animals, two mls of blood will be withdrawn at the beginning of the experiment, at the end of the second hour, and at the end of the fourth hour. This blood will be assayed for the level of scopolamine in the blood using the method of Cintron-Trevino et al. (1982 - see appended abstract and letter). The results of this assay (adjusted to register micrograms of scopolamine) will establish blood level concentrations of scopolamine over a four-hour period which will be the usual test period. The total blood volume of a pigeon is 9.2% of total body weight (Altman, 1961). The pigeons which we will use are retired male breeders whose body weight ranges from 700-900 grams (blood volume 64-83 mls). For a 700 gram animal, the blood withdrawn would be 9.3% of total blood volume; for the 900 gram animal, the blood removed would be 7.2% of the total blood volume. Following blood withdrawal, these four control animals will be returned to their home cages and not tested for 1 month. In our preliminary studies, we injected a bolus of 0.173 mg/kg of scopolamine into the heart. Ten minutes following this injection we found dramatic effects on neural activity of vestibular nuclei cells (see section II.C.3). This dose level is 10 times that shown to produce an effect in the cat vestibular nucleus in one study (Jaju et al., 1970) but one-fifth that used in the cat in a second study on the effects of scopolamine on vestibular nuclei activity. Since we observed effects at a drug level of 0.173 mg/kg in the vestibular nuclei, we will try to maintain a blood level concentration of 100 ug/kg over a period of four hours. If <u>any</u> adverse affects are noted the drug dosage level will be adjusted downward; if no effects on vestibular primary afferent activity are noted at this dose level the dosage will be adjusted upward in several animals. During all testing, scopolamine will be administered by a drug infusion pump. During rotatory testing a hydraulic slip ring will be used.

3. Testing paradigm

Rotational testing will be carried out using a Contraves Model #823 rate table. Electrical labyrinthine stimulation will be carried out by delivering voltage wave forms through a Fredrick Haer

constant current stimulator to bipolar stimulating electrodes. During a given test session, a thin shaft micropipette will be lowered to the region of postganglionic vestibular primary afferents. Once vestibular primary afferents have been identified physiologically using a series of rotations and tilts (Blanks and Precht, 1976; Perachio and Correia, 1983 b; Anastasio et al., 1983, see section II.C.1), silastic will be placed around the microelectrode in the recording well to stabilize it and drug infusion will commence. We will use slender shaft glass micropipettes (see Perachio and Correia, 1983a) with impedances in the range of 5-10 Mohms (at 1 kHz) and an electrolyte solution of 3 molar NaCl. For the animals which will receive rotational stimulation, the following paradigm will be applied: a) recording of spontaneous activity with the animal in the standard postion (horizontal SC's coplanar with the earth's horizontal plane) for 2 minutes. b) Two minutes of recording of discharge activity with the animal pitched 10 degrees-beak down. c) Recording of 2 minutes of discharge activity with the animal pitched 10 degrees-beak up. d) Delivery of 2 bandwidths of sum of sines with the peak velocity of each component constant at 20 degrees/sec. e) If a unit remains following the sinusoidal rotation, an acceleration pulse (velocity ramp) will be administered. This velocity ramp will be an acceleration of 20 degrees/sec^{-2} to a constant velocity of 60 degrees/sec-maintenance of that constant velocity for 60 sec then deceleration back to stop at 20 degrees/sec^{-2}. For otolith afferents, the sum of sinusoidal rotational stimuli will not be used but additional tilts will be substituted. These tilts will be $\pm$ 10 degrees roll to accompany the $\pm$ 10 deg pitch which will have already been administered.

Electrical stimuli will be delivered using the same programmable function generator which delivers the volatages to the Contraves-Goertz rate table. However, these voltages will be fed into a constant current source and delivered to the vestibular neuroepithelium by the electrodes described in section II.C.2. Polarizing electrical stimuli have been used by previous investigators to electrically stimulate the labyrinths (Lifschitz, 1973; Ezure et al., 1983; Goldberg et al., 1982). During all of the test paradigms, the animal will be blindfolded. The horizontal ampullary afferents will be tested with the horizontal SC's in the earth's horizontal plane. Anterior and posterior ampullary afferents will be tested with the animal rolled 90 degrees so that the sagittal head plane is coplanar with the earth's horizontal plane.

D. Data Analysis

Using standard procedures, which we have described in the past (Brassard and Correia, 1975; Brassard, et al., 1977; Ni et al., 1978; Landolt, 1978; Landolt and Correia, 1980; Anastasio et al., unpublished observations - see section II.C.1) we will analyze spontaneous and driven activity of vestibular afferents with a constant blood level of scopolamine ;(100 ug/kg-start value) and compare these data with those which we have previously derived for barbiturate anesthetized pigeons (Correia and Landolt, 1973, 1978; Landolt and Correia, 1980) and alert pigeons (Anastasio et al., 1983; Anastasio et al., unpublished observations, see section II.C.1). Spontaneous activity will be analyzed by forming ISI histograms and determining first order statistical properties (MFR, SD, CV, B1, B2). Driven responses will be analyzed by forming Bode plots

(see for example, Figs. 3A and B), obtaining best-fit transfer functions and statistically comparing time constants to those obtained from barbiturate anesthetized and unanesthetized pigeons. Those time constants which will be compared are: the adaptation time constant; the long-time constant (the so-called "cupula time constant") and the time constant associated with high frequency gain enhancement and phase advance. For the acceleration pulse data, the time constant of decay will be calculated. For the tilt data from otolith afferents, first order statistical properties will be calculated for the $\pm$ 10 degree pitch, $\pm$ 10 degree roll data after 30 sec of maintenance at each tilted position. The same analysis methods will be applied to vestibular primary afferent responses to electrical stimulation.

Only spontaneous activity will be recorded and analyzed in experiments where postsynaptic potentials are recorded in the neuroepithelium of the scopolamine dosed pigeon. Note will be made of the presence of EPSP's and IPSP's and interevent histograms will be formed for postsynaptic potentials and action potentials. These measures will be compared to control data gathered during the first half of the grant period.

E. Time Table

In the past, we have found that we can study a chronic unanesthetized pigeon preparation for 1 month with test sessions each day lasting at a maximum 4 hours. In a series of 20 pigeons we found that using the small shaft micropipettes (Anastasio et al., unpublished observations) that we can make up to 50 passes through each of the wells into the left or right vestibular nerves and still record from vetibular afferents which appear to be healthy. Also during this period of time, the pigeons do not appear to show effects of the repeated electrode penetrations through the overlying brain structures. Therefore, we propose to study one animal per month during the proposed period. Ten animals will receive rotational and tilt stimulation and 10 animals will receive electrical stimulation. Four animals will receive drug infusion and blood withdrawal to validate the constancy of drug level over a 4-hour period. Although tests will be conducted 5 days a week, no animal which has received scopalomine will be retested in the same week. Since most of the procedures in this part of the proposal will have been developed, only the drug infusion and calibration of blood level dosage will have start-up time. During the first month, we will concentrate on drug delivery systems and calculation of infusion rates to maintain a constant dose level of 100 ug/kg.

F. Pitfalls

It may be that scopolamine has no effect on the mechanoelectric transduction chain in the peripheral vestibular system. It may be that the preliminary results which we obtained from single vestibular nuclei neurons were effects specific to synapses within the vestibular nuclei themselves. However, as we stated in the Rationale, it seems that the appropriate starting place for the analysis of the effects of scopolamine on the vestibular system is in the periphery. If we determine early in this series of experiments, that scopolamine has no effect on the activity of vestibular primary afferents as evidenced by their spon-

taneous discharge and their response to rotation, tilt, or electrical stimulation, we will not conduct the series of experiments in which we propose to record postsynaptic potentials in the neuroepithelium of scopolamine dosed animals but move to the level of the vestibular nuclei and apply our test paradigms to those cells. Unfortunately, that eventuality will require additional work since we do not have control data (dynamic response recordings from single cells in the vestibular nuclei in the unanesthetized pigeon preparation without scopolamine). That data, for pigeon, which does not exist in the literature (to our knowledge) will also be gathered during the second half of the grant period. However, we have allowed a year and one-half for those studies. It seems that during that time period, we can begin to study at least one of the vestibular nuclei (probably the lateral vestibular nucleus).

FACILITIES AVAILABLE

A. Laboratory Facilities (Vestibular Neurobiology Laboratory)

1. PI's laboratory

The PI's laboratory consists of 400 sq. ft. which contains: a) rotator/tilt stand - a Contraves-Goertz Model #823 rate table mounted in a Contraves-Goertz Model #4426 tilt stand and powered by a 1,500 watt 1,500CP Hyband servo amplifier. The rotator is driven by waveforms generated by a Hewlett-Packard (HP) 3722A noise generator, a ROM programmable sum of sine wave generator and a Khron Hite 4024AR low distortion oscillator. b) Electrical stimulation equipment - (1) A WPI #1800 neural stimulation "set-up" consisting of an interval generator (WPI #1830), 2 pulse train modules (WPI #1831), and a dual isolator (WPI #1880), (2) 2 Fredrick Haer optical isolators (constant current stimulation-bidirectional with a smooth transition through zero. c) Computer - LSI 11/23 with: RX02 floppy drive/40 megabyte Winchester disk and 128 K words of memory; four A/D converters (12 bit A/D conversion at a maximum throughput of 200 kHz); two D/A converters (12 bit D/A conversion at a maximum throughput of 200 kHz); and one programmable real time clock with 2 Schmitt triggers with adjustable level and slope controls.

2. Core support facilities

a) Histology core unit - One room is used for tissue preparation and one room contains a Lietz Dialux 20 research microscope. The tissue preparation area contains several stirrers, balances, a pH meter, perfusion pumps, a cryostat, a sliding microtome, a slide warming tray, an oven, etc. The microscope room contains the Lietz Dialux 20 microscope with its attachments and capability for fluorescent, darkfield, lightfield, and interference microscopy and photography. b) Graphic arts core facility - The elements of the graphic arts facility are: a darkroom and photography copy area (Polaroid MP-4XL camera copy system). The darkroom contains an Ilfospeed 4250 print washer/dryer, an Omega Pro-Lab enlarger, and a constant temperature bath. This facility is used to develop and print photomicrographs (light and TEM); print negatives of graphs, tables, line drawings etc. c) Computer core facility - A DEC PDP 11/20 computer with 8 channels of A/D, 4 channels of D/A, a RK05 disk pack, 28 K words of memory, 2 DigiData tape drives (9 track, 800 bpi), a Tektronix 4010-VT display with 4631 hard copy unit and a LA

30 DEC writer, CSPI MAP-200 array processor (125 ns instruction time) with 12 K-32 bit words of MOS memory, and an Apple microcomputer system with 2, 5 1/4" disk drives and a digitizing pad. The resident software library includes: a single unit action potential processing package with graphical output (cycle histograms, auto-correlation, frequency of firing histograms, interspike interval histograms, poststimulus time histograms, amplitude ratio and phase calculations based on an interactive least square fit of cycle histograms; a spectral analysis package based on the fast Fourier transform with graphical output (autopower spectra, cross power spectra, coherence, amplitude ratio, phase etc.; a package to interactively determine the best-fit parameters of a transfer function after amplitude ratio and phase values have been input.

B. University Support Facilities

Support facilities (cost basis) on the UTMB campus include: an animal care facility; a service computation facility; a medical engineering facility; a medical electronics facility; and a medical illustration facility.

C. Transmission Electron Microscope Facility

A suite of rooms (500 sq. ft.) containing a JOEL-100CX transmission Electron Microscope, LKBIII ultramicrotome and a darkroom. Suite and instruments available on a rental basis ($40/hr-see appended agreement letter from Dr. Christensen, Department of Physiology & Biophysics).

REFERENCES

1. Ades, H.; Engstrom, H., IN: Symp. on the Role of the Vestibular Organs in the Exploration of Space. Washington, DC: NASA, SP-77, p.23-40; 1965.

2. Altman, P.L., IN: Blood and Other Body Bluids, D.S. Dittmer, ed. Fed. Amer. Soc. for Exp. Biology, Washington, D.C., 1961.

3. Anastasio, T.J.; Correia, M.J.; Perachio, A.A., Soc. Neurosci. Abstr. 9: 525; 1983.

4. Bergstrom, B.; Engstrom, H., Equilibrium Res. 3: 37-32; 1973.

5. Blanks, R.H.I.; Precht, W., Exp. Brain Res. 25: 369-390; 1976.

6. Brassard, J.R.; Correia, M.J., Computer Prog. Biomed. 7: 1-20; 1977.

7. Brassard, J.R.; Correia, M.J.; Landolt, J.P., Computer Prog. Biomed. 4: 1-20; 1974.

8. Brassard, J.R.; Correia, M.J.; Landolt, J.P., Computer Prog. Biomed. 5: 11-38; 1975.

9. Caston, J., Pflug. Arch. 331: 365-370; 1972.

10. Caston, J.; Gribenski, A., Pflug. Arch. Ges. Physiol. 372: 139-143; 1977.

11. Caston, J.; Gribenski, A., J. Neurophysiol. 47: 55-59; 1982.

12. Chat, M.; Sans, A., Neurosci. 4: 651-657; 1979.

13. Cintron-Trevino, N.M.; Chen, Y., Annual Meeting of the Aerospace Medical Assoc., pp. 83-84; 1982.

14. Correia, M.J.; Landolt, J.P., Adv. Oto-Rhino-Laryng. 20: 134-148; 1973.

15. Correia, M.J.; Landolt, J.P., Biol. Cybern. 27: 199-213; 1978.

16. Correia, M.J.; Landolt, J.P.; Cardin, R.P.S.; Anderson, P.J.; Lee, M.A., DCIEM Report #927, Defence and Civil Institute of Environmental Medicine, Downsview, Ontario, Canada; 1973.

17. Correia, M.J.; Landolt, J.P.; Ni, M.-D.; Eden, A.R.; Rae, J.L., IN: The Vestibular System: Function and Morphology. T. Gualtierotti, ed. New York, Springer-Verlag: 280-316; 1981.

18. Dohlman, G.F.; Farkashidy, J.; Salonna, F., J. Laryng. 72: 1984; 1958.

19. Dunn, R.F., J. Comp. Neurol. 193: 255-264; 1980.

20. Eccles, J.C., Springfield, IL, C.C. Thomas, 1969.

21. Eden, A.R.; Correia, M.J., Physiol. Behav. 27: 947-949; 1981.

22. Eden, A.R.; Correia, M.J. Brain Res. 248:201-208; 1982.

23. Engstrom, H., IN: Symp. on the Role of the Vestibular Organs in Space Exploration. Washington, DC, NASA, SP-187: 123-135; 1968.

24. Engstrom, H.; Ades, H.W.; Hawkins, Jr., J.E., Symp. Biol. Hung. 5: 21-41; 1965.

25. Engstrom, H.; Bergstrom, B.; Ades, H.W., Acta Otolaryng. Suppl. 301: 75-126; 1972.

26. Ezure, K.; Cohen, M.S.; Wilson, V.J., J. Neurophysiol. 49: 639-648; 1983.

27. Fernandez, C.; Goldberg, J.M., J. Neurophysiol. 34: 661-675; 1971.

28. Fex, J., Acta Physiol. Scand. Suppl. 189: 1-68; 1962.

29. Flock, A.; Russell, I., Nature 243: 89-91; 1973.

30. French, A.S.; Holden, A.V., Kybernetik 8: 165-171; 1971a.

31. French, A.S.; Holden, A.V., Comp. Prog. Biomed. 2: 1-7; 1971b.

32. Friedmann, I.; Bird, E.S., J. Ultrastruct. Res. 20: 356-365; 1967.

33. Furukawa, T.; Ishii, Y., J. Neurophysiol. 30: 1377-1403; 1967.

34. Gacek, R.R.; Nomura, Y; Baloh, K., Acta Otolaryng. 59: 541-553; 1965.

35. Gleisner, L.; Henriksson, N.G., Acta Otolaryng. Suppl. 192: 90-103; 1963.

36. Goldberg, J.M.; Fernandez, C., Acta Otolaryngol. 80: 101-110; 1975.

37. Goldberg, J.M.; Fernandez, C., J. Neurophysiol. 43: 986-1025; 1980.

38. Goldberg, J.M.; Fernandez, C.; Smith, C.E., Brain Res. 252: 156-160; 1982.

39. Highstein, S.M.; Baker, R., Abstr. Midwinter ARO Meeting p. 87; 1983.

40. Hilding, D.; Wersall, J., Acta Otolaryng. 55: 205-217; 1962.

41. Homick, J.L., Acta Astronaut 6: 1259-1272; 1979.

42. Ireland, P.E.; Farkashidy, J., Trans. Amer. Otolaryng. Soc. 49: 20-30; 1961.

43. Ishii, S.; Matsura, S.; Furukawa, T., Jap. J. Physiol. 21: 79-89; 1971.

44. JaJu, B.P.; Kirsten, E.B.; Wang, S.C., Am. J. Physiol. 219: 1248-1255; 1970.

45. Jorgensen, J.M., Vidensk. Meddr dansk naturh. Foren. 133: 121-147; 1970.

46. Jorgensen, J.M., Acta Zool. 53: 155-163; 1972.

47. Jorgensen, J.M.; Andersen, T., Acta Zool. 54: 121-130; 1973.

48. Kemmerer, C.E.; Correia, M.J.; Perachio, A.A., Abstr. from the First Southern Biomedical Conference, Shreveport, LA, 1982.

49. Kirsten, E.B.; Schoener, E.P., Neuropharmacol. 12: 1167-1177; 1973.

50. Kirsten, E.B.; Sharma, J.N., Brain Res. 112: 77-90; 1976.

51. Kitamura, K.; Kimura, R.A., Adv. Oto-Rhino-Laryng. 31: 118-134; 1983.

52. Klinke, R.; Galley, N., Physiol. Rev. 54: 316-357; 1974.

53. Kohl, R.L.; Homick, J.L., Neurosci. Biobehav. Rev. 7: 73-85; 1983.

54. Landolt, J.P.; Correia, M.J., J. Neurophysiol. 43: 1746-1770; 1980.

55. Landolt, J.P.; Correia, M.J.; Young, E.R.; Cardin, R.P.S.; Sweet, R.C., J. Comp. Neurol. 159: 257-287; 1975.

56. Lifschitz, W.S., Brain Res. 63: 43-57; 1973.

57. Matsuoka, I.; Domino, E.F.; Morimoto, M., Acta Otolaryngol. 80: 422-428; 1975.

58. Money, K.E.; Myles, W.S., Nature 247: 404-405; 1974.

59. Ni, M.-D.; Correia,M.J.; Rae, J.L.; Koblasz, A.J., MIMI 77, Proc. International Symposium on Mini and Microcomputers. IEEE Cat. #77CH1347-4C, p. 205-212; 1978.

60. Parker, D.E., Scientific Amr. 243: 118-135; 1980.

61. Pearson, E.S.; Hartley, H.O., Biometrika Tables for Statisticians, Vol. 1., Cambridge: Cambridge University Press, 1970.

62. Perachio, A.A.; Correia, M.J., J. Neurosci. Meth. (in press, 1983a).

63. Perachio, A.A.; Correia, M.J., Brain Res. (in press, 1983b).

64. Perachio, A.A.; Correia, M.J.; Kevetter, G.A., Soc. Neurosci. Abstr. 9: 739; 1983.

65. Pernier, J.; Gerin, P., Bull. Math. Biophys. 3: 129-151; 1971.

66. Precht, W., IN: The Vestibular System: Function and Morphology. T. Gualtierotti, ed. New York, Springer-Verlag: 227-250; 1981.

67. Ramon-y-Cajal, S., Trabajos Lab. Invest. Biol. Univ. Madrid, 6: 161-176; 1908.

68. Reason, J.T.; Brand, J.J., IN: Motion Sickness. New York, Academic Press, 1975.

69. Rossi, M.L.; Prigioni, I.; Valli, P.; Casella, C., Brain Res. 185: 125-137; 1980.

70. Sala, O., Acta Otolaryng. Suppl. 197: 1-34; 1965.

71. Schessel, D.A.; Highstein, S.M., Vestibular and Oculomotor Physiology: International Meeting of the Barany Society. B. Cohen, ed. ANYAS 374: 210-214; 1981.

72. Schmidt, R.S., Acta Otolaryng. 56: 51-64; 1963.

73. Schneider, L.W.; Anderson, D.J., Brain Res. 112: 61-76; 1976.

74. Schwarz, D.W.F.; Schwarz, I.E.; Tomlinson, R.D., Soc. Neurosci. Abstr. 4: 614; 1978.

75. Stewart, W.W., Cell. 14: 741-759; 1978.

76. Weisberg, A.; Beatty, G.H., Technometrics 2: 483-500; 1960.

77. Wersall, J.; Flock, A.; Lundquist, P.G., Cold Spr. Harb. Symp. on Quant. Biol. 30: 115-132; 1965.